

Tasmanian Geological Survey

Record 1997/03

Geology of the Islands of Southwestern Bass Strait

**A contribution to the
National Geoscience Mapping Accord**



MINERAL RESOURCES TASMANIA

Geology of the islands of southwestern Bass Strait

by J. L. Everard, C. R. Calver, J. Pemberton, J. Taheri and G. Dixon*
with an Appendix by P. G. Quilty#

* Earth Science Section, Parks and Wildlife Service, Department of Environment and Land Management (Tasmania)

Australian Antarctic Division, Department of Environment, Sport and Territories (Commonwealth of Australia)

A contribution to the National Geoscience Mapping Accord

CONTENTS

ABSTRACT	4
INTRODUCTION	4
REGIONAL SETTING	7
COUNCILLOR ISLAND	7
<i>Petrography of metabasalt</i>	9
<i>Petrography of hornblende porphyry dyke</i>	11
<i>Geochemistry</i>	11
<i>Discussion</i>	14
BRIG ROCKS	17
REID ROCKS	17
<i>Petrography</i>	17
<i>Geochemistry</i>	19
<i>Discussion</i>	19
BLACK PYRAMID	21
<i>Petrography</i>	27
<i>Geochemistry</i>	27
<i>Discussion</i>	27
ALBATROSS ISLAND	29
<i>Petrography</i>	31
<i>Geochemistry of dolerite boulders</i>	31
<i>Discussion</i>	31
SMALL ISLETS WEST OF HUNTER ISLAND	32
North Black Rock	32
South Black Rock	32
Steep Island	32
Nares Rocks	32
Delius Islet	33
Brown Rocks	33
Bird Island	33
Seacrow Islet	33
Stack Island	33
HUNTER ISLAND	33
Cuvier Bay	33
<i>Petrography</i>	33

<i>Geochemistry of dolerite dyke</i>	34
Shepherds Bay.....	34
Cave Bay	34
<i>Petrography</i>	34
PENGUIN ISLET	34
<i>Granite petrography</i>	36
<i>Basalt petrography</i>	36
<i>Geochemistry</i>	36
THREE HUMMOCK ISLAND	36
Chimney Corner	36
West of Neils Rock	38
Granite petrography	38
Petrography of melanocratic enclaves	38
Granite geochemistry	41
<i>Discussion</i>	44
Geochemistry of melanocratic enclaves	47
<i>Discussion</i>	47
ROBBINS ISLAND (MARYS ISLAND and GUYTON POINT)	48
<i>Petrography</i>	48
<i>Geochemistry</i>	50
PETREL ISLANDS and WALKER ISLAND	50
DREDGING	50
East of King Island	50
Hope Channel	50
<i>Petrography – basalt</i>	52
<i>Discussion</i>	52
SE of Albatross Island ('Anomaly Alpha')	52
<i>Petrography – basalt</i>	53
<i>Discussion</i>	54
SW of Albatross Island ('Anomaly Beta')	54
<i>Petrography – orthoquartzite and basalt</i>	54
<i>Discussion</i>	54
NW of Albatross Island ('Anomaly Gamma')	54
<i>Petrography – orthoquartzite, limestone and basalt</i>	55
<i>Discussion</i>	55
W of Black Pyramid ('Anomaly Delta')	55
NOTE ON BASS-3 DRILLHOLE	55
CONCLUSIONS	56
ACKNOWLEDGEMENTS.....	56
REFERENCES	57
APPENDIX 1: Palaeontology and age of limestone from Black Pyramid and a dredged limestone pebble, Bass Strait (<i>P. G. Quilty</i>).....	59
APPENDIX 2: Sample locations and treatment.....	61
APPENDIX 3: Approximate mineralogy (approximate wt% by X-ray diffraction) of samples.....	62

FIGURES

1. Generalised onshore geology, far northwest Tasmania to King Island	63
2. Enlargement of onshore geology, Fleurieu (Hunter) Group of islands	5
3. Magnetic image of southwest Bass Strait	64
4. Enlargement of magnetic image, Fleurieu (Hunter) Group of islands.....	6
5. Geological sketch map of Councillor Island	8
6. Geochemical comparison of picrites from Councillor Island and King Island	15
7. Chondrite-normalised rare-earth element plot of Councillor Island picrite and hornblende porphyry, compared with range displayed by King Island picrites	16
8. Sketches of Black Pyramid showing rock units	21
9. Total alkali (Na ₂ O + K ₂ O) : silica (SiO ₂) plot for Tertiary basalts from Reid Rocks, Black Pyramid, Robbins Island and northwest Tasmania	29
10. Geological sketch map of Penguin Islet	35

11. Quartz-alkali feldspar-plagioclase plot of calculated pseudomodes of granites from Penguin Islet, granites and melanocratic enclaves from Three Hummock Island, and hornblende porphyry from Councillor Island.	42
12. Selected variation diagrams of granites from Penguin Islet and granites and melanocratic enclaves from Three Hummock Island	45
13. Plot of Fe ₂ O ₃ /FeO against Rb for granites from Penguin Islet and Three Hummock Island, with generalised fields for Sn-W, W, Mo and Cu-Au mineralised granitoids in the Lachlan Fold Belt ...	47
14. Dredging traverses, magnetic anomalies and onshore geology, Hope Channel	51

TABLES

1. Chemical analyses of picrites and hornblende porphyry dyke, Councillor Island	13
2. ICPMS analyses of two Councillor Island samples for rare-earth elements and Nb, Hf, Ta and Th...	14
3. Chemical analyses of Tertiary basalts from Reid Rocks, Black Pyramid and Robbins Island	20
4. CIPW norms of Tertiary basalts....	21
5. Chemical analyses of Neoproterozoic(?) dolerites from Albatross Island and Cuvier Bay	31
6. Chemical analyses of Devonian granitoids and melanocratic enclaves from Penguin Islet and Three Hummock Island	43
7. CIPW norms of granitoids and melanocratic enclaves	44
8. Summary of dredging results, Hope Channel ...	52
9. Summary of dredging results, western Bass Strait	53

PHOTOGRAPHS

1. Pillows in picritic basalt, Councillor Island ...	10
2. Hornblende porphyry dyke in picritic basalt, Councillor Island	10
3. Photomicrograph of metamorphosed picrite from pillow lava, Councillor Island	12
4. Photomicrograph of hornblende porphyry dyke, Councillor Island	12
5. Jointing in Tertiary basalt, Reid Rocks	18
6. Jointing and associated alteration, Tertiary basalt, Reid Rocks	18
7. Photomicrograph of Tertiary basalt, Reid Rocks	19
8. Black Pyramid, viewed from the east ...	22
9. Black Pyramid, viewed from the northwest	22
10. Tongue-like flow, northern side of Black Pyramid	24
11. Columnar jointing passing laterally into 'knobby' Tertiary basalt, Black Pyramid	24
12. Amygdaloidal basalt with Neptunian limestone dykes, Black Pyramid ...	25
13. Vertical and inclined columnar jointing, Black Pyramid	25
14. Graded granule-pebble conglomerate overlying calcareous sandstone, 'unit 2', eastern median ridge, Black Pyramid	26
15. Graded bedded sandstone with thin pebble conglomerate interbeds, cliff exposure south of eastern median ridge, Black Pyramid	26
16. Photomicrograph of glassy tuff, middle unit, Black Pyramid	28
17. Photomicrograph of Tertiary basalt, Black Pyramid	28
18. Albatross Island, viewed from the northeast, showing dipping conglomerate	30
19. Siliceous cobble-conglomerate, northern end of Albatross Island	30
20. Dipping Tertiary volcanic rocks, South Black Rock	32
21. Schlieren in granite, Chimney Corner, Three Hummock Island	37
22. Potash feldspar phenocryst alignment in granite, Chimney Corner, Three Hummock Island	37
23. Melanocratic enclave swarm in megacrystic granite, west of Neils Rock, Three Hummock Island ...	39
24. Close-up of melanocratic enclave swarm in megacrystic granite, west of Neils Rock, Three Hummock Island	39
25. Photomicrograph of granite, Chimney Corner	40
26. Photomicrograph of enclave within granite, Chimney Corner	40
27. Photomicrograph of enclave, Chimney Neils Rocks ...	42
28. Photomicrograph of Tertiary basalt, Marys Island	49
29. Photomicrograph of Tertiary basalt, Guyot Point	49

Abstract

Geological observations have been made on several islands between northwest Tasmania and King Island.

Councillor Island is composed of pillowed to tabular metabasalt, and is a northerly extension of the middle picritic unit of the Neoproterozoic volcanosedimentary succession on the nearby southeast coast of King Island. A thin hornblende porphyry dyke is compositionally unrelated, and probably much younger.

Reid Rocks consists of somewhat altered basalt of inferred Tertiary age. On the basis of major element chemistry it is a slightly potassic, relatively fractionated transitional olivine basalt, but its affinities are clearly mildly alkalic, especially on petrographic and trace element criteria.

Black Pyramid consists of a lower unit of glassy olivine tholeiite basalt and breccia enclosing minor bodies of early Miocene limestone, overlain by a horizontal well-bedded unit of vitric tuff, conglomerate and limey sandstone with graded bedding, and capped by a basaltic breccia of near-oversaturated tholeiitic affinities. Probably the entire succession was deposited subaqueously, providing further evidence for high relative sea-level in the early Miocene.

The siliciclastic conglomerate on Albatross Island is most likely a correlate of the Neoproterozoic Forest Conglomerate at the base of the Togari Group in the Smithton Synclinorium. Beach boulders of dolerite on the island are petrographically and geochemically broadly similar to the dolerite of the Rocky Cape Dyke Swarm.

The Devonian granite on Three Hummock Island, examined at two localities, displays several interesting mesoscopic features including biotite-rich layering and schlieren parallel to a flow lamination defined by potash feldspar phenocryst alignment, and fine-grained melanocratic enclaves. An outstanding example of an enclave swarm is hosted by megacrystic granite on the south coast. Most of the enclaves probably represent globules of mafic magma that were entrained in a liquid state into the granitoid pluton and subsequently partly equilibrated with it, but some angular enclaves of differing petrography may be true xenoliths.

Penguin Islet consists of a highly fractionated felsic S-type granite, probably an apophysis of the similar Three Hummock Island Granite.

Hunter Island consists of orthoquartzite and subordinate pelite assignable to the Rocky Cape Group. A highly altered dolerite dyke occurs at Cuvier Bay. To the west and south, Delius Islet, Brown Rocks, Bird Island and Stack Island appear to be composed of similar orthoquartzite, whilst North Black Rock, South Black Rock, Steep Island and Nares Rocks consist of Tertiary basalt and associated volcanoclastic rocks.

A Tertiary hawaiite flow occurs at Guyot Point, at the eastern end of Robbins Island, but nearby at Marys Island a domal structure of massive tabular basalt is a petrographically and chemically distinct nepheline hawaiite.

Samples were dredged from the seafloor, mainly over magnetic anomalies, in several areas. No bedrock was recovered, but well-rounded pebbles of Tertiary basalt, Cainozoic limestone and Proterozoic quartzite were retrieved at some sites. Re-examination of samples of basement from the Bass-3 oil exploration well suggests that they are correlates of the Black River Dolomite, and thus may represent an extension of the Togari Group 80 km northward of known exposure.

INTRODUCTION

Interest in the shallow continental shelf between Tasmania and King Island was stimulated by the acquisition of detailed aeromagnetic coverage of this area (reproduced in part in Figures 3 and 4) by the Australian Geological Survey Organisation (AGSO) in 1994/1995, as part of the Tasmanian National Geoscience Mapping Accord (NGMA) project. During interpretation of the aeromagnetic data it became apparent that knowledge of the geology of several offshore rocks and islands, critical for a correct interpretation, was lacking. Notable amongst the poorly-known or unknown islands were Councillor Island, Reid Rocks, Black Pyramid and Penguin Islet.

In order to investigate these locations a 14 m oceanographic research catamaran, the ORV *Alguita*, was chartered out of Stanley by the Tasmanian Geological Survey from 28 November to 6 December

1995. As well as these islands, this report documents observations on Hunter, Three Hummock, Robbins and Albatross Islands. Attempts were made to dredge selected seafloor magnetic anomalies, but no pre-Tertiary bedrock material was obtained. Comments are made on the interpretation of magnetic surveys in the area.

This report is based on field observations and collections made by three of us (JLE, CRC, JP), followed by petrographic studies (JLE, CRC), x-ray diffraction and chemical analysis of selected samples (JT). Any weathering rinds present were removed and the samples crushed in a steel jaw crusher. Separate grindings in chrome steel and tungsten carbide mills were made for each sample to avoid contamination and interference problems involving Cr, W and Nb. Glass discs and pressed pellets were prepared for x-ray fluorescence determination of major and trace elements respectively, using standard techniques. FeO was

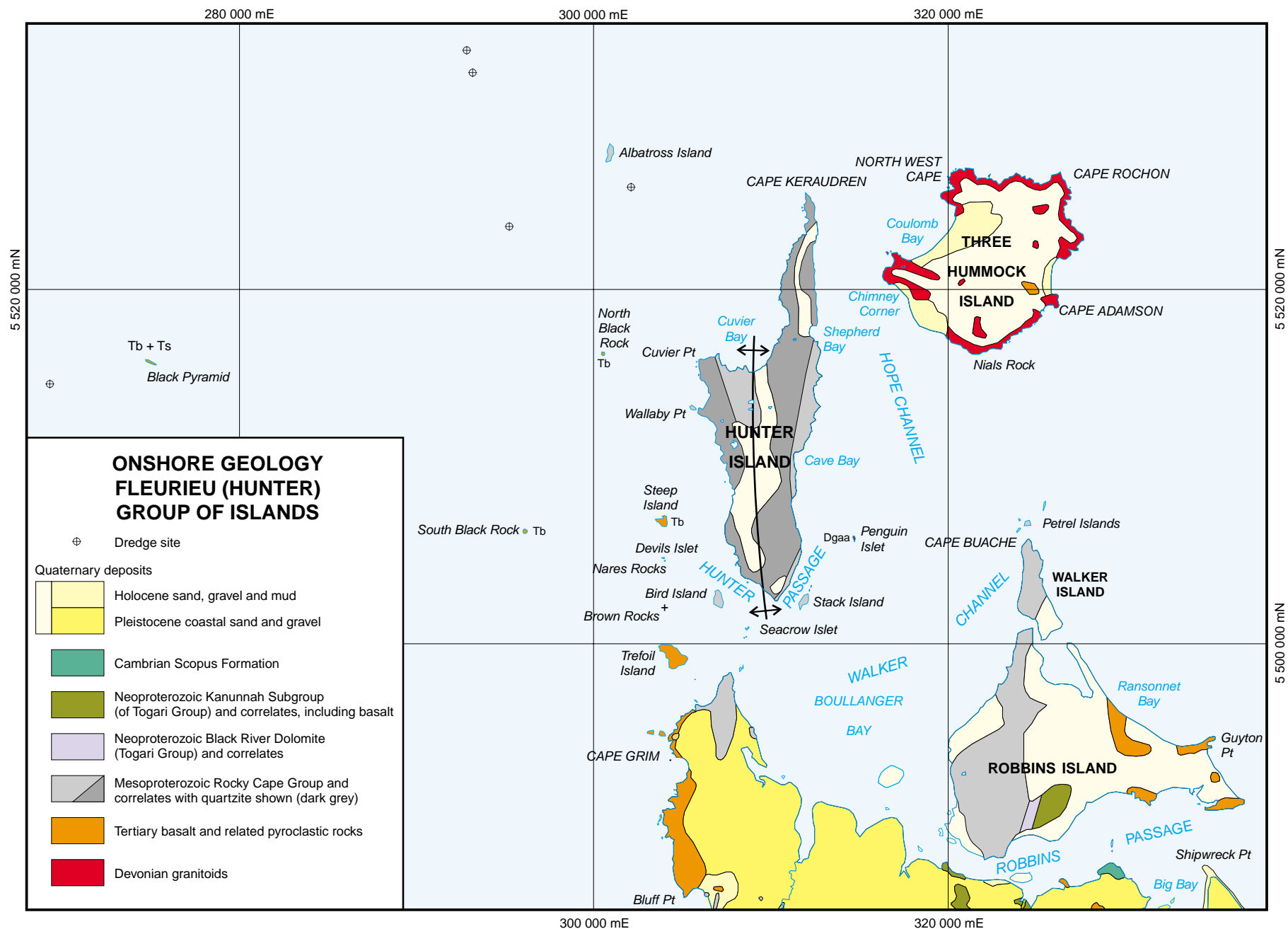


Figure 2 Enlargement of onshore geology, Fleurieu (Hunter) Group of islands (modified from Calver et al., 1995).

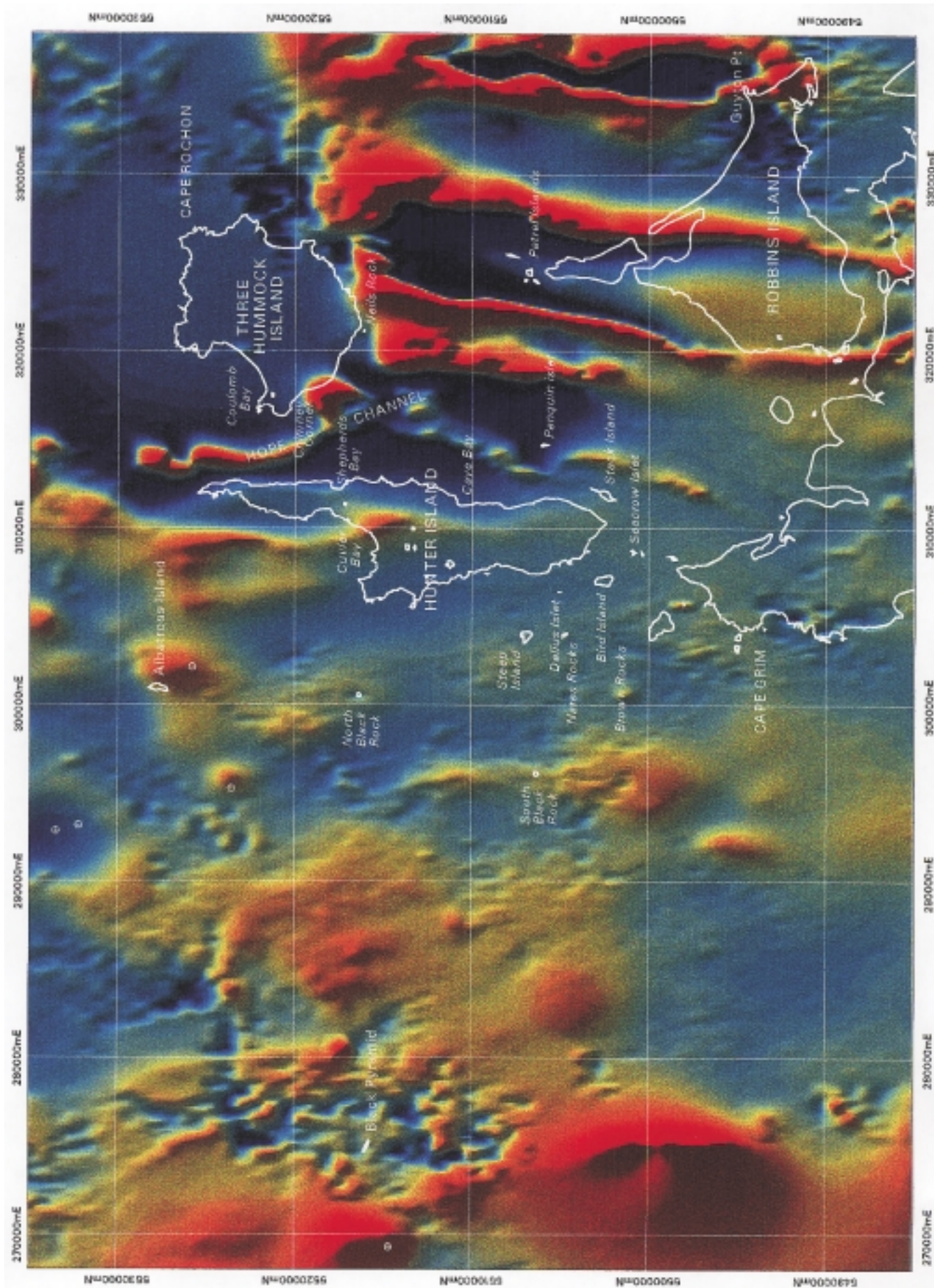


Figure 4

Enlargement of coloured image (total magnetic intensity) in vicinity of Fleurieu (Hunter) Group of islands.

determined by HF/H₂SO₄ attack in a platinum crucible followed by titration with KMnO₄, and Fe₂O₃ calculated by difference. A Leco induction furnace was used to measure evolved CO₂ by weight in an inert atmosphere. H₂O was calculated by difference using loss-on-ignition and CO₂ results, correcting for sulphide as required. For two samples, rare earth elements (REE) were determined by the ICPMS method by Analabs, Perth, Western Australia.

Mr G. Dixon, then an earth scientist with the Parks and Wildlife Service, accompanied us on part of the voyage and incorporated his findings in a separate report (Dixon, 1996).

Regional setting

A lengthy discussion of the regional geology of the area (fig. 1, 2) is outside the scope of this report. The reader is referred to Seymour and Calver (1995) and Morrison and Davidson (1989), and the references therein, for further details.

A multiply deformed Mesoproterozoic, dominantly siliciclastic shelf sequence (Rocky Cape Group) underlies most of northwest Tasmania, northwest of the Arthur Lineament. In a downfolded region, the Smithton Synclinorium, the Rocky Cape Group is unconformably to disconformably overlain by a Neoproterozoic sequence (Togari Group) of dominantly dolomite with a middle interval of basalt, diamictite and mudstone/siltstone. A Middle to Late Cambrian fossiliferous mudstone/lithicwacke sequence, the Scopus Formation, disconformably overlies the Togari Group in the core of the synclinorium.

Apparently similar geology occurs on southeast King Island, where a presumed Neoproterozoic volcanosedimentary sequence, including dolomite and basalt, overlies possible correlates of the Rocky Cape Group. Sedimentary sequences on western King Island are more metamorphosed, probably older, and are intruded by Proterozoic granite dated at 760 Ma (Black, 1994).

No rocks of Middle Palaeozoic to Mesozoic age are known in the region, except for the Devonian granitoids of Three Hummock Island and eastern King Island. The extent of Devonian deformation in the region is uncertain, as it is difficult to distinguish its effects from the Middle Cambrian and possible Proterozoic orogenies.

Commencing in the late Mesozoic, at about the time of separation of Antarctica from Australia, rifting of the continental crust between Tasmania and Victoria resulted in downwarping and the commencement of sedimentation in Bass Basin, which now consists of a sedimentary pile more than 12 km thick at its depocentre. Bass Basin is bounded by ridges with outcropping basement to the east, between Flinders Island and Wilsons Promontory (Bassian Rise), and to the west between northwest Tasmania, King Island,

and the Mornington Peninsula. During the Cainozoic, extensive basaltic volcanism occurred both in northwest Tasmania and Bass Basin. Repeated fluctuations in sea-level in the Quaternary (the last transgression commencing 17,000 years BP) caused the area to alternate between being land (the Bassian Plain), a lake, a marine embayment, and sea several times. Bass Strait today is mostly between 30 m and 90 m deep.

A shallow seismic survey (Jones and Holdgate, 1980) has shown areas of Proterozoic to Palaeozoic basement, with little or no Cainozoic sediment cover, surrounding the Fleurieu (Hunter) Group and King Island and extending as a broad ridge from Cape Grim to King Island. The ridge is overlapped by Miocene limestone to the south (King Island Sub-basin) and east (Bass Basin). For the most part the shelf lies at depths of 40 m to 60 m in this area. Jones and Davies (1983) described the superficial sediments of the shelf area under study.

Councillor Island

This small island is located (39°49.9'N, 144°09.6'E; 256 900 mE, 5 587 100 mN) about three kilometres east of Cowper Point on the central east coast of King Island and rises to height of 24 m above sea level. Together with its southern extension, Flying Squirrel Reef, to which it is connected by a cobbly tombolo emergent at low tide, the island is about 900 m long and up to 300 m wide, and elongate in a NE to NNE direction.

No previous information was available on the geology of Councillor Island. According to the compilation map of Jennings and Cox (1978) only Quaternary deposits and minor Tertiary limestone are exposed on immediately adjacent parts of King Island, and the nearest exposed bedrock is the Devonian Sea Elephant Granite which outcrops about seven kilometres to the northeast near the lower Sea Elephant River. Relatively unmetamorphosed but cleaved argillaceous siltstone and mudstone of inferred Precambrian age are exposed in the vicinity of Naracoopa, ten kilometres to the south of Councillor Island. This sequence, which has similarities to parts of the Rocky Cape Group of northwest Tasmania, probably underlies most of eastern King Island, but is concealed beneath Quaternary deposits north of Naracoopa. It is overlain, with apparent unconformity, to the east by an east-facing volcanosedimentary sequence of dolomite, mixtite, siltstone, sandstone and major units of tholeiitic and picritic basalt (Waldron and Brown, 1993). This latter sequence is exposed as a north-trending strip along much of the coast between Naracoopa and Grassy, where it is intruded by Devonian granodiorite and forms the host rocks of the King Island scheelite deposit, a skarn. The volcanosedimentary sequence has some similarities, particularly in its lower part, to the Neoproterozoic Togari Group of the Smithton district, but a direct correlation was not substantiated by Waldron and Brown (1993).

Geological sketch map of Councillor Island

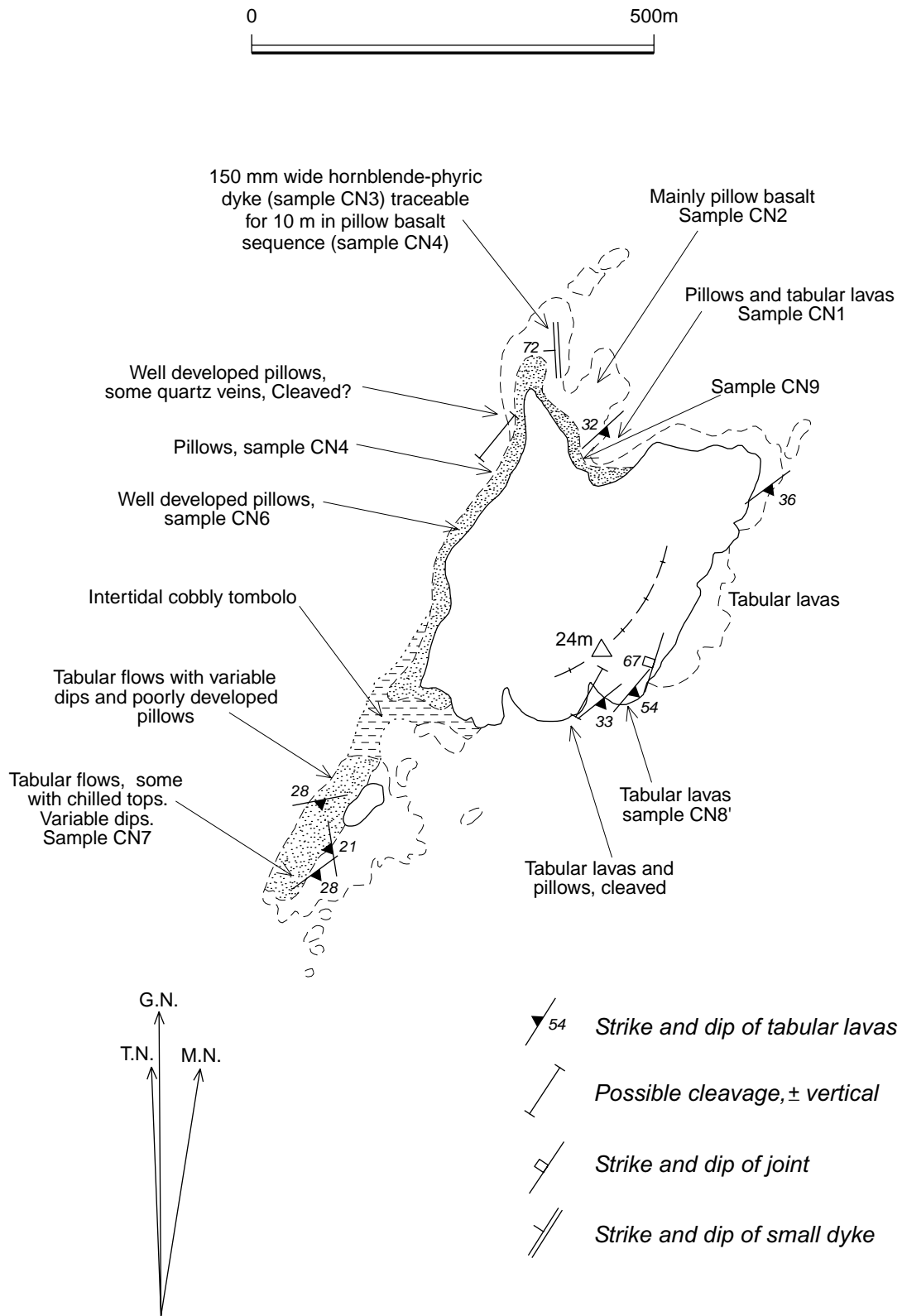


Figure 5

Geological sketch map of Councillor Island, drawn from field observations and aerial photographs (King Island Run 10: T485-217, 218; 1967).

The new AGSO aeromagnetic data (fig. 3) shows a magnetically low and mostly quiet area to the west of Councillor Island, although there is a weak to moderate anomaly on the King Island coast just south of Cowper Point and some short wavelength weak anomalies in the immediate vicinity of Councillor Island. Immediately to the east is a strong, broad, linear positive anomaly which trends SSW and extends onshore near Bold Head, where basaltic components of the Neoproterozoic(?) volcanosedimentary sequence are exposed. Further north along the coast of King Island this sequence, including the intercalated basalts, has a much weaker magnetic response, and the main anomaly lies just offshore.

A shore traverse around Councillor Island and Flying Squirrel Reef (fig. 5) showed that both consist of basalt, occurring as well-developed to poorly-developed pillows (typically 0.4 m across), tabular lava flows several metres thick and apparently massive bodies. Exposure is good along the shore and adjacent rock platforms, but there is little outcrop in the interior of the island, which is vegetated with long grass and coastal shrubs.

The best examples of pillows occur on the western shore of Councillor Island where they are tightly packed, rounded, 0.3–0.6 m across and have little or no inter-pillow hyaloclastite or sedimentary material (plate 1). Pillows are less well developed and intercalated with tabular flows on the northern shore and on Flying Squirrel Reef. The steep eastern shoreline of Councillor Island, cut by several sea-eroded clefts, offers nearly complete exposures of dominantly thick tabular basalt with subordinate pillows.

In the field the basalt is fine-grained and apparently aphyric, with shiny black weathered surfaces and a medium to dark grey to blue-grey interior. Ropy surfaces were noted locally, for example on the central northern shore platform. Possible original vesicles were noted in tabular flows with chilled tops near the southern extremity of Flying Squirrel Reef, but the basalt is usually mesoscopically massive. Quartz veins are present in pillow basalt about 100 metres south of the northwestern headland.

Dips measured on the top surfaces of tabular flows on the northern and eastern shores are consistently moderate (21° to 44°) to the south southeast (strike 047° to 078°), except at the southern end of Flying Squirrel Reef where they are more variable and fairly shallow. A well developed flattening compaction fabric, observed in pillows 50 metres south of the northeast headland of the island, is subparallel at 053E36 (strike/dip). These features are thought to be primary and indicative of horizontality at the time of extrusion (i.e. equivalent to bedding). Poorly developed subvertical cleavage was measured in pillows in the west (strike 043°) and tabular lavas in the east (strike 030°).

These bedding-cleavage relationships suggest that the sequence dips and youngs to the southeast.

A narrow (150 mm), straight, steeply-dipping (175W72) dyke is traceable for about ten metres within the pillow sequence on the northern shore platform, a few tens of metres from the northwestern headland of Councillor Island (plate 2). Dark green-grey prismatic to splintery phenocrysts of hornblende are discernible against a paler grey groundmass. The dyke is fairly constant in width and possibly terminates against small faults at each end.

The magnetic susceptibility of the basalt is quite variable, even on an outcrop scale. Although the mean value of 59 field measurements on the island is 2.86 ($\times 10^{-3}$ SI), the range is 0.38 to 18.4. A series of twenty measurements from pillows at one locality on the northern shore platform has a distinct bimodal distribution, with six samples lying between 0.45 and 0.71, and fourteen between 1.86 and 18.4 (mean 7.28). Most readings from the western shore are low (29 readings between 0.38 and 0.84, but others of 1.34 and 3.61 were recorded). Tabular lavas from Flying Squirrel Reef (average 6.06) and the eastern shore of Councillor Island (average 2.77) are relatively high. As there is little or no visible difference in the mesoscopic appearance of the rocks, the variability in susceptibility is probably due to varying amounts of fine-grained secondary magnetite produced by metamorphism and/or alteration (see below). There is some suggestion that the higher susceptibility basalt is more abundant on the east of the island, possibly correlating with the increased ratio of tabular lavas to pillow lavas, and consistent with the aeromagnetic survey showing the main anomaly lying east of the island.

The narrow hornblende-phyric dyke is essentially non-magnetic ($X = 0.24 \times 10^{-3}$ SI), as are its host rocks (0.50).

Petrography of metabasalt

All the basalts sampled were essentially similar in thin section (plate 3). They are metamorphosed, with few primary igneous minerals remaining and most of the igneous texture obliterated. All contain about 5–15% of chloritised pseudomorphs after olivine, with the euhedral to subhedral crystal form occasionally well preserved, in a matrix of mainly fibrous tremolite-actinolite. In some specimens there are also irregular patches of chlorite that lack crystal form; these may be amygdaloids. X-ray diffraction shows that some samples (CN6, 8, 9 and 10) contain relict clinopyroxene, but because of the fine grain size this is usually difficult to identify in thin section. Some relatively coarse-grained epidote occurs in a few specimens, mainly associated with chlorite in the olivine pseudomorphs.

Texturally the main differences between specimens are in the grain size of the splintery tremolite-actinolite matrix, which ranges from relatively fine grained (30 μm , e.g. CN6) through medium grained (50–150 μm , e.g. CN1, 2, 4, 8) and coarse grained (200 μm , e.g. CN7) to very coarse grained (500 μm , e.g. CN10). There is an apparent tendency for the matrix to be coarser grained



Plate 1

Pillows in picritic basalt, northwest shore, Councillor Island. The hammer is 350 mm long.

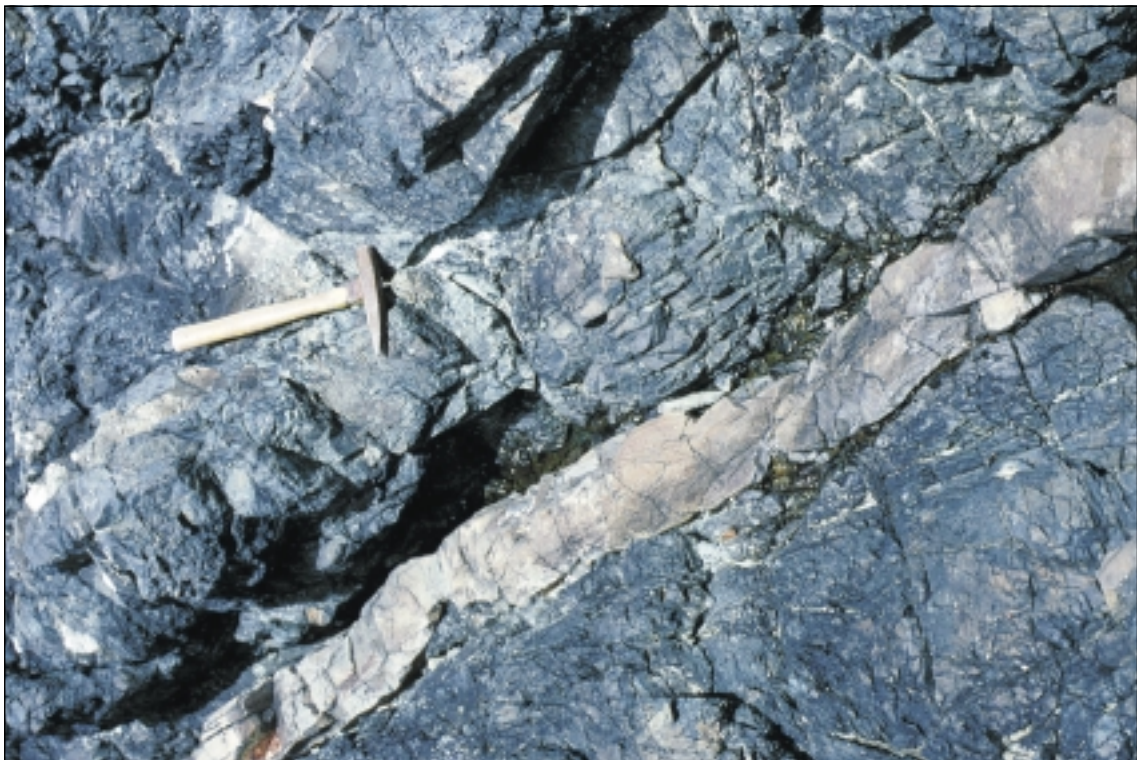


Plate 2

Hornblende porphyry dyke in picritic basalt, Councillor Island. View looking approximately vertically downward, southwest to left.

in the tabular lavas (e.g. CN7, CN10) than in the pillows, but this may not be significant as in some specimens several domains of differing grain size are present in a single thin section (e.g. CN5).

Typical specimens from the northern shore platform (CN1, 2, 4) contain about 5% scattered equant euhedral pseudomorphs up to 500 μm across after olivine in a matrix of tremolite-actinolite. The pseudomorphs, sometimes clumped into glomeroporphyritic aggregates, are now composed of colourless clear chlorite which is nearly isotropic to very low dark grey in birefringence. Under strong illumination a distinct fibrous fabric is recognisable, either throughout each pseudomorph or in randomly oriented small domains in each pseudomorph. The optical orientation is cleavage-fast and the chlorite is thus probably a Mg-Si rich variety such as penninite. The matrix consists almost entirely of splintery prisms of tremolite-actinolite mostly 50–150 μm long, both randomly oriented and locally radially aligned to form vaguely spherulitic to fanning pseudo-variolitic structures up to a few millimetres across. Some of the larger tremolite-actinolite splinters are weakly pleochroic (α , β colourless, γ pale green). A very tenuous dissemination of fine-grained (5 μm to dust-sized) opaques is present.

In a sample of a tabular flow from Flying Squirrel Reef (CN7) a foliation is defined by the alignment of the long axes of pseudomorphs of fine-grained chlorite after olivine, in a matrix of unoriented relatively coarse-grained (up to 200 μm) tremolite-actinolite. A few small (up to 200 μm) anhedral of pale yellow epidote occur within or at the margins of the pseudomorphs.

The samples with high magnetic susceptibility from the east and north of the island (CN8, 9, 10) differ mainly in containing a higher proportion of magnetite, although it is still not strikingly abundant in thin section. The magnetite tends to be concentrated as anhedral aggregates within and adjacent to the olivine pseudomorphs, but also occurs as inconspicuous disseminated dust and blebs (<20 μm in CN9) in the matrix. The magnetite is probably mainly of metamorphic origin, although recrystallised primary magnetite may also be present. These samples also contain relict clinopyroxene (identified by x-ray diffraction), which in the coarser grained areas can be optically distinguished from tremolite-actinolite by higher relief. The clinopyroxene is colourless and is probably augite, but it is fine grained, anhedral, probably recrystallised and possibly partly hydrated, making further optical identification impossible.

A few euhedral to subhedral grains of chromite up to 100 μm across, distinguished from magnetite by their form and deep red colour under strong illumination, were observed in one sample (CN5) from the northwest of the island, but not in any others. Minute red anisotropic crystals present in many samples may be secondary hematite.

Petrography of hornblende porphyry dyke

In thin section (sample CN3; plate 4) the narrow dyke contains elongate euhedral prisms of hornblende up to 2.5 mm long, with hexagonal cross sections up to 500 μm across. They grade in size downward to sparsely distributed, small (<20 μm) euhedra in the groundmass, which also contains rather sparsely distributed laths of plagioclase (mostly 40–80 μm \times 10–20 μm). Both hornblende and plagioclase tend to be aligned to form a 'fluidal' flow texture. The fine-grained, low birefringence fibrous mesostasis which forms most of the rock is optically unresolvable. The hornblende is pleochroic (α very pale straw yellow, β pale to medium brown, γ medium brown with a very slight greenish tint), optically positive, has maximum extinction angles ($\gamma:c$) of about 19° and displays (100) simple twinning. It is probably common hornblende. Small (up to 150 μm but generally <50 μm), generally cubic opaque euhedra of pyrite are scattered throughout the groundmass and also occur as inclusions within hornblende phenocrysts. Other accessory minerals include traces of apatite, turbid sphene and possibly epidote. Irregular patches up to 500 μm across of fine-grained secondary carbonate are present in parts of the groundmass, but adjacent hornblende is unaltered. X-ray diffraction showed that quartz, plagioclase, potash feldspar and mica are present in the groundmass.

Geochemistry

Five analyses of pillow basalts and two of tabular lavas (Table 1) confirm that all are depleted tholeiitic picrites, with up to 20.7% MgO, high Ni and Cr, and low alkalis. Incompatible elements, including both the large-ion lithophile elements (LILE) K, Rb, Ba, Sr and Th, and the high field strength elements (HFSE) P, Zr, Nb, Y and Ce are very low and many are below XRF detection limits.

The five analysed pillow basalts are very similar, but the tabular lavas (on the basis of two analyses) appear to show more variability. Both the tabular lavas have slightly lower SiO₂ and slightly higher Al₂O₃ and Na₂O than the pillows (also true if analyses are calculated to 100% anhydrous). The higher CaO and very high Cr of sample CN8 probably reflects the presence of clinopyroxene (noted petrographically) and possibly spinel. Anomalous Cu (140 ppm) in CN8 may indicate traces of copper sulphides, but none were noted petrographically; the higher Sr may be the result of seawater alteration. In contrast sample CN7 has low CaO and high MgO, possibly indicating particularly abundant olivine, although Ni is relatively low. The tabular lavas CN8 and CN7 may respectively contain cumulate clinopyroxene and cumulate olivine, but because of alteration it is not possible to confirm this petrographically. However lack of covariance between MgO or Mg# and other elements suggests that fractional crystallisation of olivine (or other phases) was not an important process in the evolution of these lavas (however, for the five pillow basalt analyses, Ni correlates *negatively* with Mg#).

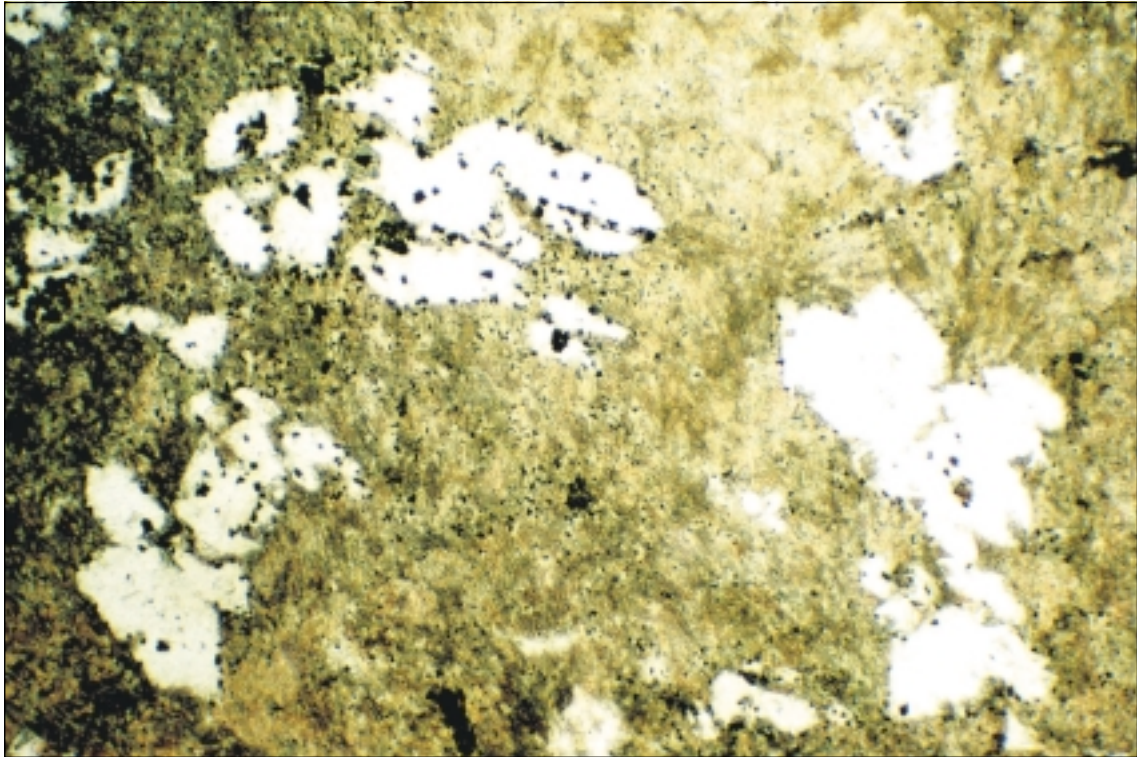


Plate 3

Sample CN9, metamorphosed picrite from pillow lava, Councillor Island. Olivine pseudomorphs (now chlorite) in a groundmass of mainly tremolite-actinolite.

Plane polarised light, field of view 4.4×2.9 mm.

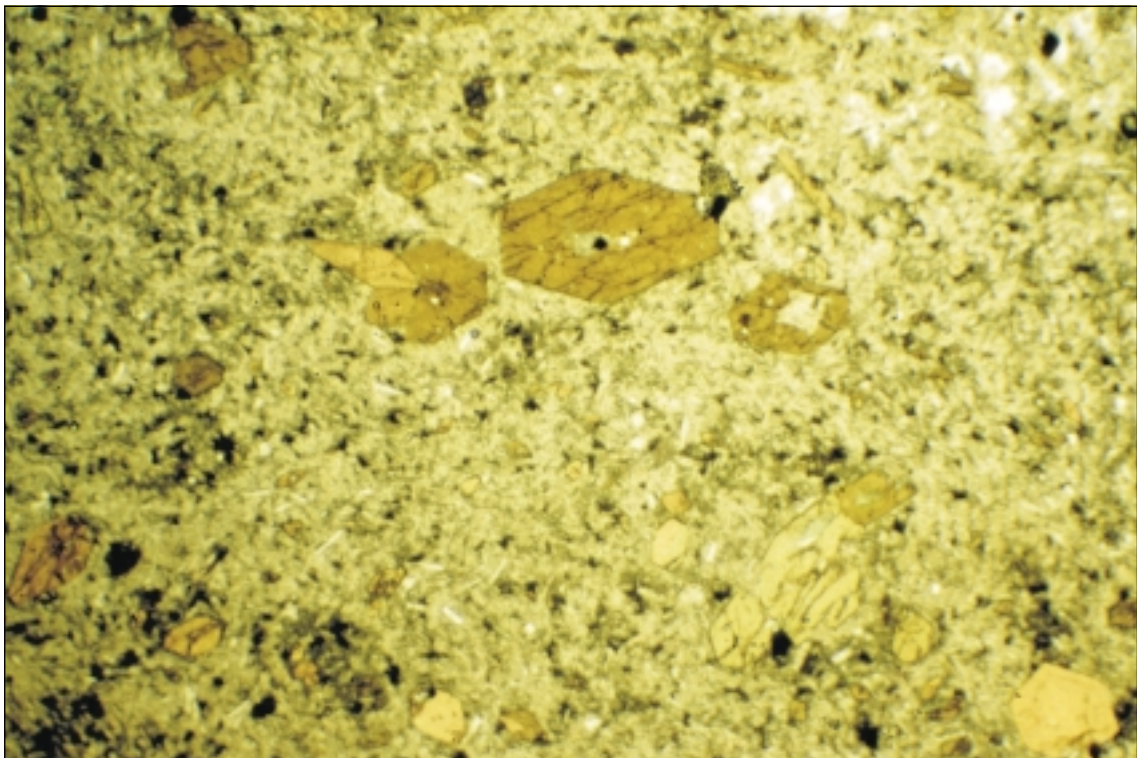


Plate 4

Sample CN3, hornblende porphyry dyke, Councillor Island. Euhedral phenocrysts of brown to yellow hornblende in a fine-grained quartzofeldspathic groundmass.

Plane polarised light, field of view 4.4×2.9 mm.

Table 1

Chemical analyses of picrites and hornblende porphyry dyke, Councillor Island

	Councillor Island								King Island Picrites	
	Dyke	pillows					tabular flows		flow	pillow
	CN3	CN2	CN4	CN5	CN6	CN9	CN7	CN8	R33032	R33033
SiO ₂	61.64	46.61	45.65	48.56	46.35	44.38	43.29	42.79	43.67	46.41
TiO ₂	0.70	0.25	0.26	0.24	0.21	0.25	0.26	0.29	0.33	0.21
Al ₂ O ₃	16.24	9.70	10.56	8.36	8.62	9.84	11.14	12.02	10.36	7.81
Fe ₂ O ₃	1.36	1.20	1.26	1.57	1.62	2.55	2.47	4.26	9.15 [#]	8.37 [#]
FeO	4.09	7.71	8.26	6.81	6.97	7.02	6.73	6.46	nd	nd
MnO	0.10	0.16	0.15	0.17	0.15	0.17	0.17	0.20	0.17	0.15
MgO	2.61	18.72	17.87	18.68	19.69	19.03	20.71	13.02	20.22	21.21
CaO	4.96	10.41	10.34	11.47	11.14	11.15	8.64	14.97	10.77	9.64
Na ₂ O	3.44	0.50	0.48	0.57	0.33	0.22	0.63	0.91	0.22	0.19
K ₂ O	2.39	0.10	0.11	0.22	0.08	0.06	0.09	0.23	0.01	0.01
P ₂ O ₅	0.35	0.09	0.10	0.10	0.11	0.12	0.09	0.14	0.02	0.02
H ₂ O ⁺	1.59	4.20	4.27	3.41	4.39	4.79	5.67	2.73}		
CO ₂	0.06	0.13	0.17	0.10	0.11	0.07	0.10	0.38}	4.66 [‡]	4.61 [‡]
SO ₃	0.08	0.08	0.09	0.08	0.08	0.09	0.08	0.23}		
Total	99.61	99.86	99.57	100.33	99.85	99.73	100.07	98.64	99.58	98.54
Sc	11	43	42	39	35	37	41	44	38	28
V	84	195	200	190	180	210	210	280	nd	nd
Cr	39	2850	2950	2300	2250	2900	1800	10800	1627	2347
Co	14	82	89	71	64	81	63	63	76	77
Ni	42	1080	1200	980	920	1150	470	425	738	1213
Cu	74	43	22	12	7	25	<5	140	11	33
Zn	73	53	57	47	54	55	61	94	49	42
Ga	17	8	7	6	6	7	8	9	nd	nd
As	<20	<20	<20	<20	<20	<20	<20	<20	nd	nd
Rb	170	<10	<10	16	<10	<10	<10	<10	2	<1
Sr	410	15	25	23	14	22	13	100	4	4
Y	24	12	12	11	11	13	14	14	12	7
Zr	290	23	23	22	22	21	23	20	15	10
Nb	30	*36.9	3	<3	<3	3	*12.7	4	<3	nd
Mo	<5	<5	<5	<5	<5	<5	<5	<5	nd	nd
Sn	<9	<9	<9	<9	<9	<9	<9	<9	nd	nd
Ba	648	<23	<23	25	<23	<23	<23	<23	17	14
La	65	*53.1	<20	<20	<20	<20	*0.70	<20	0.18	0.26
Ce	118	*96.1	<28	<28	11	<28	*0.91	<28	0.22	0.62
Nd	51	*37.1	<20	<20	<20	<20	*1.00	<20	0.7	0.69
Hf		*13.9	nd	nd	nd	nd	*0.9	nd	nd	nd
Ta		*3.3	nd	nd	nd	nd	*2.8	nd	nd	nd
W	<10	<10	<10	<10	<10	<10	<10	<10	nd	nd
Pb	15	<10	<10	<10	<10	<10	<10	<10	nd	nd
Bi	<5	<5	<5	<5	<5	<5	<5	<5	nd	nd
Th	16	*13.2	10	<10	10	<10	10	*0.31	11	10
U	<10	<10	<10	<10	<10	<10	<10	<10	nd	nd

* denotes ICPMS data # total iron as Fe₂O₃ ‡ denotes loss on ignition nd: not determined

R33032 and R33033 from Waldron and Brown (1993)

The two analysed samples with higher magnetic susceptibility, CN8 and CN9, also have higher Fe₂O₃/FeO, consistent with greater abundance of magnetite.

One picrite sample (CN9) was analysed for REE by the ICPMS method (Table 2). The chondrite-normalised pattern is characterised by low overall REE levels and extreme depletion in LREE. The terbium (Tb) peak is probably spurious and may be attributable to dissolution difficulties or analytical error, as many unrelated rocks submitted in the same batch show a similar feature.

The radically different chemistry of the hornblende porphyry dyke rock indicates that it is unrelated to the picrites. The major element chemistry is close to the average tonalite of Le Maitre (1976), and the CIPW-norm based pseudomode straddles the tonalite-granodiorite boundary when plotted on the Q-A-F granite classification diagram (fig. 10) of Streckeisen (1973). The fairly high K₂O/Na₂O and molar Al₂O₃/(CaO+Na₂O+K₂O) of 1.273 may indicate S-type affinities if granitoid petrogenetic concepts are applicable. The chondrite-normalised rare-earth element (REE) plot (Table 2, fig. 7) is strongly light REE enriched ((La/Yb)_N = 17.0), unlike picrite CN9. The absence of any europium anomaly suggests plagioclase fractionation has not occurred.

Discussion

The common pillow forms of the basalt indicate subaqueous eruption, but tabular flows are also

common and there is little associated hyaloclastite. These morphologies may be indicative of a variable effusion rate affecting the nature of the interaction with seawater, specifically explosivity and rapidity of quenching.

The tabular lavas may have been produced by rapid extrusion, producing thick volumes of lava that were able to flow some distance down topographic irregularities in the sea floor before solidifying. The pillows may represent either lower rates of intrusion, or more distal equivalents of the tabular lavas. In either case, the smaller volumes of lava were chilled more rapidly by seawater to form solid outer carapaces, which were periodically disrupted allowing the liquid interior to ooze out and budding off new pillows, some of which may have become completely detached. The lack of glassy pyroclastic material and low vesicularity of the lavas may indicate relatively deep water and non-explosive extrusion. The lack of any intercalated sedimentary material suggests that the rate of sedimentation was insignificant relative to that of volcanism.

The mineralogical dominance of tremolite-actinolite and chlorite, the abundance of olivine pseudomorphs and the lack of plagioclase is consistent with the highly magnesian, picritic composition.

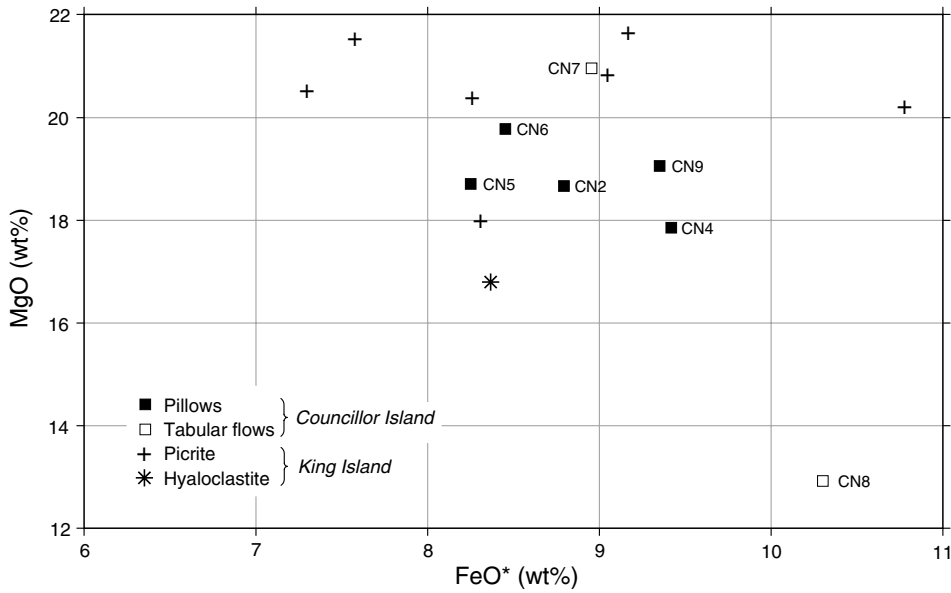
Broadly similar pillowed and tabular basalts are a major component of the volcanosedimentary succession on the southeast coast of King Island (Scott, 1951; Solomon, 1969; Waldron and Brown, 1993).

Table 2

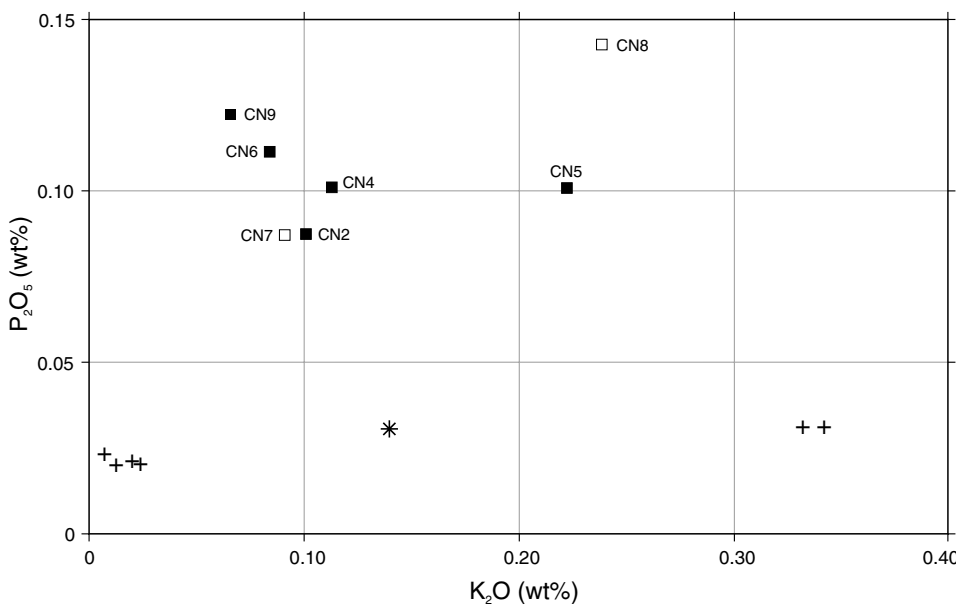
ICPMS analyses, Councillor Island samples

Rock type	<i>hornblende porphyry (CN9)</i>		<i>picritic pillow basalt (CN3)</i>		
	<i>ppm</i>	<i>ppm/ chondrite</i>	<i>ppm</i>	<i>ppm/ chondrite</i>	<i>average chondrite*</i>
La (ppm)	53.1	171.3	0.7	2.26	0.310
Ce	96.1	118.9	0.91	1.13	0.808
Pr	11.5	94.3	0.23	1.89	0.122
Nd	37.1	61.8	1.0	1.67	0.600
Sm	5.9	30.3	0.5	2.56	0.195
Eu	1.54	21.0	0.18	2.45	0.0735
Gd	3.5	13.5	1.6	6.18	0.259
Tb	nd	nd	0.69	14.56	0.0474
Dy	3.8	11.8	2.1	6.52	0.322
Ho	0.78	10.9	0.51	7.10	0.0718
Er	1.6	7.6	2.1	10.00	0.210
Tm	0.32	9.9	0.26	8.02	0.0324
Yb	2.1	10.0	1.4	6.70	0.209
Lu	0.3	9.3	0.2	6.21	0.0322
Nb	36.9		12.7		
Ta	3.3		2.8		
Hf	13.9		0.9		
Th	13.2		0.31		

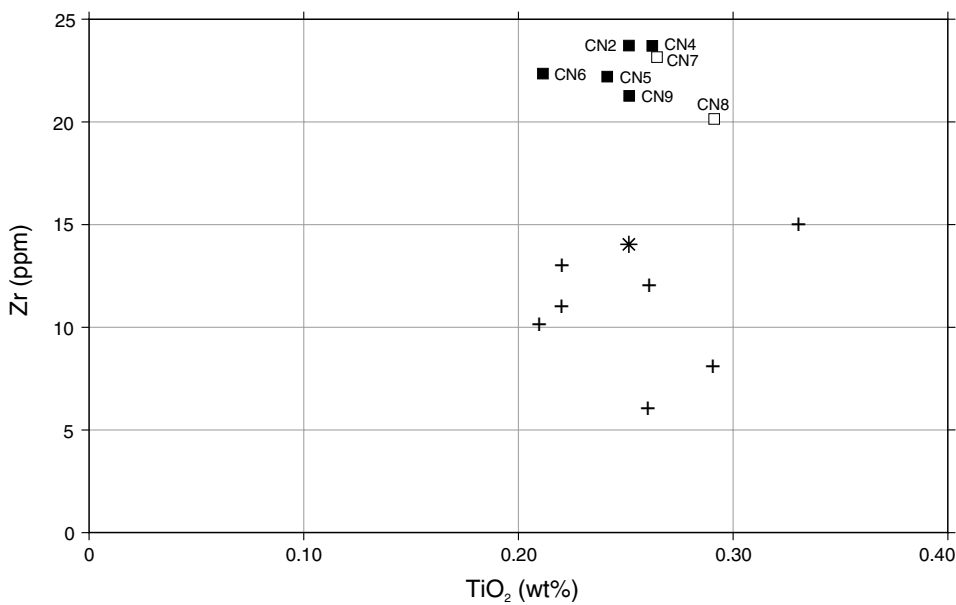
* (Boynton, 1984)



(a) plot of MgO against total iron (FeO*)



(b) plot of P₂O₅ against K₂O



(c) plot of Zr against TiO₂

Figure 6

Geochemical comparison of picrites of Councillor Island and King Island (data for latter from Waldron and Brown, 1993).

A Neoproterozoic age has been inferred for the King Island succession, partly by analogy with the Togari Group of the Smithton area. In detail, however, the Councillor Island rocks differ in the lack of associated sedimentary units and the paucity of hyaloclastite, and may represent a deeper water environment.

The structural evidence from the Councillor Island metabasalts, suggesting a southeastward younging sequence, and the adjacent linear magnetic anomaly support the view that these rocks represent a northward extension of the King Island succession.

Waldron and Brown (1993) suggested a tripartite division of the basaltic component of the King Island succession into a Lower Tholeiite Sequence, overlain by a Picrite Sequence and finally an Upper Tholeiite Sequence. The Councillor Island rocks most resemble the Picrite Sequence, which is "usually porphyritic and consist(s) of pseudomorphs after olivine (0.1–3 mm) and small (0.05–0.2 mm) chromite euhedra in a quenched clinopyroxene groundmass [in which variolitic to spherulitic textures are reported].... All the phenocrysts are completely pseudomorphed by colourless chlorite (pycnochlorite). Other secondary minerals present include abundant epidote, minor clinzoisite and small fibrous crystals, possibly tremolite, with minor interstitial pyrite and chalcopyrite." Although the clinopyroxene in these rocks is described as 'remarkably fresh', it appears to be largely replaced by tremolite-actinolite in the more metamorphosed rocks on Councillor Island. The Lower and Upper Tholeiite Sequences, in contrast, are much

less magnesian, and plagioclase (including some fresh labradorite) is a major phase.

The picrites of Councillor Island also geochemically resemble those of King Island (Table 1; fig. 6a, b, c). However there are some subtle differences in detail. Most of the King Island picrites are more highly depleted in incompatible elements, notably Na_2O , K_2O , Sr and especially P_2O_5 and Zr. This is illustrated in plots of P_2O_5 against K_2O (fig. 6b) and of Zr against TiO_2 (fig. 6c). As Zr, Ti and P are relatively immobile during alteration and metamorphism, this is thought to be a primary feature.

The chondrite-normalised rare earth pattern of Councillor Island sample CN9 lies within or just above the envelope defined by the King Island picrites (Waldron and Brown, 1993) (fig. 7), and is quite different to the less depleted and flat to LREE-enriched pattern of both the lower and upper tholeiitic sequences on King Island. The slightly less LREE-depleted nature of King Island picritic hyaloclastite R33041 was attributed to seawater alteration by Waldron and Brown (1993). Such a process seems unlikely as an explanation for the higher abundances of Zr and P in the Councillor Island picrites.

All the picrites are essentially unfractionated, near-primitive magmas, probably produced by a high degree of partial melting of a mantle source that had been depleted in fertile components, possibly by an earlier episode of partial melting.

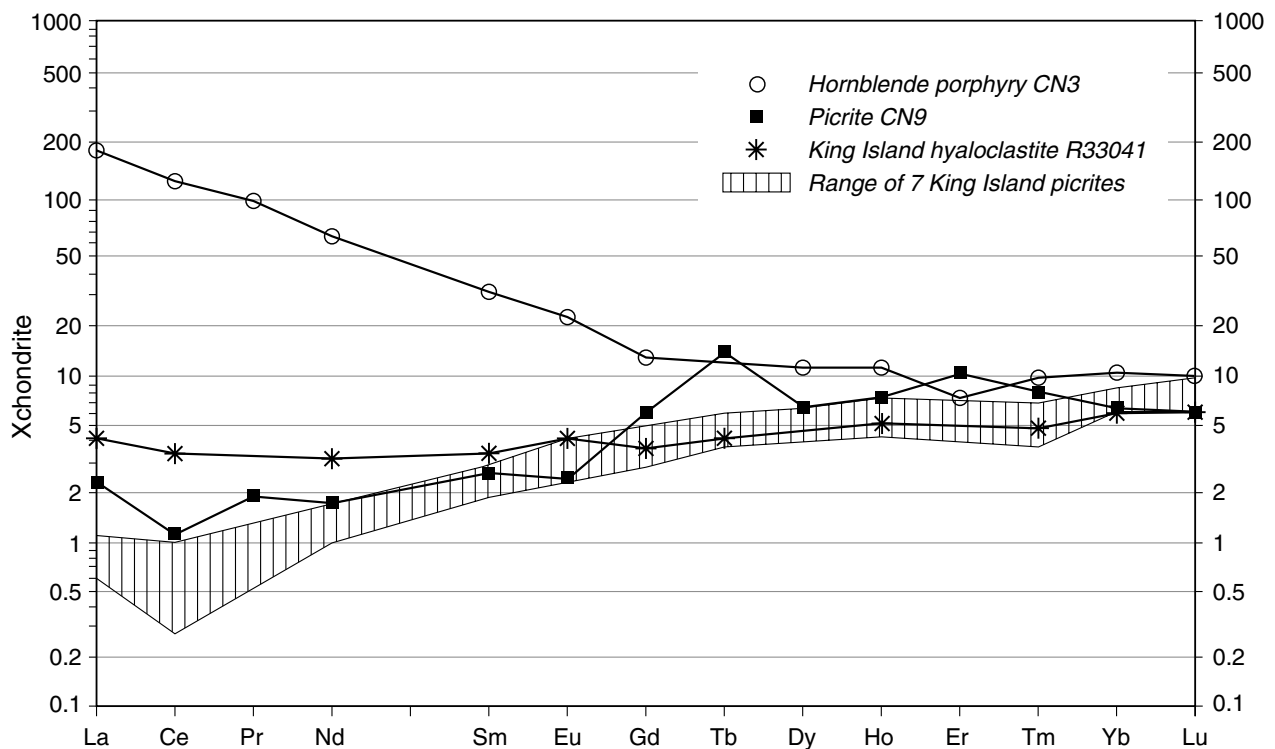


Figure 7

Chondrite-normalised rare-earth element plots for a Councillor Island picrite (CN9) and hornblende porphyry (CN3), compared with range displayed by King Island picrites (data for latter from Waldron and Brown, 1993).

Chondrite normalisation factors from Boynton (1984).

Possible correlates on the Tasmanian mainland include the uppermost lavas in the sequence at Double Cove (Macquarie Harbour) and plugs intruding the Crimson Creek Formation in the Dundas Trough (Crawford and Berry, 1992).

The age and affinities of the hornblende porphyry dyke are unknown, although its field relationships and relative freshness suggest that it is much younger than the host metabasalt. A post-orogenic Late Devonian age seems most probable. The presence of quartz precludes affinity with lamprophyres, and it may represent a minor phase of granite-related magmatism.

Brig Rocks

We sailed between these isolated outcrops, located 0.8–1.4 km off the southeast coast of King Island (around 246 800 mE, 5 556 300 mN) at dawn. No landing was attempted. Despite the poor light, the smaller, nearer shore North Brig Rock could clearly be seen to consist of granite (presumably the Grassy Granodiorite) forming a jagged, steep, tor-like islet rising to 15 m above sea level. The larger but lower (13 m) South Brig Rock, which is situated about 500 m to the south, is composed of a darker rock. Possible pillow structures seen through binoculars suggest that it may be composed of basalt, possibly representing an extension of the Neoproterozoic sequence on the eastern coast of King Island and Councillor Island.

Reid Rocks

This isolated group of rocky islets is located about 21.5 km ESE of Stokes Point on the southern extremity of King Island, and about 54 km from Cuvier Point on Hunter Island. The main islet (40°14.9'S, 144°09.3'E; 258 000 mE, 5 540 800 mN) is shown on marine charts as approximately 500 m long, elongated in a east-west direction and rising to 13 m above sea-level. A smaller group of islets (South Reid Rocks) is located about 3 km to the SSE.

No previous information was available on the geology, although examination of an aerial photograph obtained by the Parks and Wildlife Service suggested the presence of vertical columnar jointing, presumably in (mafic?) igneous rock, and showed the islet was transected by a number of north-trending slot-like gulches (G. Dixon, pers. comm.).

Reid Rocks is entirely devoid of vegetation, with nearly complete rock exposure. The most obvious feature is a well developed, undulating, subhorizontal layering or stratification, 0.3–0.5 m thick. This stratification is defined by fairly evenly spaced subhorizontal sheet joints and is cut by less conspicuous, well-spaced subvertical joints (plate 5).

A landing was made on the northern side of the island, although with some difficulty due to the large number (several thousand) of Australian fur seals, both on the rocks and in the sea. Because of their dense population

and aggressive behaviour it was not possible to move more than about ten metres from the landing site.

Well developed columnar jointing was observed in cliffs on the southeast side of Reid Rocks, but at the landing site it is relatively poorly developed, defining crudely polygonal to rounded columns 0.5–1.4 m across. Alteration zones 20–50 mm wide, composed of soft creamy-white to pale brown secondary minerals, have developed along both the vertical joints and the cross-cutting subhorizontal joints, to form a network throughout the rock (plate 6).

X-ray diffraction studies later identified the white material as a moderately crystalline apatite-type mineral, and the brown ('beige') material as a mixture of struvite ($\text{NH}_4\text{MgPO}_4 \cdot 6\text{H}_2\text{O}$) and monohydrocalcite ($\text{CaCO}_3 \cdot \text{H}_2\text{O}$) (R. N. Woolley, pers. comm.). It is likely that the source of the ammonium and phosphate is seal droppings and urine, which together with seawater have reacted with weathered basalt in the joints.

A gulch a few metres east of the landing site is 3–10 metres wide and trends at 150° (true). It further restricts access as the sea surges through it to the other side of the islet.

Mesoscopically the rock is a tough, massive, fairly coarse-grained weathered basalt, blue-grey in colour where relatively fresh. Weathered surfaces are grey-green with pseudobreccia texture, in which irregularly shaped pseudoclasts, 'poorly sorted' with sizes typically 5–50 mm across, have indistinct, diffuse rounded outlines. Small equant olivine phenocrysts and sparsely distributed angular vesicles and amygdales, up to 1 mm across, are visible in hand specimen.

The mean magnetic susceptibility of the basalt (22 field readings from outcrop) is 2.43×10^{-3} SI units (range 1.73–3.12). Because of weathering this should be considered a minimum value for fresh rock.

Petrography

Thin sections (samples RR1, RR4) show that the rock is an altered, coarse-grained alkali olivine basalt. No real distinction can be made between phenocrysts and groundmass. The rock consists mainly of titanite, completely altered olivine, plagioclase and opaque iron-titanium oxide. A poorly developed subophitic texture is evident in RR1 (plate 7), and grades to an intergranular texture in RR4.

Polygonal equant euhedra of former olivine, 0.5–1.0 mm across, are completely replaced by fine-grained dark brown to greenish brown alteration products. Similar but paler material in smaller, irregular to angular patches is probably after smaller grains of 'groundmass' olivine. Irregularly polygonal equant platelets of pale pink to nearly colourless titanite, 200 μm to 1 mm across, may partly enclose disoriented oblong laths of plagioclase, 400 μm to 1 mm long and 50–100 μm wide. The plagioclase is often zoned but is probably mainly labradorite. Opaque



Plate 5

Vertical columnar jointing, with closely spaced horizontal cross-joints, in Tertiary basalt, Reid Rocks.



Plate 6

Jointing and associated inter-columnar alteration, Tertiary basalt, Reid Rocks. The outcrop surface is subhorizontal and the lens cap is 50 mm diameter.

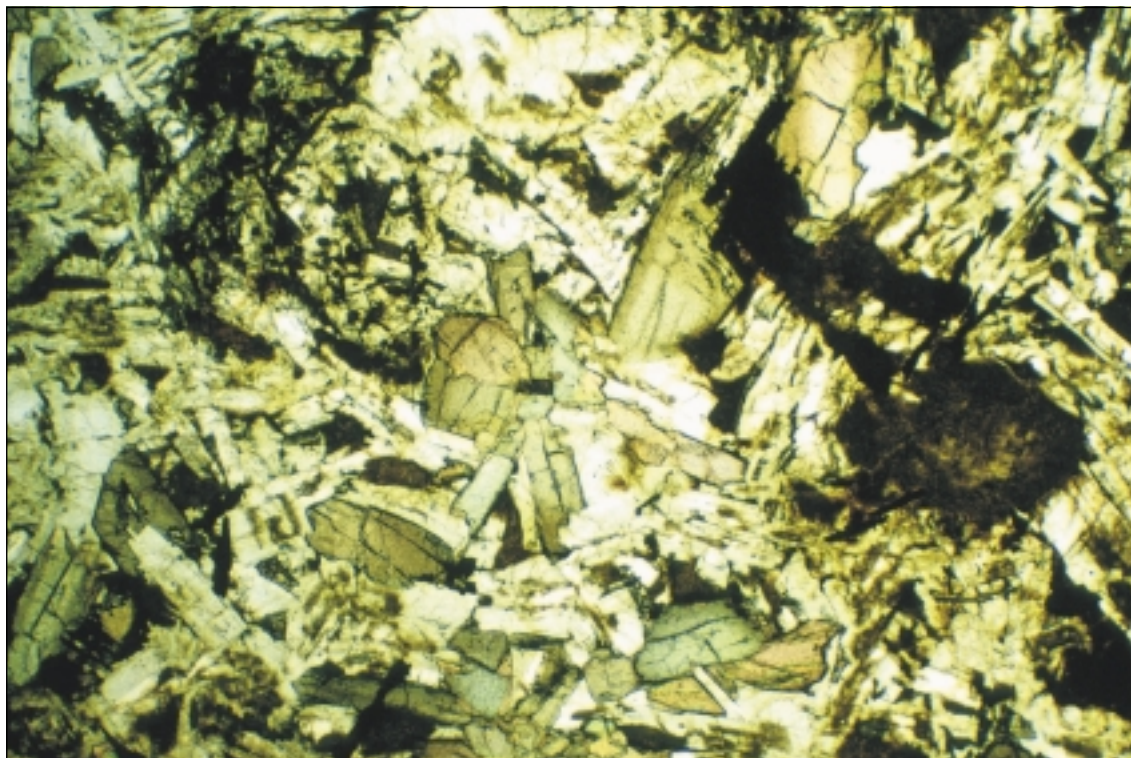


Plate 7

Sample RR1, Tertiary basalt (transitional olivine basalt with alkalic affinities), Reid Rocks. Altered olivine (brown), titanite (pale pink), plagioclase (white) and opaque minerals, subophitic texture.
Plane polarised light, field of view 4.4×2.9 mm.

minerals occur as jagged, angular, commonly elongate to acicular grains up to $500 \mu\text{m}$ long, but commonly $100\text{--}300 \mu\text{m}$, or as clusters of jagged angular aggregates. The opaque phases may be partly enclosed by titanite and olivine, and therefore began to form fairly early in the crystallisation process. Acicular apatite, up to several hundred micrometres long and about $5 \mu\text{m}$ wide, is a common accessory mineral.

Irregularly shaped vesicles up to 3 mm long are abundant in sample RR4 (about 15% void).

Geochemistry

The major element analysis (Table 3; RR4) shows slightly higher SiO_2 , Al_2O_3 and K_2O than might be expected from the petrography. The high Fe_2O_3 relative to FeO is due to the oxidation and alteration of particularly olivine, as seen in thin section. The CIPW norm (Table 4, calculated at $\text{Fe}_2\text{O}_3/\text{FeO} = 0.20$) indicates that the rock is a transitional olivine basalt ($0 < \text{hy} < 10$) in the classification scheme of Johnson and Duggan (1989), although its affinities are undoubtedly more alkalic than tholeiitic. The fairly low MgO and Mg\# (i.e. $\text{Mg}/(\text{Mg} + \text{Fe})$, also calculated at $\text{Fe}_2\text{O}_3/\text{FeO} = 0.20$) indicate that the rock is relatively evolved, probably mainly by low pressure fractionation of olivine. K_2O is relatively high for a saturated basalt; this may be a source inherited characteristic.

These conclusions are reinforced by the trace element data. The Nb/Y ratio, slightly greater than unity, is consistent with mildly alkalic affinities. Ni is far below

the levels (300–500 ppm) considered typical of primary magmas and is consistent with appreciable olivine fractionation.

The major and trace element levels are generally comparable to the range displayed by similar northwest Tasmanian Tertiary basalts (e.g. Everard, 1989 and unpublished data; fig. 9), except perhaps for Co which is unusually low.

Discussion

Although no direct evidence was found on Reid Rocks, consideration in a regional context leaves little doubt that the basalt is of Tertiary age. The samples collected are probably too altered for radiometric dating.

The presence of titanite, late-stage 'groundmass' olivine and relatively abundant apatite is diagnostic of alkali olivine basalt. Therefore Reid Rocks represents a different phase of volcanism, possibly of differing age to the tholeiites of Black Pyramid (see below) or the Cape Grim area. The nearest similar rocks in northwest Tasmania are at Mt Cameron West (Sutherland and Corbett, 1967; Seymour and Baillie, 1992; J. L. Everard, unpublished analyses) where two K/Ar dates of 14.5 and 15.5 Ma have been obtained (Seymour and Baillie, 1992; A. V. Brown, unpublished data). The present data do not justify a direct connection.

Little evidence for depositional environment was seen. The apparent lack of pillows, hyaloclastites or

Table 3
Chemical analyses of Tertiary basalt samples

	<i>Reid Rocks</i>	<i>Black Pyramid</i>			<i>Robbins Island</i>		
	<i>RR4</i>	<i>unit 1 BP1</i>	<i>unit 1 BP7</i>	<i>unit 3 BP5</i>	<i>Marys Is RI1</i>	<i>Guyot Point RI3</i>	<i>Guyot Point RI4</i>
SiO ₂ (wt%)	50.42	50.42	50.04	50.52	47.02	47.76	47.15
TiO ₂	2.00	1.79	1.77	1.60	2.31	2.27	2.31
Al ₂ O ₃	16.01	14.22	14.44	14.82	14.36	14.33	14.24
Fe ₂ O ₃	4.85	2.76	3.16	3.24	2.73	1.58	1.99
FeO	4.89	7.92	7.09	8.13	7.99	9.17	8.83
MnO	0.14	0.16	0.14	0.18	0.15	0.15	0.16
MgO	5.33	8.66	8.42	7.53	7.96	7.89	8.25
CaO	8.63	8.54	8.54	8.89	6.66	7.33	7.25
Na ₂ O	3.85	2.97	3.11	2.88	4.29	3.68	3.78
K ₂ O	1.48	0.90	0.86	0.56	2.16	2.21	2.26
P ₂ O ₅	0.37	0.31	0.32	0.24	0.69	0.75	0.72
H ₂ O ⁺	1.93	1.37	1.56	1.29	2.84	2.48	2.16
CO ₂	0.08	0.08	0.15	0.15	0.18	0.14	0.11
SO ₃	0.10	0.13	0.11	0.15	0.10	0.12	0.13
TOTAL	100.09	100.24	99.71	100.18	99.42	99.97	99.33
Mg#	66.02	66.09	67.92	62.28	63.98	60.53	62.48
Mg#(0.20)*	53.82	62.74	63.17	57.97	60.65	60.11	61.11
Sc (ppm)	18	24	24	27	13	14	13
V	195	190	190	185	160	165	180
Cr	155	335	330	245	190	145	165
Co	26	40	47	51	44	40	39
Ni	67	120	135	200	155	140	150
Cu	41	19	16	45	33	27	26
Zn	105	92	96	110	97	105	105
Ga	24	21	20	20	24	24	25
As	27	<20	<20	<20	<8	<8	<8
Rb	33	18	13	10	21	40	43
Sr	410	370	380	290	380	940	930
Y	24	23	24	23	24	23	23
Zr	165	140	145	105	260	275	270
Nb	26	22	23	12	47	51	51
Mo	<5	<5	<5	<5	<5	<5	<5
Sn	<9	<9	<9	<9	<9	<9	<9
Ba	184	159	158	56	246	254	255
La	<20	<20	<20	<20	25	24	35
Ce	39	42	44	35	92	93	94
Nd	27	25	34	17	42	50	42
W	<10	<10	<10	<10	<10	<10	<10
Pb	13	<10	<10	<10	<10	10	<10
Bi	<5	<5	<5	<5	<5	<5	<5
Th	13	10	13	10	13	16	14
U	<10	<10	<10	<10	<10	<10	<10

* molar 100Mg/(Mg + Fe₂) calculated as analysed, and at Fe₂O₃/FeO = 0.20

Table 4
CIPW Norms of Tertiary basalt samples

	Reid Rocks	Black Pyramid			Robbins Island		
	RR4	unit 1 BP1	unit 1 BP7	unit 3 BP5	Marys Is RI1	Guyot Point RI3	Guyot Point RI4
or	8.95	5.39	5.19	3.35	13.26	13.42	13.77
ab	33.36	25.49	26.91	24.74	25.47	26.40	23.92
an	22.57	23.15	23.44	26.27	14.08	16.51	15.70
ne	-	-	-	-	6.63	3.04	4.91
di	15.41	14.44	14.41	13.85	12.64	12.87	13.44
hy	2.40	18.42	15.94	24.14	-	-	-
ol	10.18	6.31	7.38	1.21	19.00	18.64	19.28
mt	2.32	2.59	2.49	2.75	2.66	2.67	2.69
il	3.88	3.44	3.43	3.08	4.55	4.62	4.52
ap	0.86	0.71	0.74	0.55	1.63	1.75	1.69
TOTAL	99.93	99.94	99.93	99.94	99.92	99.92	99.92
mol% An	38.94	46.12	45.08	50.02	34.25	37.08	38.22

calculated at Fe₂O₃/FeO = 0.20

intercalated sediments suggests that the basalt may well have been extruded subaerially.

Reid Rocks lies near the northwestern end of a zone of short wavelength positive magnetic anomalies about 25 km north-south by 10 km east-west (fig. 3). This may delineate the extent of Tertiary basalt of similar age.

Black Pyramid

Black Pyramid is a steep-sided island located on the basement ridge about halfway between King Island and the Tasmanian mainland (40°28.7'S, 144°20.7'E; 275 000 mE, 5 516 000 mN). Sutherland and Corbett

(1967, p. 88) and Sutherland (1980, p. 84) briefly discussed the island's geology as inferred from photographs and a single thin section of a sample collected during a visit by a zoologist (R. H. Green). As noted by these authors, Black Pyramid consists of Tertiary basaltic volcanic rocks in which a clear three-fold horizontal layering is visible.

The island is about 750 m long, elongate in a WNW-ESE direction with a marked median ridge which rises to a more-or-less flat summit 73 m above sea level near the western end (plates 8, 9; fig. 8). On the southern side and western end, sheer cliffs about 30 m high rising directly from the sea define the lowermost unit. A

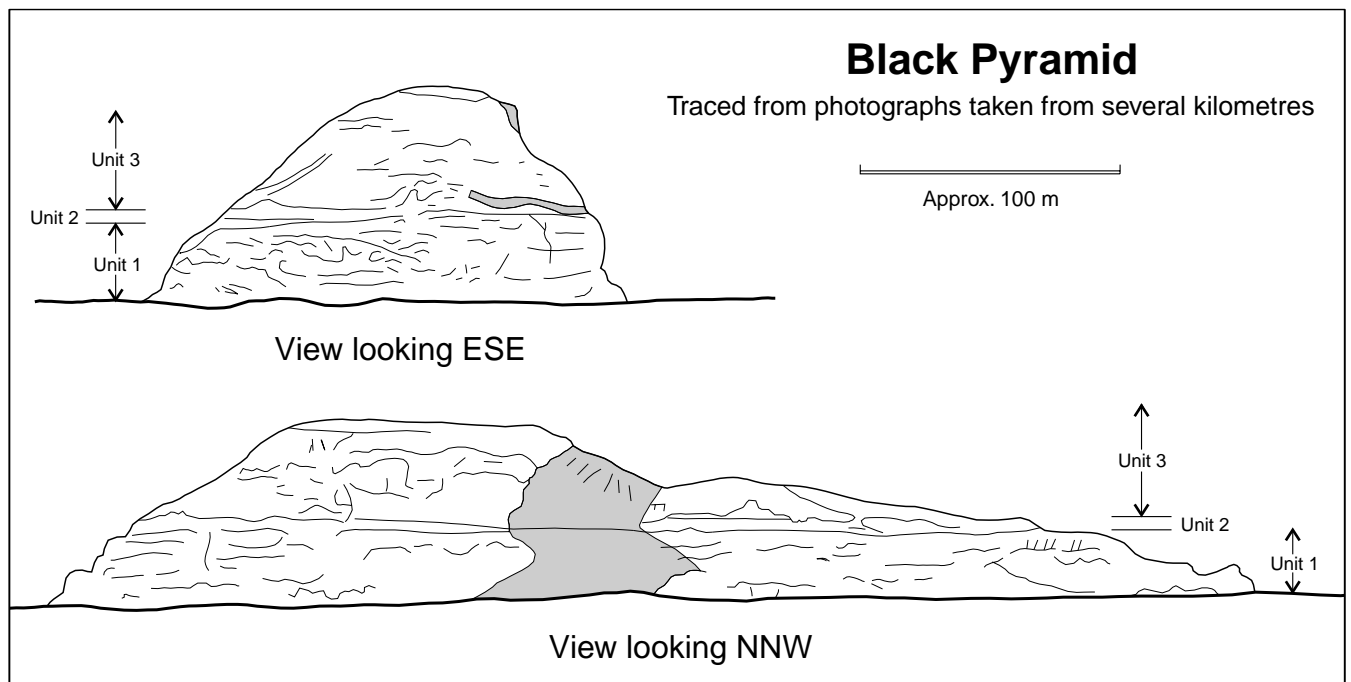


Figure 8



Plate 8

Black Pyramid, viewed from the east.



Plate 9

*Black Pyramid, viewed from the northwest.
The three-fold layering with a middle sedimentary unit is clearly visible.*

discontinuous ledge, best developed on the southern side near the eastern end, lies above the cliffs and marks a distinctive horizontally-bedded unit. Above the ledge the ground again rises very steeply to the median ridge, and smaller cliffs are developed south and east of the summit. Only low discontinuous cliffs occur at sea level on the northern side of the island, above which there is little outcrop on ground rising very steeply (at 40 to 45°) to the median ridge and summit, with only a slight indentation marking the bedded unit.

We landed on the northern side near the eastern end, where a small shore platform a few metres wide is developed, and traversed the median ridge through the middle-bedded unit to about the base of the overlying upper unit. To avoid disturbing the large gannet colony on the ridge and northern flank of the island, we then followed the bedded unit around the south flank of the island until blocked by cliffs.

Close inspection shows that the three units are:

Unit 1

A lower unit, extending from at least sea level to about 30 masl, of basaltic lava flows and subordinate volcanoclastic rocks. A crude horizontal stratification, suggestive of a series of thin overlapping and/or interdigitating flows, can be observed in many places in the cliffs encircling the island. A near-vertical cross section through a discrete tongue-like flow is exposed in the cliff a few metres above sea level about halfway along the northern side of the island (plate 10). The flow is about 25 m wide at its base and at least 10 m thick, although its top is not well exposed. It displays well-developed, generally vertical, columnar jointing. More closely spaced inclined jointing occurs locally, adjacent and perpendicular to its lateral margins and presumed cooling front. This flow is underlain and laterally adjoins a volcanoclastic, possibly hyaloclastite deposit consisting of large (0.3–1 m), angular black basalt fragments in a pale orange-brown matrix, which in turn rests on another basalt flow containing possible pillows, extending to sea level. The tongue-like flow probably burrowed through, and was chilled against, slightly older unconsolidated, possibly cold wet pyroclastic debris. Similar, probably partially burrowing tongue-like flows are preserved a few metres to the west on the same northern side, and also display columnar jointing perpendicular to their bottom, side and top margins.

At the landing site the basalt displays polyhedral to irregular 'knobby' jointing with a joint spacing of 200 to 400 mm. The basalt is massive to locally very vesicular, fairly fresh-looking with a medium-grey interior and is mesoscopically aphyric.

Above the eastern end of the shore platform, well developed columnar jointing is exposed in a 15 m cliff (plate 11). The columns are 200–400 mm wide and are closely segmented by horizontal transverse joints near their base, and both pass laterally and rest on irregularly jointed non-columnar 'knobby' basalt,

which in turn is underlain by poorly jointed vesicular glassy basalt at sea level. This sequence probably represents the basal part of a flow, the gradation in morphology being caused by cooling rate.

Very vesicular basalt near the base of cliffs at the extreme eastern tip of the island contains amygdalites 1–4 mm across filled with calcite, and is criss-crossed along fractures with narrow anastomosing Neptunian dykes of fine-grained pinkish-cream limestone (plate 12).

Very well developed polygonally jointed basalt is exposed at the top of a small knoll about 15 masl near the eastern end of the island. The columns are about 0.5 m across and vertically oriented at the top of the knoll, but towards the base on either side are inclined and diverge away (plate 13). Similar features elsewhere have been termed *colonnade-and-entablature*, but normally the inclined columns (the entablature), which are attributed to an irregular cooling front, occur at the top of the flow (e.g. Cas, 1989).

A number of irregular bodies of limestone surrounded by vesicular basalt are exposed near the top of this unit on the eastern ridge. The limestone bodies tend to be tabular, up to 3 m × 0.2 m in size and with ragged to more or less straight margins. Bedding in one example with ragged margins is oriented subvertically and is slightly warped, suggesting an origin as a xenolith of semiconsolidated sediment caught up in a flow. Other examples, including one with a horizontal bedding contact between micritic limestone below and bioclastic limestone above, appear to be Neptunian dykes.

The bioclastic limestone was sampled and the palaeontology indicates an early Miocene age and an inner neritic environment (see Appendix 1).

Unit 2

This middle, well-bedded, flat-bedded unit is about five metres thick (about 30–35 masl). On the eastern ridge the unit can be subdivided into an off-white to brown, possibly calcareous sandstone (Unit 2a) about three metres thick, overlain by a two metre-thick poorly sorted, graded granule-pebble conglomerate (Unit 2b) (plate 14) with very angular clasts of weathered basalt. A few metres further west, below and south of the eastern ridge, the conglomerate (Unit 2b) lenses out and the sandstone (Unit 2a) directly underlies the top agglomerate (Unit 3). A good section through Unit 2 is exposed in a seven metre high cliff further west. There it consists of well-bedded sandstone with graded bedding, intercalated with several thin (up to 200 mm) beds of pebble conglomerate (plate 15), and passes upwards into Unit 3.

Near the bottom of Unit 2, on the southern side of the eastern ridge, there is a bed of a distinctive porous and very light, pale mustard-coloured brownish-yellow rock with thin (1–10 mm) diffuse horizontal lamination. In the field this was thought to be a leached limestone, but a thin section (BP6) shows that it consists entirely of



Plate 10

*Tongue-like flow (about 25 m across),
northern side of Black Pyramid.*



Plate 11

*Columnar jointing passing laterally into 'knobby'
Tertiary basalt, eastern end of Black Pyramid.*



Plate 12

*Amygdaloidal basalt with Neptunian limestone dykes, Black Pyramid.
The width of view is about one metre.*



Plate 13

Vertical and inclined columnar jointing, eastern end of Black Pyramid.



Plate 14

Graded granule-pebble conglomerate overlying calcareous sandstone, 'unit 2', eastern median ridge, Black Pyramid.



Plate 15

Graded bedded sandstone with thin pebble conglomerate interbeds, cliff exposure south of eastern median ridge, Black Pyramid.

small beads, bubbles, shards and fragments of pale yellow glass, completely isotropic under crossed nicols (plate 16). X-ray diffraction confirms that this rock is composed of amorphous material, apart from minor anatase. It is probably a subaqueously deposited, reworked vitric tuff.

Unit 3

This topmost unit extends from about 35 masl to the pinnacle (73 masl) of the island. It comprises poorly exposed unbedded agglomerate with boulder-sized basalt clasts, including pillows and pillow fragments, set in a brown to orange, poorly sorted, sandy to pebbly, weathered volcanoclastic matrix.

Petrography

In thin section the lower basalt unit (unit 1; samples BP1, 7; plate 17) consists of 5–10% of olivine phenocrysts in a 'fluidal' fine-grained intersertal groundmass of flow-aligned plagioclase laths, small interstitial ferromagnesian granules, black glass and dirty-grass-green to greenish-brown alteration. The olivine phenocrysts are mostly equant euhedra (generally 1 mm or less) although a few are slightly embayed, suggesting resorption. They are frequently clumped in glomerocrysts. Some contain scattered inclusions of tiny (5–10 μm), almost opaque, equant square chromite euhedra. The olivine phenocrysts show varying degrees (incipient to total) of alteration to finely fibrous pale greenish-brown 'bowlingite', initially around their rims and along fractures. Plagioclase laths in the groundmass (typically 100–250 μm \times 30–60 μm) are mostly labradorite (about An_{60}). The interstitial ferromagnesian granules are mostly too small (5–40 μm) for optical determination, but both olivine and colourless augite are definitely present. Under high magnification, acicular to dust-sized opaque blebs can be resolved in the black glass. The brown alteration is fibrous and similar to the 'bowlingite' after olivine phenocrysts, but the greener patches are extremely fine grained and unresolvable.

A fine-grained limestone (BP3) from one of the limestone bodies in the lower unit shows faint lamination representing variation from even-grained micritic texture to micropelletal texture. A bioclastic limestone (BPC4) shows abundant foraminifera, fragments of calcareous algae and echinoderm elements in a micritic or micropelletal matrix similar to BP3. Fibrous calcite cement partly fills intragranular pore space. Angular grains of quenched basalt are also present. The palaeontology of this sample is described in Appendix 1.

A sample (BP5) of a pillow fragment from the base of the upper unit (unit 3) is petrographically very similar to the lower unit. It contains slightly smaller (<500 μm) olivine phenocrysts, grading in size downward to ferromagnesian granules in a more glassy intersertal groundmass in which the plagioclase laths are slightly larger (150–400 μm) than in BP1 or 7. The ferromagnesian granules appear to consist mainly of

olivine, and the presence of pyroxene was not confirmed. The interstitial glass, as in samples from the lower unit, is black due to the abundant opaque dust. Much of the olivine, particularly of the larger phenocrysts, is altered to pale greenish-brown fibrous 'bowlingite' or oxidised red-brown 'iddingsite'.

Geochemistry

The two samples (BP1, BP7) of the lower unit (unit 1) from near sea level at the eastern end are chemically (Tables 3, 4) very similar olivine tholeiites ($ol; hy \gg 10$) in the classification of Johnson and Duggan (1989). The Mg numbers (at $\text{Fe}_2\text{O}_3/\text{FeO} = 0.20$) and Ni contents are below values considered characteristic of primary magmas (Mg number 68–72; Ni 300–500 ppm; e.g. Frey *et al.* 1978) but fairly typical of Tasmanian Tertiary tholeiites, and suggest about 10–15% low pressure fractionation of olivine (and/or of orthopyroxene at higher pressures?) has occurred. This is also consistent with the moderate depletion of Ni. The relatively high Cr contents (330–335 ppm) and lack of significant Sr depletion suggest that neither clinopyroxene nor plagioclase were important fractionating phases. This is entirely consistent with the observed phenocryst assemblage. Nb/Y ratios are consistent with mildly tholeiitic affinities.

Sample BP5 from the upper basalt unit (unit 3) is also an olivine tholeiite, but the much lower ol (1.21%) indicates that it is transitional to quartz tholeiite. Lower Nb and Nb/Y are also consistent with a more strongly tholeiitic character. On the basis of lower Mg number it may be more strongly fractionated than the older lower unit. Distinctly higher Ni and lower Cr suggest that pyroxene fractionation may have been relatively more important, although this is not evident in CaO. In any case, the lower levels of incompatible elements (K_2O , P_2O_5 , Rb, Zr, Nb, Ce and Ba) indicate that it could not have been derived from the lower unit composition by simple low pressure fractionation in a crustal magma chamber. Rather, it may represent a separate batch of higher degree partial melting. Mixing of magmas may have occurred at various levels, but this is impossible to resolve, even qualitatively, with the present data.

These rocks are broadly similar in both major and trace elements to similar Tertiary tholeiites from northwest Tasmania (e.g. Everard, 1989 and unpublished data, fig. 9).

Discussion

The presence of marine limestone and possible hyaloclastites in the lower unit, the well-bedded middle sedimentary unit including limestone, and pillows in the upper unit indicate entirely subaqueous volcanism. Together with the early Miocene fauna within the limestone intercalated with basalt near the top of the lower unit (Quilty, see Appendix 1), this provides further evidence for a high stand of relative sea level in Bass Strait at this time.

On the colour magnetic image (fig. 4), Black Pyramid lies in a meridional belt of short wavelength negative

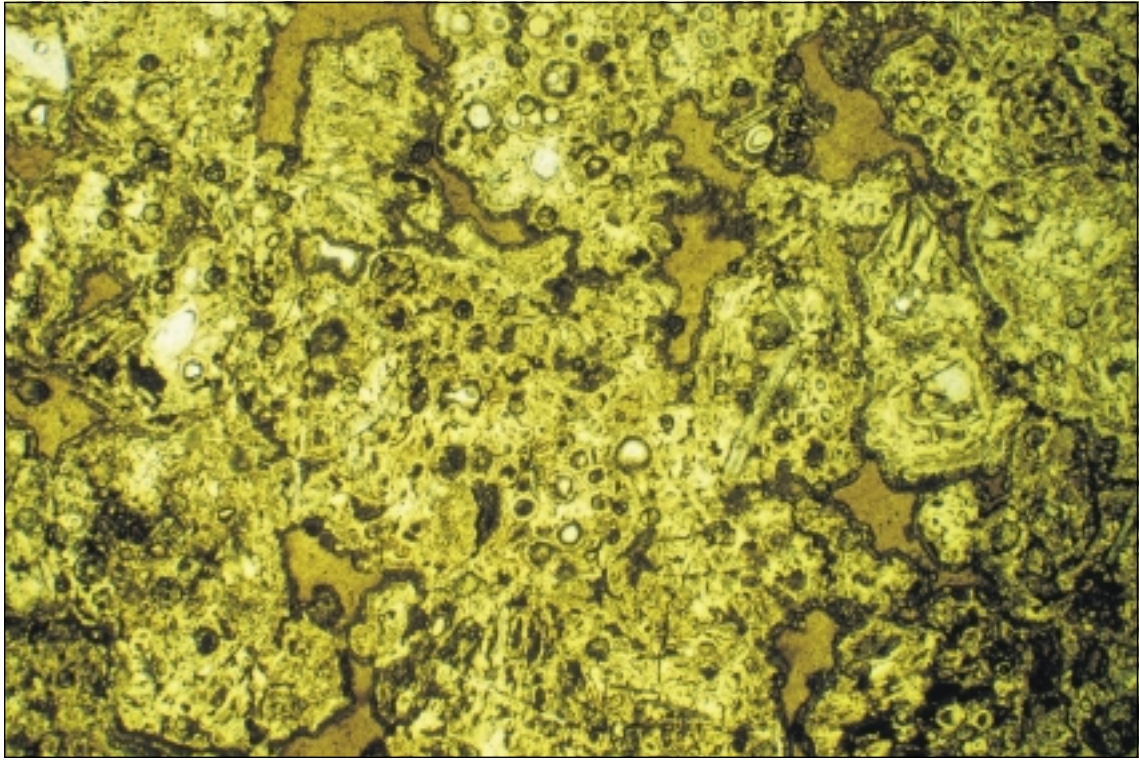


Plate 16

*Sample BP6, glassy tuff, middle unit, Black Pyramid.
Plane polarised light, field of view 4.4 × 2.9 mm.*

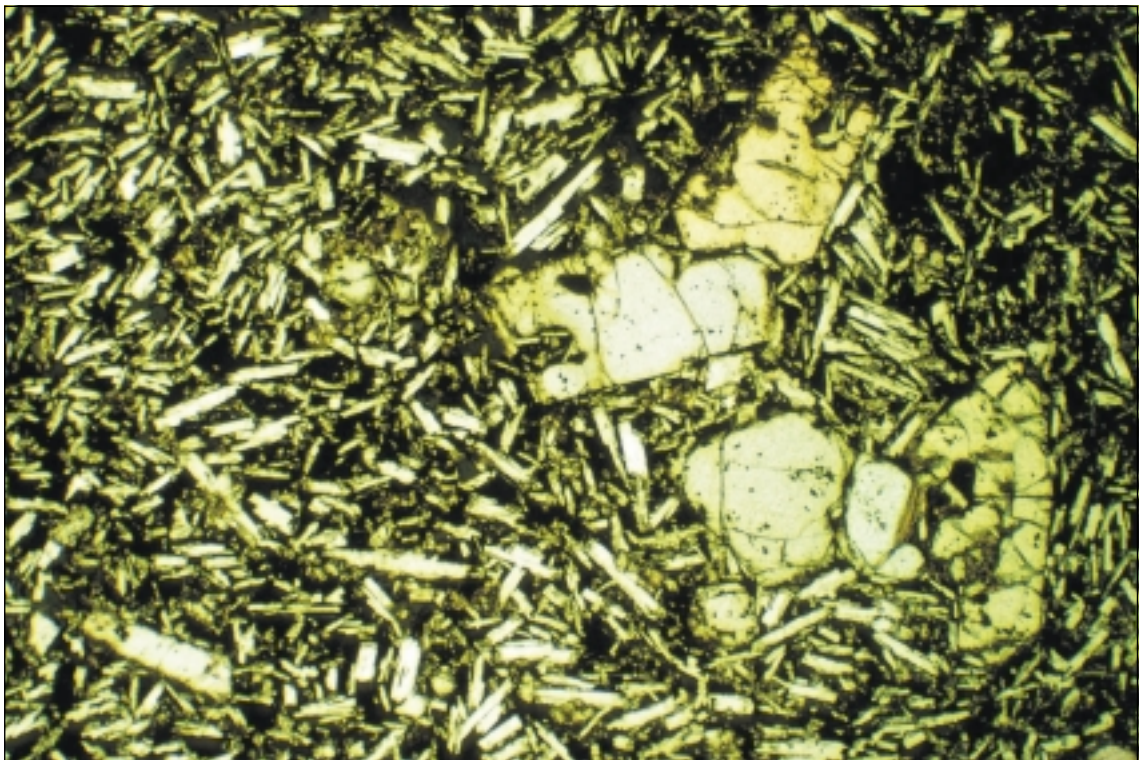


Plate 17

*Sample BP7, Tertiary basalt (olivine tholeiite), lower unit, Black Pyramid. Slightly embayed olivine phenocrysts in an intersertal groundmass of mostly plagioclase laths and black glass.
Plane polarised light, field of view 4.4 × 2.9 mm.*

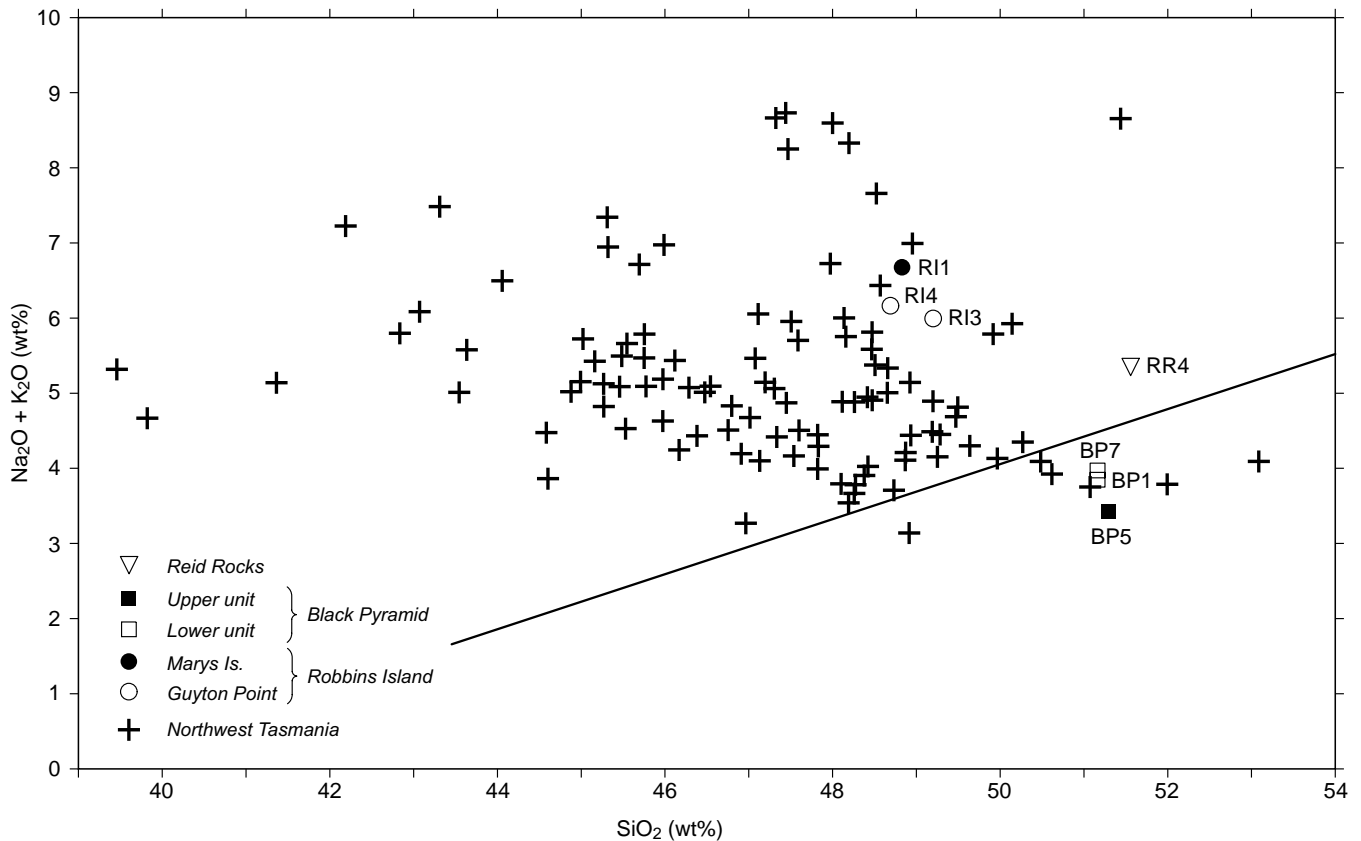


Figure 9

Total alkali ($\text{Na}_2\text{O} + \text{K}_2\text{O}$): silica (SiO_2) plot for Tertiary basalts from Reid Rocks, Black Pyramid and Robbins Island. Data from Tertiary basalts of Rocky Cape tectonic region of northwest Tasmania shown for comparison (data sources Brown, 1986, 1989; Cromer, 1972; Edwards, 1950; Everard, unpublished data; Gee, 1971; Geeves, 1982; Sutherland, Baillie and Colwell, 1989; Sutherland et al., 1989, 1996; Sutherland and Corbett, 1967; Varne, 1977; Yaxley, 1981). Analyses recalculated to 100% anhydrous. Empirical alkalic-tholeiitic field boundary of Macdonald and Katsura (1964) also shown.

anomalies extending for about 24 km to the north and nine kilometres to the south, and which is mostly less than five kilometres wide. This probably indicates the extent of similar basalt on the sea floor. The different polarity supports a different age to the more alkalic basalt of Reid Rocks. As numerous magnetic reversals occurred in the early Miocene, reversed polarity is compatible with the age of the fauna in the intercalated limestone.

Albatross Island

Albatross Island is located about 11 km west of Cape Keraudren (the northern tip of Hunter Island) at $40^{\circ}22.7'S$, $144^{\circ}38.8'E$ (301 000 mE, 5 627 500 mN). The island is about one kilometre long, elongate in a NNE-direction, and up to 250 m wide. The geology and geomorphology of the island were described in detail by Banks (1989): essentially it is a strike ridge of siliciclastic conglomerate, dipping moderately (35° to 10°) to the WNW (plate 18). The northern third of the island (as far south as 'The Trap') was briefly examined for this study.

The dominant lithology is a thick-bedded to massive, clast-supported cobble to (small) boulder conglomerate (plate 19). Most clasts are well rounded and typically 100–300 mm across. The vast majority are of fine-grained white or pink quartzite resembling the

quartzitic lithologies within the Rocky Cape Group. A few clasts show cross bedding. There are also rare, generally smaller and more angular clasts of dark grey siltstone (resembling pelitic units in the Rocky Cape Group such as the Cowrie Siltstone) and laminated red siltstone. The matrix is a coarse quartzose sand. About 5% of the succession consists of impersistent beds of coarse-grained sandstone 300–600 mm thick. A weakly developed cleavage dips steeply west.

Rare rounded beach boulders, up to 600 mm across, of pale green, weathered dolerite were sampled from the eastern end of the 'Northern Gulch', a depression which cuts across the northern part of the island. This gulch trends about 080° , is about 20 m wide and is floored by cobbles and boulders. The dolerite boulders may be derived from close offshore (Banks, 1989) or perhaps from an outcrop concealed beneath superficial deposits in the floor of the gulch.

An interesting geomorphological feature on the eastern side of the northern part of the island is the presence of two sea tunnels, each about 50 m long, aligned parallel to the main axis of the island and 15–20 m above present sea level. The northern tunnel is up to about eight metres high, and its extension south of the 'Northern Gulch' is about 3–5 m high and opens out to a small amphitheatre-like depression ('The Trap'). In this



Plate 18

Albatross Island, viewed from the northeast, showing dipping conglomerate.



Plate 19

Close-up of siliceous cobble-conglomerate, northern end of Albatross Island.

vicinity, lenticular sandy beds up to 500 mm thick persist for several metres within the conglomerate. The tunnels have been shown to have formed by erosion along a fault at a time of higher sea-level, probably in the Last Interglacial (Banks, 1989).

Petrography

A thin section cut from a clast in the conglomerate (AI2) is a supermature orthoquartzite, consisting of a mosaic of equant quartz grains mostly in the 200 µm to 500 µm size range. Authigenic overgrowths and well-rounded original detrital grain outlines can be distinguished on many grains. Grain boundaries are irregular to slightly sutured. There are rare grains of polycrystalline quartz and a single ragged flake of white mica was noted. Minute grains of dark brown rutile, zircon and possible apatite are present in trace quantities.

A thin section from a sandstone bed within the conglomerate near the northern end of the island (AI3) shows a moderately sorted, coarse-grained lithic sandstone, with well-rounded quartz grains and sand to small pebble-sized clasts (mostly 200–800 µm) of quartzite, phyllite and quartzose siltstone. An opaque mineral is relatively abundant as irregular grains to up to 500 µm across, but ranging down to dust size.

In thin section the dolerite boulder (AI1) is aphyric, relatively coarse grained and metamorphosed but with a clear relict igneous texture. It now consists mainly of ragged prismatic laths up to 500 µm long of tremolite-actinolite representing 'uralitised' pyroxene, pale green chlorite, minor epidote and a turbid interstitial mesostasis of feldspar and quartz. Turbid angular grains of sphene (<250 µm) are abundant and an opaque phase is sparingly disseminated. The tremolite is weakly pleochroic from pale yellow to pale green, but locally grades into better crystallised cores of a more strongly coloured, darker green to orange-brown hornblende. The interstitial feldspar is poorly twinned and at least some is optically negative; x-ray diffraction indicates plagioclase is the only feldspar present, so it may be oligoclase to albite. Mica (presumably sericite) was also detected by x-ray diffraction. Angular interstitial quartz anhedral are clear and up to 400 µm across, although generally smaller.

The rock is a quartz metadolerite, in which peak metamorphism reached the lower amphibolite facies, followed by pervasive greenschist retrogression. It strongly resembles samples collected from the Neoproterozoic Rocky Cape Dyke Swarm from northwestern Tasmania.

Geochemistry of dolerite boulders

Caution is needed in interpreting a chemical analysis of sample AI1 (Table 5) because of the likelihood of element mobility during metamorphism and alteration. The high total FeO/MgO suggests a relatively evolved composition and the low alkalis and Nb/Y indicate subalkaline, probably tholeiitic, affinities. These features are also common to many

Table 5

Chemical analyses, Neoproterozoic (?) dolerite

	<i>Albatross Is</i>	<i>Cuvier Bay</i>
	<i>AI1</i>	<i>CB5</i>
SiO ₂ (wt%)	52.98	41.29
TiO ₂	0.64	3.45
Al ₂ O ₃	13.12	11.06
Fe ₂ O ₃	4.27	2.04
FeO	8.41	12.02
MnO	0.20	0.22
MgO	5.16	4.86
CaO	9.60	6.55
Na ₂ O	1.90	2.22
K ₂ O	0.17	0.64
P ₂ O ₅	0.35	0.43
CO ₂	0.18	10.10
H ₂ O	3.12	4.40
SO ₃	0.09	0.51
Total	100.19	99.79
Sc (ppm)	70	33
V	310	390
Cr	50	30
Co	36	38
Ni	88	61
Cu	3	175
Zn	98	125
Ga	15	22
As	<20	35
Rb	23	35
Sr	240	420
Y	27	38
Zr	78	280
Nb	15	42
Mo	40	<5
Sn	<9	<9
Ba	38	<23
La	<20	<20
Ce	31	92
Nd	<20	58
W	<10	<10
Pb	<9	11
Bi	<5	<5
Th	15	23
U	<10	<10

dolerites in the Rocky Cape Dyke Swarm, but in detail there are some differences. Sample AI1 has lower K₂O, TiO₂ and Zr and higher P₂O₅ and Sc. It also has some similarities, particularly in major element chemistry, to the Neoproterozoic 'lower tholeiitic sequence' of southeast King Island described by Waldron and Brown (1993), but P₂O₅, Sc, Sr, Zr, Zr/Y, and Ce are significantly higher.

A direct correlation with any of these rock suites is not justified, but the boulders on Albatross Island indicate the presence of nearby dolerite outcrops which may broadly belong to the same episode of Neoproterozoic magmatism.

Discussion

We concur with Banks (1989) that the conglomerate is most likely a correlate of the Forest Conglomerate

(Neoproterozoic), which occurs discontinuously at the base of the Togari Group in the Smithton Basin. The unit also strongly resembles certain Late Cambrian siliceous conglomerates of the Denison Group. However correlation with these sequences is considered less likely, because no Denison Group outcrop is known northwest of the Arthur Lineament.

Small islets west of Hunter Island

North Black Rock

Located about 5.5 km west of Hunter Island, this small islet rising to 10 masl consists of black, blocky to columnar-jointed basalt. Landing was not attempted.

On the basis of aerial inspection, Sutherland (1980) reported that both North and South Black Rock consisted of flow foot breccias with contrary dips; we are unable to confirm this in the case of the former.

South Black Rock

This somewhat larger islet, rising to 39 masl, is located 11 km SSW of North Black Rock and eight kilometres west of Steep Island. It also consists of Tertiary volcanic rocks, including massive basalt, some pillows and possibly pyroclastic rocks (plate 20). A crude layering dips at about 35° to the west. A small shore platform is developed and landing would be feasible in calm seas.

Steep Island

Steep Island has an area of about 0.2 km²), rises to 64 masl and is located 3.5 km west of southern Hunter

Island. Cliffs plunging directly into the sea make access difficult or impossible except on the eastern side. Unfortunately because of adverse sea conditions we were unable to land, but G. Dixon briefly visited the island on a previous occasion. The island clearly consists of Tertiary basaltic volcanic rocks, mainly volcanoclastics. Horizontal layering is well developed in cliffs on the eastern side.

The geology of Steep Island was briefly noted by Sutherland (1980), on the basis of circumnavigation by plane and boat and samples supplied by others, to include westerly-dipping flow-foot breccias on the northwest side. G. Dixon has noted weathered pillow forms in this area. Sutherland's samples were reported to be petrographically olivine tholeiites. Similar debris on the adjacent shore of Hunter Island was used by Sutherland (1980) to infer an aquagene volcanic centre just east of Steep Island.

Nares Rocks

This cluster of rocks, shown rising to 10 masl on bathymetric charts, is located about two kilometres south of Steep Island and also consists of Tertiary volcanic rocks.

Delius Islet

This small wave beaten islet, about one kilometre from the west coast of Hunter Island, appears (from a distance of about 500 m) to consist of Precambrian orthoquartzite.



Plate 20

Dipping Tertiary volcanic rocks, South Black Rock

Brown Rocks

Lying between Nares Rocks and Trefoil Island, and west of Bird Island, these rocks are not named on topographic maps but are shown rising to 8 masl on marine charts. From a distance of about 500 m they also appear to consist of orthoquartzite of presumably Precambrian age. The strata dip fairly gently to the east.

Bird Island

This low-lying island (0.5 km²) just southeast of Hunter Island consists of similar orthoquartzite. No landing was made.

Seacrow Islet

This small island a few hundred metres long is located 2 km SSE of Weber Point, the southern extremity of Hunter Island. From a distance of about one kilometre it appears to consist of well-bedded orthoquartzite dipping at 10° to 20° to the west.

Stack Island

This much larger island, about one kilometre long, is located 1.5 km east of Weber Point. From a few hundred metres distance it appears to consist of orthoquartzite. On the western shore gentle open upright folds with a half-wavelength of about 50 m, possibly trending north-south and verging to the west, are apparent. At the southern end the strata dip east or southeast at about 45°.

The contrary dips on Stack Island and Seacrow Islet are consistent with them lying on opposite limbs of the north-trending major regional anticline identified by D. J. Jennings on Hunter Island (see below). The western limb extends to Woolnorth Point on the Tasmanian mainland.

Hunter Island

D. J. Jennings (Department of Mines) and F. L. Sutherland (Queen Victoria Museum) spent several days on Hunter Island in 1971 examining the entire coastline, with some reconnaissance inland. Jennings produced a geological map that remains unpublished, although results were briefly summarised by Turner (1989). Accordingly we briefly landed on the island in only three places, whilst anchoring overnight.

Essentially Jennings and Sutherland found that the island is composed entirely of correlates, mainly orthoquartzite, of the Precambrian Rocky Cape Group of the Tasmanian mainland, folded along the axis of the island into a broad north-trending regional anticline. Granite, shown in large areas on older maps as recently as 1960, does not crop out on Hunter Island.

Cuvier Bay

We landed on the eastern side of Cuvier Point and traversed southeast along the shore for about one kilometre to the next smaller headland. Cuvier Point consists of hard, white, pure orthoquartzite, dipping and facing steeply west (175W81 at base of unit,

307 200 mE, 5 515 600 mN). A very irregular network of dark-green to black ankeritic sulphide-bearing veins, associated with quartz veins also containing sulphide minerals, cuts the orthoquartzite and is indicative of some hydrothermal activity near 307 100 mE, 5 515 800 mN.

The quartzite passes conformably down into a unit of dark grey siltstone with fine-grained quartzite beds at the western end of the first beach southeast of Cuvier Point. The quartzite beds display hummocky cross-stratification, indicating deposition took place above storm wave base but below the zone of constant wave reworking. Further east, moving stratigraphically downwards, quartzite beds become progressively rarer. The siltstone has a strong cleavage consistently steeper than, and clockwise of, bedding (bedding 175W74, cleavage 014W88 at an outcrop at 307 200 mE, 5 515 600 mN near the middle of the bay).

A pale grey to off-white subvertical dyke, at least seven metres wide, has intruded parallel to the cleavage in the dark grey to black siltstone on the eastern side of this outcrop. The eastern margin of the dyke is chilled, but the western margin is obscured by beach sand. A foliation is developed parallel to the margins and cleavage in the country rock. The dyke is aphyric and aphanitic apart from minor blebs of sulphide. It is essentially non-magnetic ($X = 0.55 \times 10^{-3}$ SI, $n = 10$). In the field a felsic composition was thought likely, but a thin section (see below) shows that the rock is a highly altered dolerite.

Close to the eastern end of the bay a small outcrop consists entirely of well cleaved siltstone without any quartzite interbeds.

The adjacent headland immediately to the east consists entirely of orthoquartzite, with a much more shallow westerly dip (010W21). A faulted contact, dipping steeply east, is exposed on the extreme western flank of the headland and is marked by a zone of brecciation.

These field relationships are consistent with the interpretation implied on Jennings' map. A steeply west-dipping and facing sequence of orthoquartzite and underlying siltstone is successively repeated by north-trending normal faults, downthrown to the east. The siltstone crops out sporadically in the bays and the more resistant quartzite forms the headlands. Regionally, the siltstone occupies the core of a major anticline and is the oldest unit on Hunter Island.

Petrography

A thin section (CB1) of a quartzite from near Cuvier Point shows a fine-grained, slightly strained orthoquartzite, consisting of a mosaic of quartz grains with slightly sutured contacts and no discernible original grain outlines, together with rare polycrystalline quartz, coarse-grained chert and zircon.

A thin section (CB4) of the siltstone shows a faintly laminated silty pelite with detrital muscovite aligned in

bedding, and quartz occurring as silt-sized grains. A strong cleavage is inclined to bedding.

In thin section the dyke (CB5) is seen to be extremely altered, consisting of about 30% disseminated secondary calcite. Other minerals include fairly abundant equant quartz anheda (<250 µm); irregular patches of pale yellow-green chlorite; minor aggregates of ragged, elongate to finely fibrous, colourless tremolite-actinolite; and a few relict stubby laths of multiply twinned plagioclase (albite?), in places 500 µm–1 mm long. Opaque phases are fairly abundant as equant (<1 mm) to elongate or sometimes skeletal euhedra. Many of these are probably extremely turbid secondary growths of sphene around original ilmenite. A well developed fracture cleavage is present. Little remains of the original texture, but the mineralogy indicates a mafic to intermediate composition, probably a quartz dolerite similar to rocks of the Rocky Cape Dyke Swarm. The presence of cleavage suggests that the rock may belong to the foliated pre-tectonic group of the four-fold classification tentatively advocated by Brown (1989, pp. 62–68).

Geochemistry of dolerite dyke

The dolerite dyke (sample CB5) is so altered (CO₂ 10.1%, H₂O⁺ 4.4%, Table 5) that most major elements can only be considered semi-qualitatively. The high total iron and low MgO suggest a strongly evolved composition. The high field strength incompatible elements TiO₂, P₂O₅, Y, Zr, Nb and Ce are regarded as relatively immobile with alteration and their levels are probably indicative of primary magmatic values. They are much higher than in the tholeiitic dolerite typical of the Rocky Cape Dyke Swarm of northwest Tasmania (Brown, 1989, pp. 62–68; Everard, unpublished data) but similar to the more alkalic Cooee Dolerite further east (e.g. Brown, 1989; analysis in Black, 1994, p. 2). The high Nb/Y content is also suggestive of alkalic affinities.

Shepherds Bay

Orthoquartzite forms the northern headland of the bay. No observations additional to Jennings' work were made.

Cave Bay

The sequence exposed on the foreshore at the northern end near the slipway dips and faces east (017E35) and consists of a medium to pale grey siltstone with thin interbeds of orthoquartzite. Cross bedding and a strong cleavage (168W67) are notable. Over a distance of about 200 m along the shore to the northeast the sequence becomes generally finer grained and more pelitic, although some thin pebbly beds are present. Bedding (010E38) and cleavage (170W78) remain similar in orientation, consistent with the eastern limb of a gently S to SSE-plunging regional anticline.

According to Jennings this sequence belongs to the uppermost of three Precambrian units identified on Hunter Island, although it is considered "demonstrably

down-faulted into quartzite at several localities and inferred as fault-bounded at all other exposures". The unit was described as lithologically mixed but mainly siltstone.

Petrography

In thin section a sample (H1) of this lithology shows a weakly cleaved, uniform silty mudstone, with sparsely distributed quartz silt (<50 µm) and irregular aggregates of opaque grains (<100 µm), often oxidised, in a fine-grained matrix of sericite shreds aligned in the cleavage and barely resolvable quartz grains. Patches richer in sericite, up to 500 µm across and crudely ellipsoidal to irregular, may be deformed and metamorphosed clay pellets. Flakes of detrital muscovite (<100 µm long) and blue-green to yellow pleochroic tourmaline anheda are relatively abundant. Trace zircon is also present.

Penguin Islet

This low flat islet is located three kilometres east of the southeast coast of Hunter Island. It measures about 500 m north-south and less than 100 m wide, and rises to 15 masl near its northern end. Although he apparently did not visit, Jennings (1976) noted that "[granite] is reputed to compose Penguin Islet", and it is shown thus on the King Island–Flinders Island 1:250 000 scale geological map (Jennings and Cox, 1978). Hunter Island is composed entirely of orthoquartzite-dominated correlates of the Precambrian Rocky Cape Group, and the nearest known granite outcrop is 12 km to the NNW on Three Hummock Island.

The new aeromagnetic data show a large (35 × 25 km) area of low smooth magnetics, extending from Three Hummock Island in a northeasterly direction, surrounded by a nearly continuous narrow positive anomaly. This is readily interpretable as corresponding to the surface expression of the Three Hummock Island Granite and its surrounding contact aureole, exposed or virtually exposed on the sea floor. The apparent contact of the granite is located very close to the southwest coast of Three Hummock Island, which tends to discount the possibility of a SSW extension of the granite as sea floor bedrock to Penguin Islet. The area around of Penguin Islet is also magnetically low and quiet. Although there are small weak NNE-trending elongate anomalies just to the north and south, no similar area of granite is obvious from the magnetic image.

On the other hand, a provisional gravity interpretation of the form of the Three Hummock Island Granite (Leaman and Richardson, 1989) suggests that it shelves shallowly to the southwest, and underlies northern, central and most of eastern Hunter Island at a depth of less than one kilometre. Penguin Islet lies between the interpreted one kilometre and two kilometre depth-to-granite contours on this model.

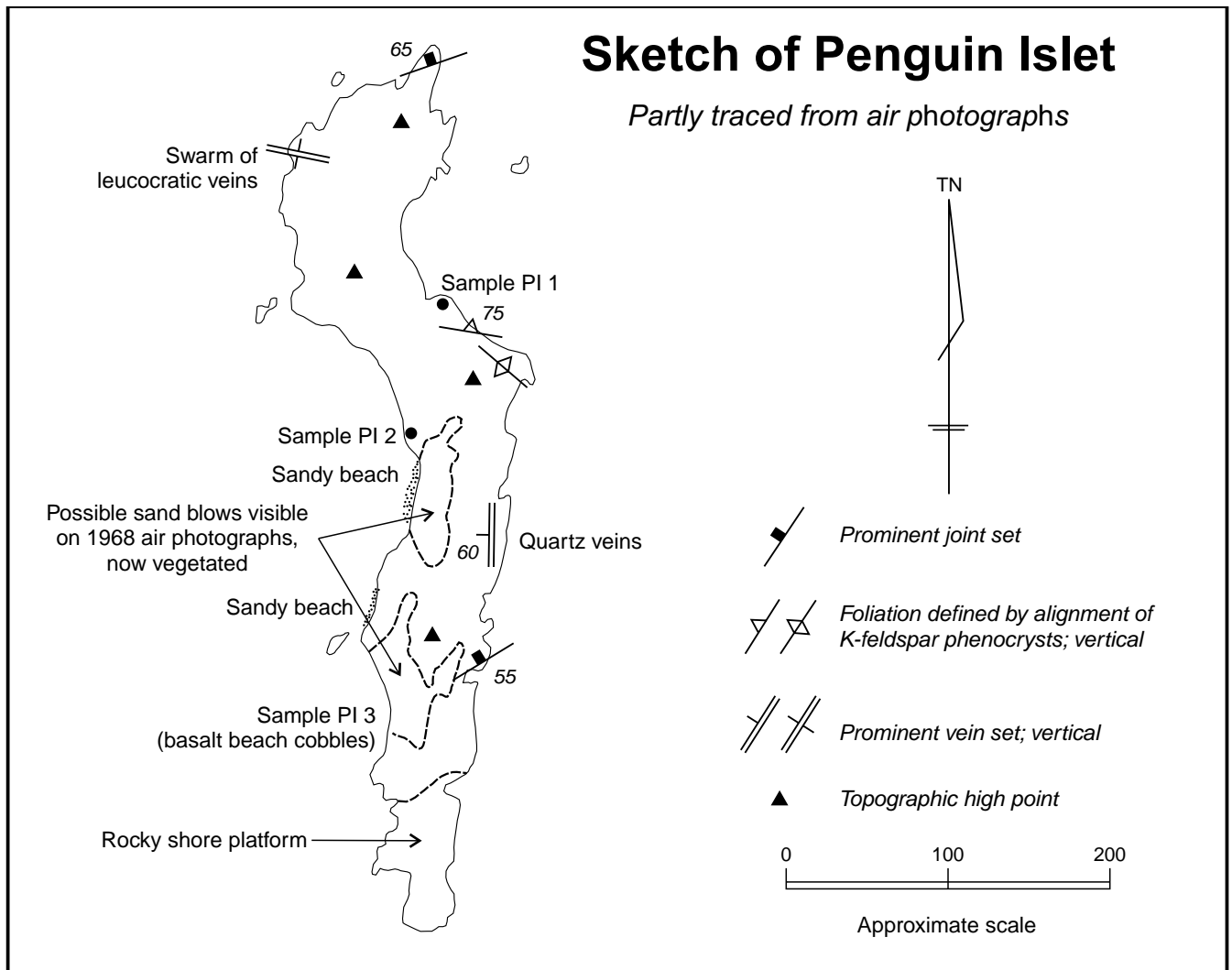


Figure 10

On landing it was confirmed that Penguin Islet consists entirely of granite (fig. 10). The shore provides nearly continuous outcrop, often in the form of rounded to jagged tors, but 'inland' there is low dense tussocky grass and heath with outcrop confined to a few mostly jagged tors, mainly on the higher points and central crest of the island.

The rock is a medium-grained, white to cream-coloured, porphyritic biotite-muscovite granite containing tabular potash feldspar phenocrysts (20–50 mm), locally aligned to define a crude phenocryst foliation (two strike-and-dips of 130 vertical and 100NE75 measured on the eastern shore about 200 m from the northern end). Fresh black biotite is quite abundant, both dispersed in the groundmass and sometimes as books up to 12 × 8 mm. Altered greenish biotite is also locally present. A patchy pinkish alteration of feldspar is locally present.

Enclaves are very rare in the granite; a single fine-grained ovoid melanocratic enclave measuring 200 × 150 mm was noted on the northwestern shore.

The granite is essentially non-magnetic, evidently lacking magnetite. The magnetic susceptibility was

measured on fresh flat surfaces as 0.064 ($\times 10^{-3}$ SI) (mean of 20 readings, range 0.04–0.09).

The granite is locally cut by finer-grained leucocratic veins up to 20 mm wide, some of which have a linear central zone of tourmaline. A swarm of subparallel veins (trending 100 vertical) was observed on the western shore of the islet about 150 m from the northern end. Narrow veinlets of aplitic material and/or tourmaline were observed elsewhere.

Several quartz veins up to 100 mm wide and striking roughly 180NW60 were noted on the eastern shore about halfway along the island.

Well-developed jointing was noted on the northwest of the island just below the highest point (070N65), and on the eastern shore about 150 m from the southern end (060N55).

A small sandy beach is developed on the western side of the island, about 100 m from the southern end. Scattered beach cobbles and boulders in the vicinity are mostly of granite, but there are a few of black glassy basalt.

Granite petrography

A sample from the northeast of the islet (PI1) is seen in thin section to consist mainly of anhedral granular interlocking quartz and perthitic feldspar, with subordinate subhedral plagioclase and probably secondary muscovite. Most feldspar is a turbid, patchy uneven intergrowth of perthite, locally grading to mesoperthite in which plagioclase patches are almost as abundant as the host orthoclase. Inclusions of ragged muscovite, often aligned, are abundant, and there are a few subhedral plagioclase inclusions. Quartz grains are equant anhedral up to 4 mm across, with jagged grain boundaries against each other and feldspar; and extinction is very slightly strained.

Oblong subhedra of plagioclase (5–0.5 mm) are albite or oligoclase and also contain abundant inclusions of muscovite and occasionally apatite. Muscovite occurs as ragged subhedral to anhedral flakes up to 2 mm across, as well as smaller inclusions in feldspar. Fresh biotite is very rare in this sample, but it is preserved in an inclusion in quartz and is pleochroic from pale to dark 'foxy' red-brown. Accessory minerals include relatively abundant, large (to 500 μm) euhedral to subhedral colourless to red-brown cassiterite; colourless, virtually isotropic, apatite anhedral up to 200 μm across; and amber to occasionally bluish subhedral tourmaline. Occasional opaque grains up to 500 μm across are identified under reflected light as arsenopyrite, and may be surrounded by an unidentified, very fine-grained colourless and straw yellow alteration product. Some smaller opaque grains are pyrite.

Another sample (PI2) from the southwest shore is similar but has a more inequigranular texture. It contains oblong phenocrysts of perthitic feldspar up to 20 mm long and anhedral quartz grains up to 5 mm across, between which is an interlocking groundmass of anhedral quartz and perthite and subhedral plagioclase and muscovite. At least some of the muscovite is secondary after biotite, as it locally retains a pale brown colour and is associated with fine-grained iron oxide alteration products. Amber tourmaline is the major accessory mineral in this sample, but apatite and rare fresh biotite (preserved as inclusions in quartz) are also present. Unlike sample PI1, cassiterite was not observed.

The granite is a highly felsic alkali feldspar granite that has been affected by late stage subsolidus alteration. It has some petrographic similarities to the Three Hummock Island Granite, but biotite is altered and the host phase of the perthite is orthoclase rather than microcline.

Penguin Islet may therefore represent the altered roof zone of a small pluton or apophysis.

Basalt petrography

Sample PI3, a beach cobble of basalt, in thin section consists of about 5 vol.% of olivine phenocrysts in an intergranular to intersertal groundmass of plagioclase,

clinopyroxene, opaque minerals and small amounts of an almost glassy mesostasis. The partly altered olivine phenocrysts, up to 1 mm across, are equant, euhedral to slightly rounded and probably were slightly resorbed. Unoriented plagioclase laths, mostly 250–500 μm but up to 1 mm long and typically 10–30 μm wide, are mostly labradorite, at least as calcic as An₆₆. Intergranular clinopyroxene granules are too small (mostly <100 μm) to determine optically, but are colourless and probably mostly augite. Elongate prismatic to almost acicular opaque minerals are up to 200 μm long and mostly 10–30 μm wide. A turbid grey interstitial mesostasis is unresolvable, but is rich in dust-sized opaque minerals. A pale orange-brown finely fibrous to amorphous mineral, birefringent to upper first order, occurs both as alteration of olivine and in the groundmass. The rock is probably an olivine tholeiite and is petrographically similar to Tertiary basalt occurring elsewhere in the region, including at Cape Grim (Sutherland and Corbett, 1967), Flat Topped Bluff and Black Pyramid (see above). The original source of the basalt cobbles cannot be identified and may well be a local flow now below sea level.

Geochemistry

Two samples (PI1 and PI2) of the granite were chemically analysed (Tables 6, 7). The results are compared with data from the Three Hummock Island granite in the following section (pages 41–47).

Three Hummock Island

Jennings (1976) reported on the geology of this large (about 70 km²) island, confirming previous reports dating back to last century that it is composed virtually entirely of granite apart from extensive cover of Quaternary sand. Some small areas of Tertiary basalt and Tertiary limestone were also mapped. Accordingly we made only brief landings in two locations to examine the granite.

Chimney Corner

Granite is well exposed in shore outcrops to the northwest of the jetty (316 800 mE, 5 520 200 mN). The granite is a medium to coarse-grained creamy-white rock, with a fairly abundant but variable biotite content, and also variably abundant, large (up to 100 mm) potash feldspar phenocrysts. Some coarse-grained muscovite is mesoscopically discernible. Finer grained more leucocratic segregations and subpegmatitic clots of tourmaline are also present.

In places well developed mineral banding, consisting of repeated layers (typically 100 mm apart) and wispy schlieren (plate 21) of finer-grained, more biotite-rich granite, defines a frequently subhorizontal but very variable, swirling flow foliation. The potash feldspar phenocrysts are oriented and aligned parallel to this fabric (plate 22).

Occasional fine-grained melanocratic enclaves are small (up to 100 mm across) and ovoid in shape. They



Plate 21

Schlieren in granite, Chimney Corner, Three Hummock Island.



Plate 22

Potash feldspar phenocryst alignment in granite, Chimney Corner, Three Hummock Island.

contain scattered polygonal phenocrysts a few millimetres across of bone-coloured feldspar set in a medium-grey, barely phaneritic (<0.5 mm) groundmass.

The granite is essentially non-magnetic (mean susceptibility 0.065×10^{-3} SI, range 0.04–0.11, $n = 10$).

West of Neils Rock

A landing was made on the southern coast of the island, about 1.5 km WNW of Neils Rock, to examine the 'rafts' and 'xenoliths' of 'sediment' and 'dark hybrid rock' reported by Jennings (1976).

The shore exposures at this locality are of very porphyritic medium to coarse-grained granite with abundant large oblong potash feldspar phenocrysts, up to 150 mm long and typically 50–100 mm wide, hosting extremely abundant fine-grained melanocratic enclaves which comprise 30–40% of overall outcrop.

The enclaves are rounded to subrounded, irregularly shaped blob-like masses, ranging widely in size from 100 mm to four or five metres across (plates 23, 24). They are variably melanocratic; some are aphanitic and virtually black, whilst others, generally the less fine-grained ones, contain more feldspar and are grey and almost granitic in appearance. Some enclaves contain large feldspar phenocrysts, but these are generally not as abundant as in the host granite.

Of particular interest are 'double enclaves'. These are generally slightly less melanocratic and relatively coarse grained, sometimes porphyritic enclaves, which themselves enclose sharply or diffusely defined, finer grained and highly melanocratic sub-enclaves.

Rare angular laminated or foliated inclusions within the granite are distinct from the enclaves and in the field appeared to be possibly true metasedimentary xenoliths.

Late leucocratic veins up to 200 mm wide cut both the enclaves and the host granite. The narrower (20–50 mm) veins are fine grained and are composed of aplite or leucogranite, whilst the wider veins commonly have a central micropegmatitic zone up to 100 mm wide with margins (50 mm) of aplite on both sides. Clots of tourmaline occur in the host granite, particularly adjacent to these veins.

Again the granite is essentially non-magnetic (susceptibility 0.1110^{-3} SI, range 0.07–0.16, $n = 10$) with somewhat higher values from the enclaves (0.36×10^{-3} SI, range 0.14–0.48, $n = 10$).

Granite petrography

A sample (TH5) from a blasted site behind the boat shed at Chimney Corner contains abundant oblong potash feldspar phenocrysts up to 30 mm long in a medium-grained (mostly 2–5 mm) cream-coloured groundmass of quartz, feldspar and fairly abundant (5–10%) flakes of black biotite, mostly 1–2 mm across. In thin section (plate 25) the rock has a typically granitic

subhedral-granular texture. There is a continuous range in grain size from the phenocrysts to the groundmass which has a large range of grain size (100 μm –5 mm) (seriate texture). The phenocrysts are microcline with both mesoscopic simple twinning and microscopic cross-hatched combined albite-pericline twinning. Microperthitic stringers of albite exsolution and small subhedral inclusions of plagioclase, and less commonly quartz, are abundant. In the groundmass plagioclase is less abundant than microcline and occurs as subhedra up to 3 mm long. These are often zoned but the extinction angles and positive optic sign suggest that compositionally they are sodic oligoclase to albite. Usually plagioclase is turbid due to partial sericitisation. Quartz is anhedral and occurs as small grains of less than 100 μm to equant sometimes polycrystalline globules 5 mm across. Ragged flakes of biotite (<2 mm) have very low 2V and a pleochroic scheme (α pale pinkish yellow to nearly colourless, β and γ medium–dark red-brown) typical of biotites from S-type granites (Whalen and Chappell, 1988). Dark metamict haloes around small zircon inclusions are common. Colourless muscovite has a similar form to biotite with which it is often associated, sometimes in crystallographic alignment. It is clearly at least partly an early alteration of biotite.

Accessory minerals include small anhedral (rarely up to 1.5 mm) of pale yellow to amber-yellow tourmaline, which may be associated with a later generation of coarse muscovite, and small equant anhedral of apatite. Opaque phases are virtually absent. Some of the turbid groundmass phases are possibly altered cordierite but, as associated pleochroic haloes are not present, microprobe studies would probably be needed to confirm this.

A sample from northwest of Neils Rock (TH9) is similar but somewhat coarser grained, with phenocrysts up to 50 mm or more and much groundmass feldspar in the 10–15 mm size range, and is richer in biotite (10–15%). In thin section it is mineralogically similar to the Chimney Corner sample. Plagioclase may be slightly more abundant, rare opaque grains are present and tourmaline was not noted. Overall it is probably slightly more mafic than the sample from Chimney Corner (TH4).

Petrography of melanocratic enclaves

Two thin sections (TH1, TH4) were cut from separate enclaves collected from Chimney Corner.

Sample TH1 (plate 26) contains phenocrysts (<5 mm) of plagioclase and anhedral quartz in a fine-grained, very biotite-rich groundmass. The plagioclase phenocrysts are well rounded, slightly embayed and typically zoned. They are very poikiloblastic, containing numerous tiny inclusions of quartz locally forming myrmekitic zones, and also larger inclusions of globular to vermiform quartz and biotite flakes aligned parallel to the (010) twin plane. The anhedral quartz phenocrysts are poikiloblastic only near their margins,



Plate 23

Melanocratic enclave swarm in megacrystic granite, west of Neils Rock, Three Hummock Island.



Plate 24

Close-up of melanocratic enclave swarm in megacrystic granite, west of Neils Rock, Three Hummock Island.



Plate 25

Sample TH5, granite, Chimney Corner. Part of a microperthitic potash feldspar phenocryst; plagioclase, quartz, biotite and muscovite also present. Crossed nicols, field of view 1.8×1.1 mm.

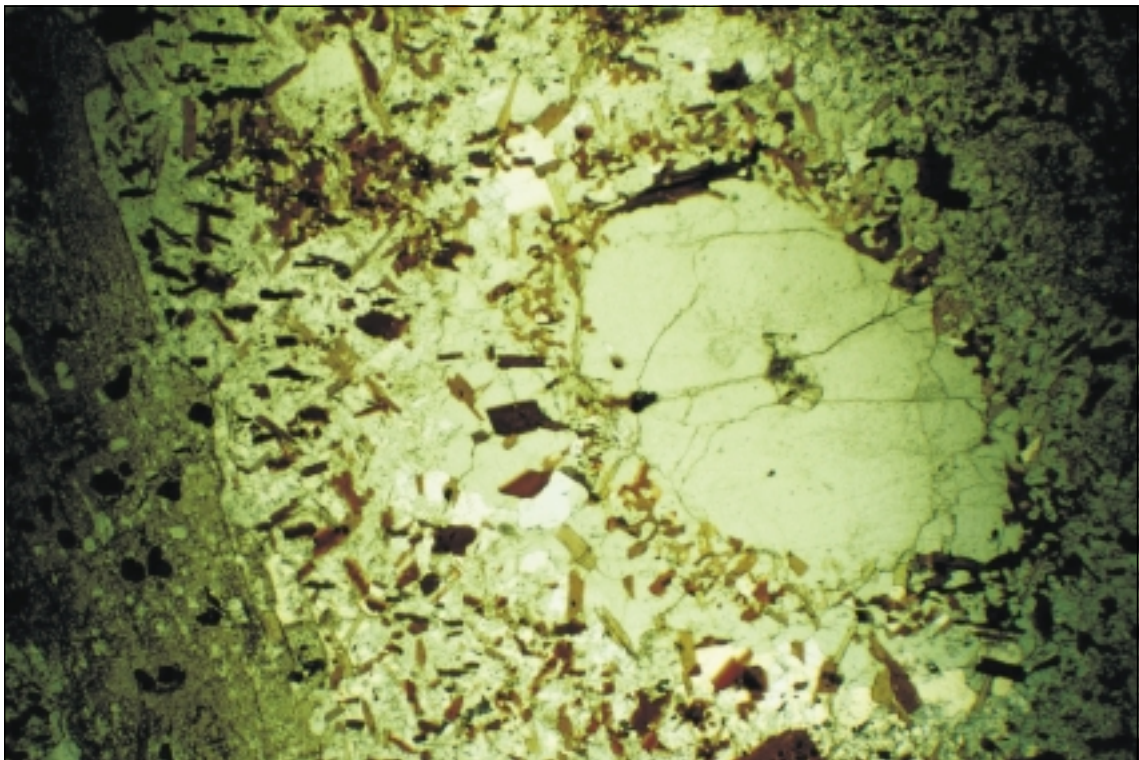


Plate 26

Sample TH1, enclave within granite, Chimney Corner. Note anhedral quartz phenocryst with poikiloblastic margin containing biotite inclusions, and relatively coarser-grained reaction halo of biotite-rich groundmass. Plane polarised light, field of view 1.8×1.1 mm.

where they may contain inclusions of biotite and occasionally plagioclase. Both plagioclase and quartz phenocrysts are frequently surrounded by a halo of relatively coarse-grained groundmass, and appear to have reacted with it rather than crystallised from it. The groundmass itself consists of abundant (c. 30%) subhedral red-brown biotite flakes (commonly <500 μm but up to 1 mm), similar to those of the host granite, and intergrown subhedral plagioclase and anhedral quartz grains typically 50–200 μm across. The biotite occurs both as isolated grains and locally concentrated into clots. Haloes around zircon inclusions are abundant. Very finely acicular (typically $50 \times 2 \mu\text{m}$) apatite is abundant in the quartzofeldspathic groundmass, and an opaque phase (presumably ilmenite) occurs as equant blebs up to 50 μm across. Potash feldspar was not seen.

Another sample (TH4) is broadly similar but coarser grained. The plagioclase phenocrysts (<10 mm) are not embayed, are less poikiloblastic and may have relatively clear cores apart from a few inclusions of globular quartz. In the groundmass biotite is perhaps less abundant (c. 20%) and more even grained (commonly c. 500 μm). It is partly altered to nearly isotropic and colourless chlorite and rare ragged flakes of muscovite. The groundmass is mostly in the 200–400 μm size range, with the sparsely distributed opaque phase mostly 50–100 μm . Acicular apatite is much less abundant than in TH1. Potash feldspar was neither seen in thin section nor detected by x-ray diffraction.

Three enclave samples (TH6, TH7, TH8) from the swarm west of Neils Rock are texturally similar but are more melanocratic, and in particular contain amphibole. They contain poikiloblastically mottled, zoned phenocrysts of plagioclase (<3 mm) with corroded margins, and a few embayed anhedral quartz phenocrysts (<5 mm in hand specimen) in a very micaceous groundmass (100–400 μm to 150–600 μm). This consists of similar red-brown biotite, abundant amphibole, plagioclase and only minor anhedral quartz. Amphibole is a pale yellow-green, weakly pleochroic, optically negative hornblende, forming equant interlocking euhedra and subhedra closely associated with biotite. Plagioclase is fairly calcic (up to about An_{50}) with zoned rims. Chlorite may occur as an alteration of biotite. Accessory phases include anhedral zircon, both equant and finely acicular apatite, rare epidote and opaque blebs (<100 μm). Again, potash feldspar was not observed either microscopically or by x-ray diffraction. Sample TH7 is noticeably less melanocratic than the other samples, and TH6 is finer grained (plate 27).

A small angular pale grey fine-grained inclusion (TH10) in the granite was thought in the field to be a metasedimentary xenolith, but a thin section shows otherwise. It consists of abundant euhedra of hornblende (100–500 μm across, pleochroic from pale yellow to pale green), poikiloblastically riddled with groundmass phases. The groundmass is a fine-grained

(5–20 μm) saccharoidal mosaic of low and high birefringence phases, shown by x-ray diffraction to be quartz, clinopyroxene, calcic plagioclase, chlorite and mica. Equant opaque grains (<50 μm) are also fairly abundant. This rock is enigmatic. It is clearly unlike the other enclaves and is unlike any possible metasedimentary xenolith. It somewhat resembles the tonalitic dyke rock from Councillor Island, particularly in being hornblende-phyric, but the groundmass differs mineralogically and texturally.

Granite geochemistry

Four samples of granite from Three Hummock Island and Penguin Islet (see previous section), and five melanocratic enclaves, were chemically analysed (Table 6). For comparison, three analyses of the Three Hummock Island granite from the database of B. W. Chappell (two of which have been published by Sawka *et al.*, 1990) are also included. CIPW norms are presented in Table 7.

All samples of the Three Hummock Island granite are fairly felsic (SiO_2 70.0–74.3%) and moderately peraluminous (alumina saturation index, i.e. molar $(\text{Na}_2\text{O} + \text{K}_2\text{O} + \text{CaO})/\text{Al}_2\text{O}_3$, of 1.12–1.21).

The Chimney Corner sample (TH5) is very similar in both major and trace elements to the three samples of Chappell. These include an aplite from north of the airstrip, about one kilometre away, and two granites from other parts of the island. The higher Ni reported in TH5 is still close to detection limits and may be due to analytical error.

The sample from west of Neils Rock (TH9) is significantly more mafic, with lower SiO_2 and higher TiO_2 , total iron ($\text{Fe}_2\text{O}_3 + \text{FeO}$), MgO, CaO, Sr, Zr, Ba, Sc, V and Cr. In addition K_2O is higher, reflecting the abundance of potash feldspar megacrysts, and Na_2O is lower. It plots away from the thermal minimum in the haplogranite system *Q-Or-Ab* and is a less fractionated granite, possibly with some entrained restite, although no diagnostic restite minerals such as cordierite or garnet were identified in thin section.

The two analyses from Penguin Islet are more felsic and more strongly peraluminous (ASI about 1.30) than those from Three Hummock Island, and have lower TiO_2 , total FeO, MgO and CaO. Sample P11 is weakly mineralised, with anomalous As (2000 ppm), Cu (90 ppm) and Sn (490 ppm) consistent with observed sulphide (arsenopyrite) and cassiterite. Both Penguin Islet samples are weakly anomalous for tungsten.

When the IUGS recommended granite classification of Streckeisen (1973) is applied to the computer-calculated pseudomodes derived from the CIPW norms, the Three Hummock Island samples (fig. 11) range from adamellite (TH9, WT67) through granite *sensu stricto* (WT66) to alkali feldspar granite (TH5, WT65). This is mainly a function of variable CaO content, and does not indicate any major chemical discontinuities amongst these samples; it is partly an artifact of this classification system, whereby albitic

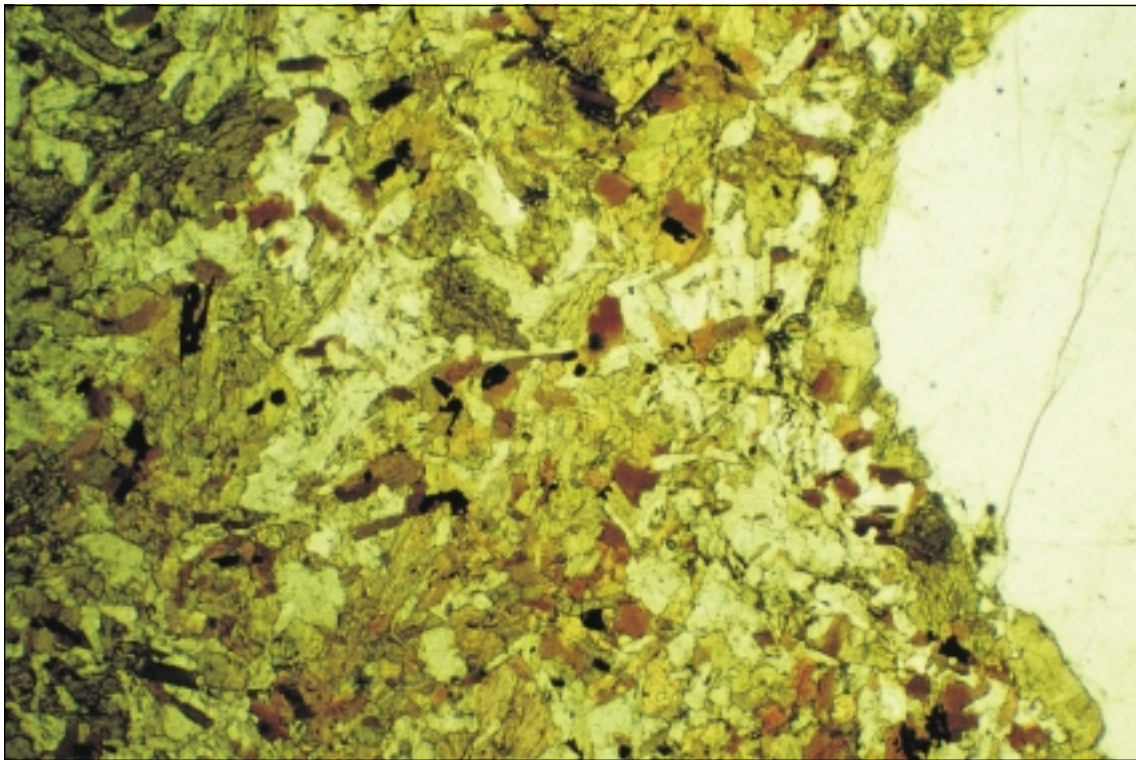


Plate 27

Sample TH6, enclave, Neils Rocks. Part of an anhedral quartz phenocryst in a groundmass of biotite, amphibole, plagioclase and minor quartz. Plane polarised light, field of view 4.4×2.9 mm.

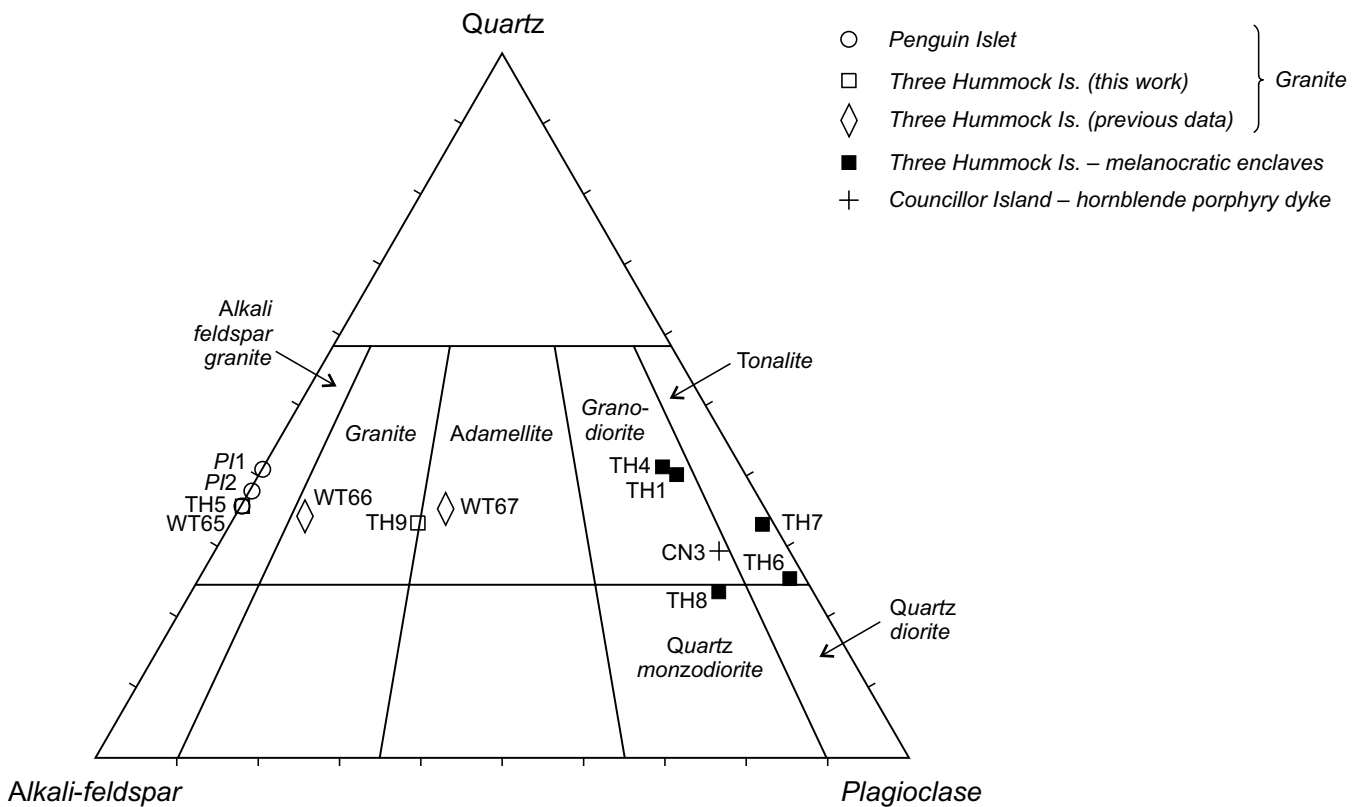


Figure 11

Quartz (Q)-alkali feldspar (A)-plagioclase (P) plot of pseudomodes (calculated from chemical analyses) of granites from Penguin Islet, granites and melanocratic enclaves from Three Hummock Island, and hornblende porphyry from Councillor Island. Some additional data (3 analyses) from Sawka et al. (1990) and B. W. Chappell (database). Granitoid classification of Streckeisen (1973) also shown.

Table 6
Chemical analyses, Penguin Islet and Three Hummock Island

Sample No.	PI1	PI2	TH5	TH9	WT65	WT66	WT67	TH1	TH4	TH6	TH7	TH8
SiO ₂ (wt%)	73.70	74.25	72.93	70.05	73.19	72.71	72.60	61.63	61.42	51.84	56.31	55.70
TiO ₂	0.17	0.10	0.19	0.55	0.21	0.21	0.20	0.88	1.53	1.77	1.56	1.57
Al ₂ O ₃	13.87	14.36	14.28	14.66	14.50	14.65	14.85	15.92	15.96	15.63	15.44	15.26
Fe ₂ O ₃	0.43	0.31	0.29	0.49	0.24	0.13	0.13	0.83	0.98	1.41	1.31	1.38
FeO	0.90	0.52	1.11	2.68	1.19	1.31	1.29	5.21	6.05	7.78	6.88	6.74
MnO	0.04	0.03	0.05	0.05	0.06	0.05	0.04	0.09	0.11	0.16	0.14	0.14
MgO	0.34	0.24	0.38	0.89	0.39	0.42	0.48	3.40	2.53	7.01	5.18	5.54
CaO	0.63	0.35	0.87	1.46	0.91	1.00	1.12 ^O	3.21	3.01	7.60	6.70	6.79
Na ₂ O	2.76	3.26	3.41	2.70	3.37	3.40	3.13	2.66	2.54	1.68	1.93	2.55
K ₂ O	4.60	4.58	4.46	5.50	4.63	4.76	4.73	2.87	2.71	2.52	2.36	2.29
P ₂ O ₅	0.16	0.22	0.17	0.15	0.20	0.22	0.16	0.55	0.36	0.42	0.38	0.34
H ₂ O ⁺	1.35	0.94	0.72	0.76	0.89	0.87	1.06	2.04	2.21	1.94	1.76	1.74
H ₂ O ⁻	nd	nd	nd	nd	0.17	0.18	0.19	nd	nd	nd	nd	nd
CO ₂	0.11	0.12	0.04	0.05	0.09	0.06	0.06	0.11	0.13	0.06	0.08	0.05
SO ₃	0.10	0.05	0.08	0.07	nd	nd	nd	0.06	0.09	0.09	0.08	0.08
Total	99.14	99.33	98.98	100.06	100.04	99.97	100.04	99.44	99.63	99.91	100.17	100.17
Sc (ppm)	6	3	2	9	nd	nd	nd	12	19	27	22	23
V	11	4	13	39	10	10	10	69	180	220	180	180
Cr	8	6	9	19	5	4	8	81	10	170	120	140
Co	<8	<8	<8	<8	nd	nd	nd	18	12	35	27	30
Ni	6	6	11	8	1	1	<1i	48	19	90	65	68
Cu	90	<5	<5	9	<1	<1	<1u	<5	18	<5	6	8
Zn	39	38	43	52	42	48	32	150	95	105	83	92
Ga	19	22	18	17	20.2	20.0	18.8	21	20	18	17	19
As	2000	<20	<20	<20	nd	nd	nd	<20	<20	<20	<20	<20
Rb	660	670	500	310	491	434	318	580	560	265	200	195
Sr	52	90	71	105	50	60	76	220	140	330	330	300
Y	16	12	15	35	18	19	15	26	40	38	37	37
Zr	80	52	78	200	76	90	102	320	255	200	195	190
Nb	33	40	23	18	24.5	22.0	16.0	53	53	29	27	26
Mo	<5	<5	<5	<5	nd	nd	nd	<5	<5	<5	<5	<5
Sn	494	34	22	<9	nd	nd	nd	<9	<9	12	<9	10
Ba	163	80	176	678	135	190	340	227	399	445	473	436
La	23	<20	20	37	17	21.8	24.1	46	30	32	27	35
Ce	96	<28	<28	64	40	49.3	54.4	83	87	107	77	90
Nd	<20	<20	<20	41	nd	22.2	21.6	40	41	58	48	56
W	37	22	11	<10	nd	nd	nd	<10	10	<10	<10	<10
Pb	31	19	28	36	26	27	34	13	16	12	16	14
Bi	5	<5	<5	<5	nd	nd	nd	<5	<5	<5	<5	<5
Th	15	10	11	17	13.8	17.0	20.0	18	23	15	16	16
U	18	<10	<10	<10	5.6	8.0	5.6	<10	25	<10	<10	<10
K/Rb	58.1	57.1	74.1	147.1	78.1	91.1	123.1	41.1	40.1	79.1	98.1	97.1
ASI	1.300	1.311	1.188	1.123	1.188	1.166	1.207	1.195	1.268	0.809	0.862	0.802
FeO*	1.29	0.80	1.37	3.12	1.41	1.43	1.43	5.96	6.93	9.05	8.06	7.98

nd: not determined

WT65 from database of B. W. Chappell (unpublished)

WT66 and WT67 from Sawka *et al.* (1990)

Key to samples:	PI1	Granite, Penguin Islet [CR147060]
	PI2	Granite, Penguin Islet [CR146058]
	TH5	Granite, Chimney Corner [CR 168202]
	TH9	Granite, west of Neils Rock [CR 198172]
	WT65	Granite, Cape Rochon [CR 264264]
	WT66	Granite, Coulomb Bay [CR 204241]
	WT67	Aplite, Three Hummock Island airstrip [CR 172213]
	TH1	Melanocratic enclave, Chimney Corner [CR 167201]
	TH4	Melanocratic enclave, Chimney Corner [CR 166202]
	TH6	Melanocratic enclave, west of Neils Rock [CR 198172]
	TH7	Melanocratic enclave, west of Neils Rock [CR 198172]
	TH8	Melanocratic enclave, west of Neils Rock [CR 198172]

Table 7

CIPW Norms, granite and enclaves; hornblende porphyry

Sample No.	PI1	PI2	TH5	TH9	WT65	WT66	WT67	TH1	TH4	TH6	TH7	TH8	CN3
Q	39.07	37.67	33.99	27.80	33.48	32.00	33.13	21.92	24.11	3.75	11.98	8.07	16.95
C	3.67	4.00	2.72	1.98	2.80	2.64	2.97	4.03	4.36	-	-	-	-
Or	27.85	27.55	26.85	32.76	27.66	28.44	28.30	17.43	16.47	15.22	14.20	13.76	14.42
Ab	23.92	28.08	29.39	23.03	28.82	29.09	26.82	23.14	22.10	14.52	16.62	21.94	29.73
An	2.13	0.30	3.26	6.31	3.24	3.56	4.56	12.67	12.94	28.29	26.99	23.84	22.29
Di	-	-	-	-	-	-	-	-	-	6.06	3.53	6.66	0.41
Hy	1.98	1.20	2.57	5.96	2.75	3.12	3.24	16.51	14.68	25.62	20.80	19.83	11.96
Mt	0.63	0.45	0.42	0.71	0.35	0.18	0.18	1.23	1.46	2.08	1.93	2.03	2.01
Il	0.33	0.19	0.36	1.05	0.40	0.40	0.38	1.71	2.98	3.43	3.01	3.03	1.35
Ap	0.37	0.50	0.39	0.34	0.46	0.50	0.36	1.28	0.84	0.97	0.88	0.78	0.81
TOTAL	99.95	99.94	99.95	99.94	99.96	99.93	99.94	99.92	99.94	99.94	99.94	99.94	99.93
100An/(An + Ab)	8.18	1.06	9.98	21.51	10.11	10.90	14.53	35.38	36.93	66.08	61.89	52.08	41.41
Key to samples:	CN3	Hornblende porphyry, Councillor Island [BR569873] For key to other samples see Table 6.											

plagioclase (molar An < 10) is classed as an alkali feldspar. Both samples from Penguin Islet classify as alkali feldspar granite.

Discussion

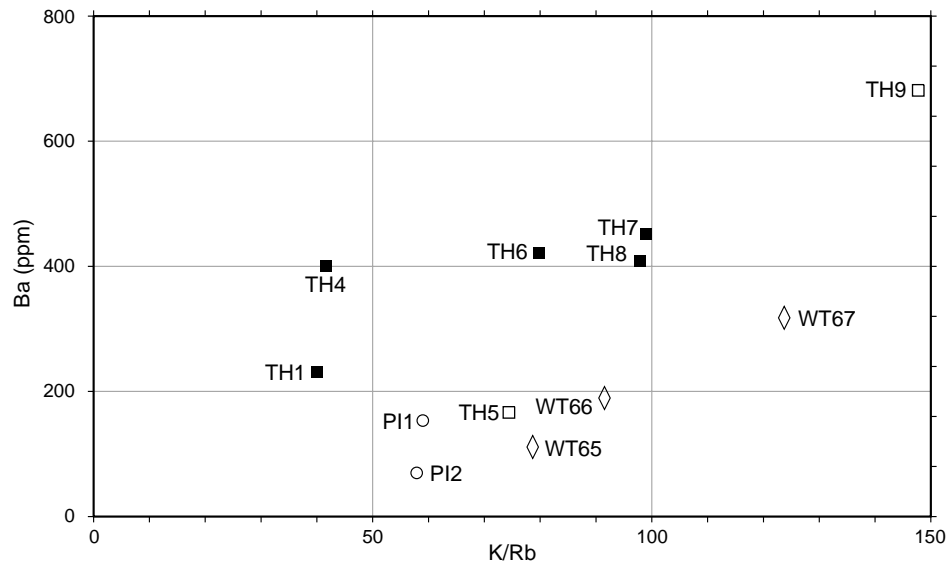
The Three Hummock Island and Penguin Islet granites may be classified as S-types (i.e. derived by partial melting of a supracrustal or sedimentary protolith; e.g. Chappell and White, 1974, 1992; Hine *et al.*, 1978). Although no definite restite minerals were identified, diagnostic criteria are their moderately to strongly peraluminous character, relatively high K₂O relative to Na₂O, high P₂O₅ and low Y, REE and Th, and red-brown colour (in thin section) of biotite. This is consistent with previous assignments of the Three Hummock Granite as S-type (McClenaghan *et al.*, 1989; Sawka *et al.*, 1990; Chappell *et al.*, 1991) and a member of the Interview Suite (also known as the Sandy Cape Suite) together with the Sandy Cape/Interview River pluton. Sawka *et al.* (1990) also includes the Conical Rocks pluton (also known as the Pieman Heads pluton) in this suite, whilst the other authors assign it to the Pieman Suite.

Provided that the influence of hydrothermal fluids is not intense, rubidium increases with fractionation in felsic melts (e.g. Blevin and Chappell, 1992). Chappell and White (1992) suggest that, in the Lachlan Fold Belt at least, granites with more than 250 ppm Rb are likely to have been modified by feldspar fractionation, which supersedes restite unmixing as the main differentiation mechanism at about this stage of their evolution. The Three Hummock Island granite is therefore fractionated, as analyses have more than 300 ppm Rb (Table 6) and samples are petrographically not strongly altered. The Penguin Islet samples and (marginally) the Chimney Corner sample, have Rb >> 500 ppm, and are thus highly fractionated. These new data, together with the gravity interpretation of Leaman and Richardson (1989), suggest that the pluton shelves gently

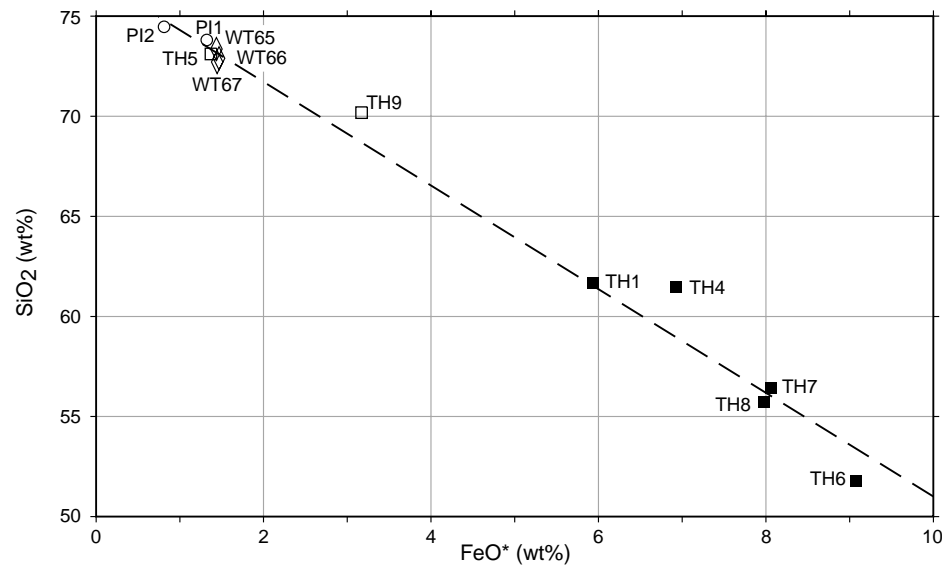
southwestward, with a highly fractionated cupola being exposed at Penguin Islet.

The data for each element were examined for correlations with K/Rb, used as a fractionation index (*decreasing* with fractionation). Only CaO and Ba (fig. 12a) show well defined strong positive correlations, suggestive of fractionation of plagioclase. Sr shows a poorer positive correlation with K/Rb, mainly due to a slightly high value in the most fractionated sample (PI2). Zr, TiO₂ and total FeO also show weak positive correlations, but are strongly correlated with each other (fig. 12c, f) and are markedly higher in sample TH9. This suggests the involvement of biotite (with zircon inclusions), possibly as restite separation. Weak negative correlations are displayed by Pb and possibly Th, and may indicate removal of accessory phases such as monazite. SiO₂, Nb, Ga and possibly P₂O₅ display moderate to weak negative correlations indicating an increase with fractionation and, in the case of these trace elements, essentially incompatible behaviour.

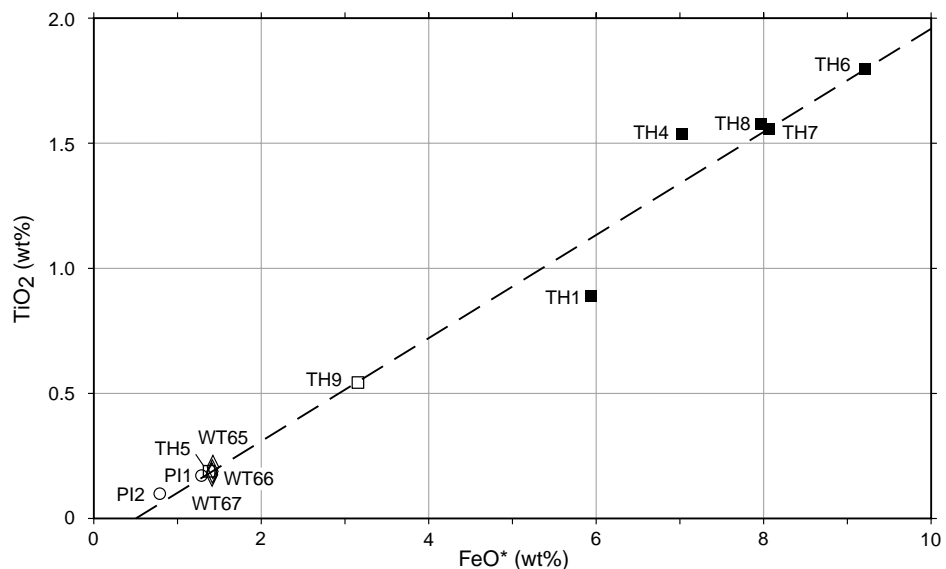
The weak magnetic response of the Three Hummock Island granite, at both the sample susceptibility and aeromagnetic survey scale (fig. 3, 4), suggests that it is a relatively reduced, 'ilmenite-series' (Ishihara, 1977) granite. However the analysed Fe₂O₃/FeO ratios (0.1 to 0.6), assuming them to be primary and not altered by secondary oxidation and weathering, are only moderately low. This strongly fractionated and relatively reduced nature is favourable for tin-tungsten mineralisation (Blevin and Chappell, 1992, 1995); strong fractionation is thought to be particularly critical in S-types, as unfractionated S-types are rarely mineralised. On the diagrams (e.g. Fe₂O₃/FeO against Rb, fig. 13; Fe₂O₃/FeO against total FeO* or SiO₂, not shown) of Blevin and Chappell (1992, 1995) the Three Hummock Island granite plots in the fields defined by Lachlan Fold Belt granites that are associated with tin (tungsten) mineralisation. The Penguin Islet granite is more fractionated than these authors' field, but this



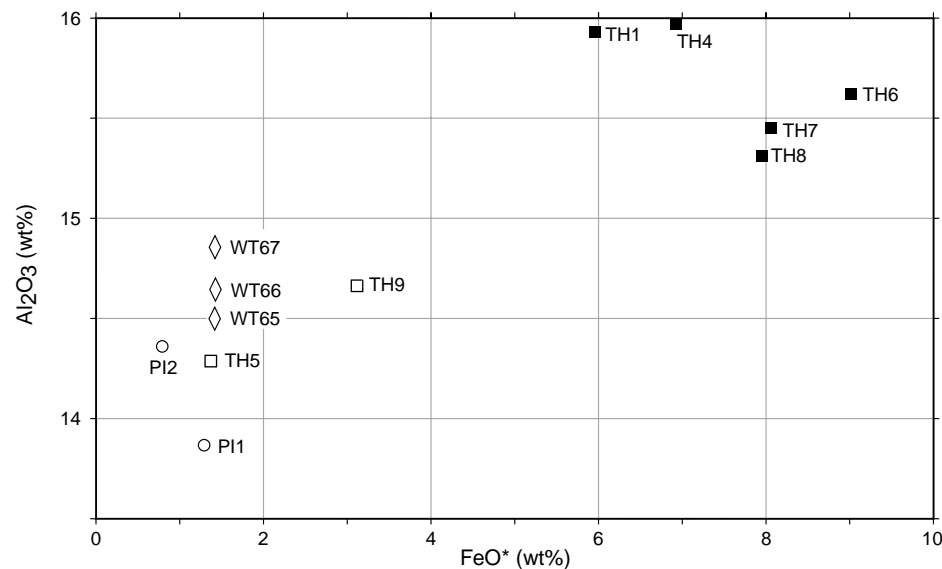
(a) Ba against K/Rb



(b) SiO₂ against total iron (FeO*)



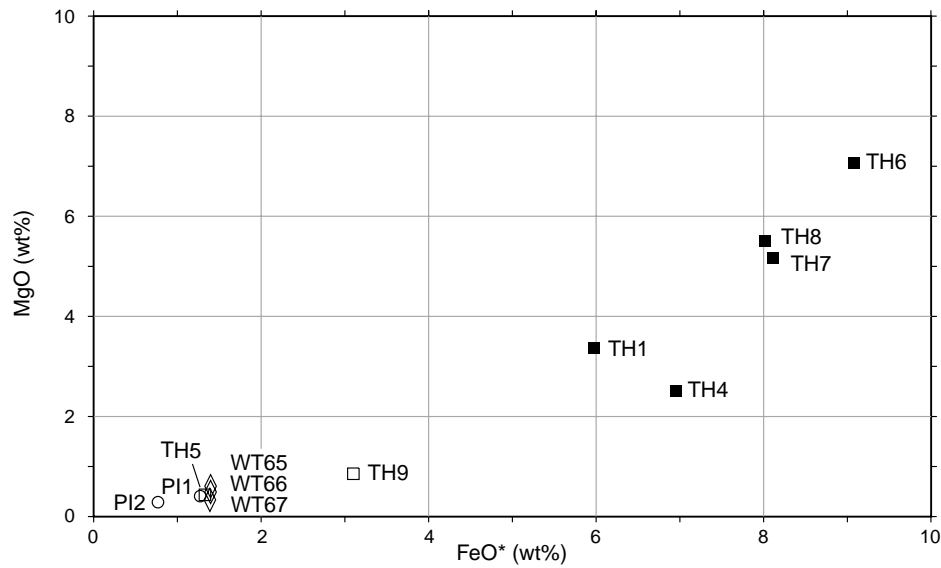
(c) TiO₂ against FeO*



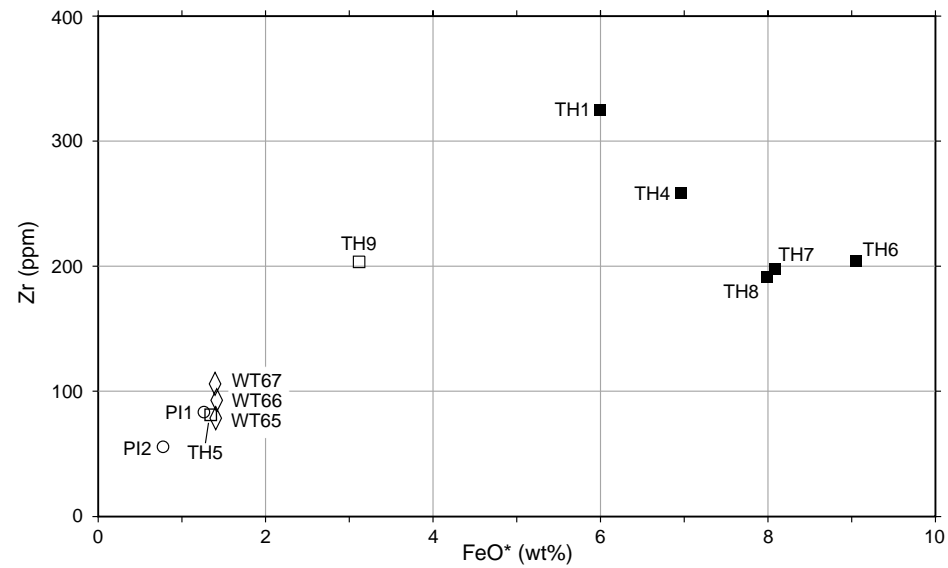
(d) Al₂O₃ against FeO*

Figure 12

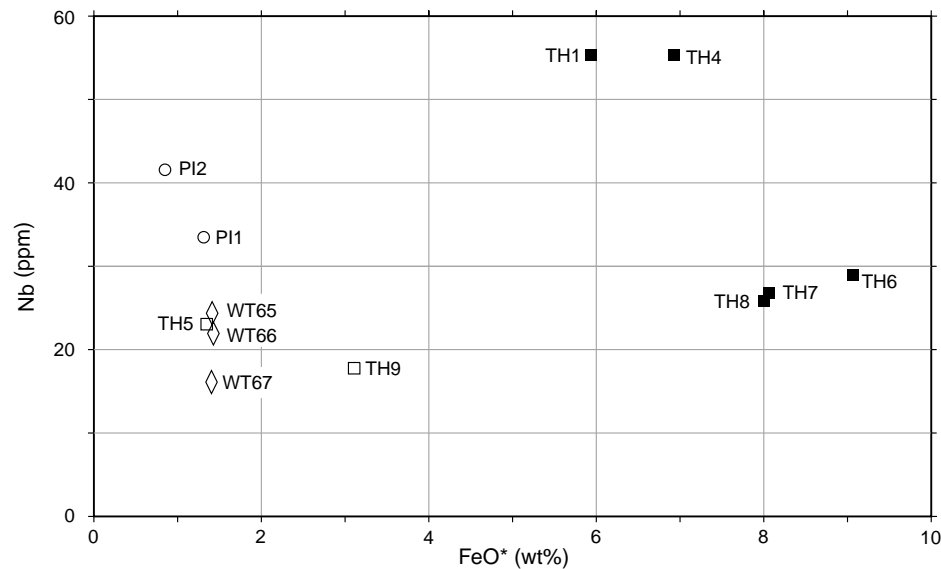
Selected variation diagrams of granites from Penguin Islet and granites and melanocratic enclaves from Three Hummock Island.



(e) MgO against FeO*



(b) Zr against FeO*



(c) Nb against FeO*

- Penguin Islet
 - Three Hummock Island (this work)
 - ◇ Three Hummock Island (previous data)
 - Three Hummock Island – melanocratic enclaves
- } Granite

Figure 12 (continued)

Selected variation diagrams of granites from Penguin Islet and granites and melanocratic enclaves from Three Hummock Island.

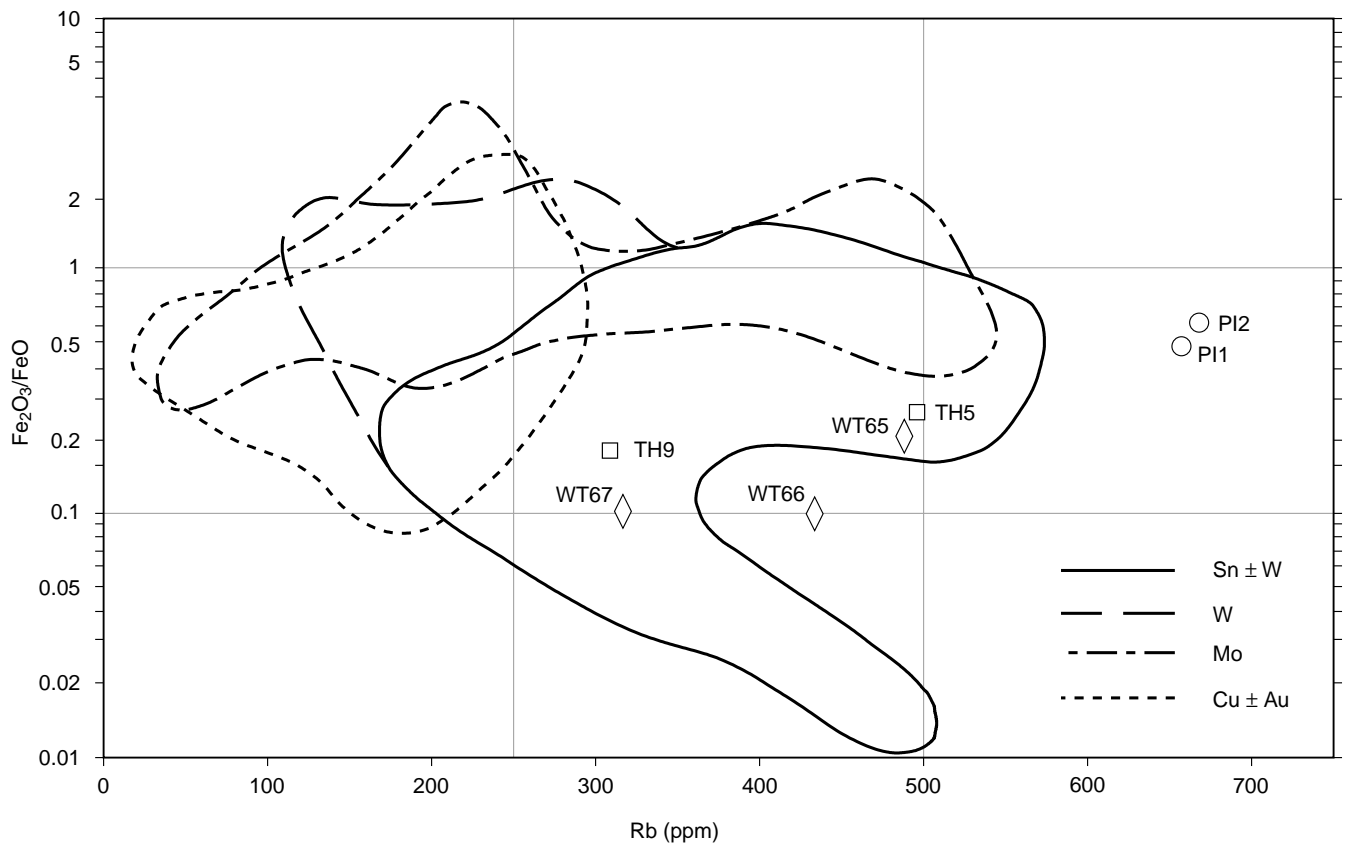


Figure 13

Plot of Fe_2O_3/FeO against Rb for granites from Penguin Islet and Three Hummock Island. Generalised fields for Sn-W, W, Mo and Cu-Au mineralised granitoids in the Lachlan Fold Belt (after Blevin and Chappell, 1992) also shown.

upgrades rather than downgrades its potential. In contrast, granites with associated copper and molybdenum mineralisation are generally more oxidised than these granites, and in particular copper-associated types are generally unfractionated oxidised I-types.

Geochemistry of melanocratic enclaves

The enclaves display a considerable range in major element chemistry.

Those at Chimney Corner (TH1 and TH4) are intermediate ('andesitic') in composition and plot as granodiorites in the QAP classification diagram (fig. 11) of Streckeisen (1973). They share some features of their host, such as peraluminous character ($ASI > 1$ and normative C), high K_2O/Na_2O and high Rb. Sample TH4 is richer in TiO_2 and poorer in MgO than TH1; this is reflected in higher V and lower Ni and Cr.

The enclaves from near Neils Rock are more mafic and most plot in the tonalite field. They are meta-aluminous and less like the host granite, although they also have high K_2O/Na_2O . The most mafic sample, TH6, is normatively a quartz tholeiite, but few known lavas have such high K_2O and P_2O_5 and low Na_2O .

The enclaves are much richer in the compatible elements Ni, Cr, Co, V and Sc than their host granites; these values are more typical of mafic mantle-derived magmas. The levels of incompatible elements, notably

Rb, Zr, Nb, the REE and Th, are broadly similar to levels in the granites.

Discussion

Although enclaves similar to these have been described in granitoids world-wide, particularly relatively mafic ones, there is no consensus as to their origin. Interpretations that have been proposed fall into three main categories:

- that they represent modified fragments ('restite') of the granitoid's source rock;
- that they represent re-incorporated chilled marginal phases or cumulates genetically related to the host granitoid; and
- that they represent globules of less viscous and more mafic magma that neither completely mechanically mixed nor chemically equilibrated with the host granitoid.

These interpretations are not necessarily mutually exclusive, as there may well be several genetically different types of enclaves. Collins (1996) considers that 'microgranitoid' enclaves occur in both I- and S-type granitoids, whilst 'gneissic' enclaves are restricted to S-types.

In the restite interpretation (e.g. White and Chappell, 1977; Chen *et al.*, 1989), the enclaves represent entrained fragments of modified restite, the residue from the

source rock that partially melted to produce the granite. In this interpretation, the enclaves and the host granites represent varying proportions (more and less) of refractory mafic minerals and a felsic melt. If this were so, the enclaves and the granites should lie on a linear mixing line on simple element-element plots, for every pair of elements (e.g. Chappell *et al.*, 1987). Certain plots, such as SiO₂ and TiO₂ against total iron (FeO*), do show a linear relationship (fig. 12b, c) consistent with simple two end member mixing, but many do not. For example, when plotted against FeO*, MgO (fig. 12e) and CaO (not shown) show curved apparent trends, Zr (fig. 12f) shows divergent trends increasing with FeO* in the granites and decreasing in the enclaves, whilst Al₂O₃ (fig. 12d), Rb (not shown), Nb (fig. 12g) and Ba (not shown) give highly scattered plots. This lack of coherence of enclave compositions and their host compositions, in simple two element variation diagrams, has been noted in other studies (e.g. Flinders and Clemens, 1996). As noted by Vernon (1983) and Elburg and Nicholls (1995), the restite interpretation is also difficult to reconcile with the presence of the 'double enclaves'.

The cumulate or chilled margin interpretation (e.g. Dodge and Kistler, 1990; Flood and Shaw, 1995) is difficult to reconcile with the chemical diversity shown by the enclaves, and especially very mafic compositions such as TH6. The likelihood of a felsic melt in a plutonic environment quenching to produce such fine-grained rocks must also be questioned, whilst there is no petrographic evidence for cumulate textures. The enclaves are typically irregular but more-or-less rounded in form, and angular or joint-bounded shapes, that might be expected if they represent incorporated fragments of solid wall-rock, were not observed.

Both our field observations and geochemical data tend to support the third hypothesis (also advanced by, for example, Reid *et al.*, 1983; Vernon, 1983, 1984; Elburg and Nicholls, 1995) that most of these enclaves represent globules of immiscible mafic magma that were injected and entrained into the granitic melt, but due to contrasts in physical properties such as viscosity and density, did not completely mix with it. However contamination by diffusive interchange of mobile elements, particularly alkalis, occurred. The compatible trace element (Ti, Sc, V, Cr, Co, Ni) signature of the enclaves remained that of a mantle-derived magma, whilst the alkali and incompatible trace element (Rb, Sr, Zr, Nb, Ba, Ce) signature is dominated by contamination from the host granite. The 'double enclaves' may have been produced by the coalescence of two or more globules of mafic magma that were at different stages of mixing and equilibration with the host.

The enclave TH10 is clearly different from the others and may well be an igneous cumulate or true xenolith.

Robbins Island (Marys Island and Guyton Point)

This area on northeastern Robbins Island was briefly examined, partly because it lies on one of a number of strong linear north-trending magnetic anomalies thought to indicate Neoproterozoic basalt in the basement. However no basement rocks are exposed. Only Tertiary basalt, previously described by Sutherland (1980), was found. These rocks are insufficiently magnetic and probably too thin to account for the anomaly.

Basalt crops out on the north, east and south shores of Marys Island, a small crudely circular headland about 100 m across and joined on its western side to Robbins Island by a short sandy to cobbly tombolo near or just above high water mark. The basalt is dark grey to black where fresh, weathers khaki-green to brown, and is massive to slightly amygdaloidal or vesicular. A distinct tabular, flaggy to platy appearance is caused by numerous subparallel, subhorizontal to shallowly dipping fractures, typically 100–300 mm apart, which pervade the rock. Individual fractures are not usually traceable far before branching or petering out, but overall they control the weathering surfaces and outcrop style. This platy fabric is consistent in orientation at any particular locality, but overall it is warped to define a domal structure, dipping away from the centre of the 'island' (059SE18 on southern side; 150E10 on eastern side, 038NW17 on northern side). Vertical fractures are not prominent and columnar jointing has not developed. The domal structure is probably an original igneous cooling feature and may indicate an undulating irregularity in either the base or eroded top of the flow. There is no evidence for an immediately local eruptive centre, although there is no outcrop in the centre of the 'island'.

Basalt crops out at the top of the beach between Marys Island and Guyot Point. At the northern end, on the south side of Guyot Point, low flat outcrops of soft weathered khaki-brown muddy to silty sediment, described as vitric tuff by Sutherland (1980), underlie 'knobby' basalt with irregularly and closely-spaced jointing. The sediments have a fine, diffuse horizontal bedding lamination. The contact is irregular but grossly subhorizontal and can be followed eastward around the southern side of Guyot Point. The overlying black basalt is fine grained, more-or-less aphyric, moderately vesicular and hard but brittle. Semi-continuous exposure of basalt continues in mostly low jagged outcrops amongst beach boulders around to the northern side of the point, where poorly developed columnar jointing appears. 'Megapillow' lavas and minor hyaloclastites were reported by Sutherland (1980) further to the west towards Big Bluff.

Petrography

A thin section (RI1; plate 28) of the flaggy basalt from Marys Island shows that it is a slightly altered holocrystalline porphyritic rock, containing abundant,

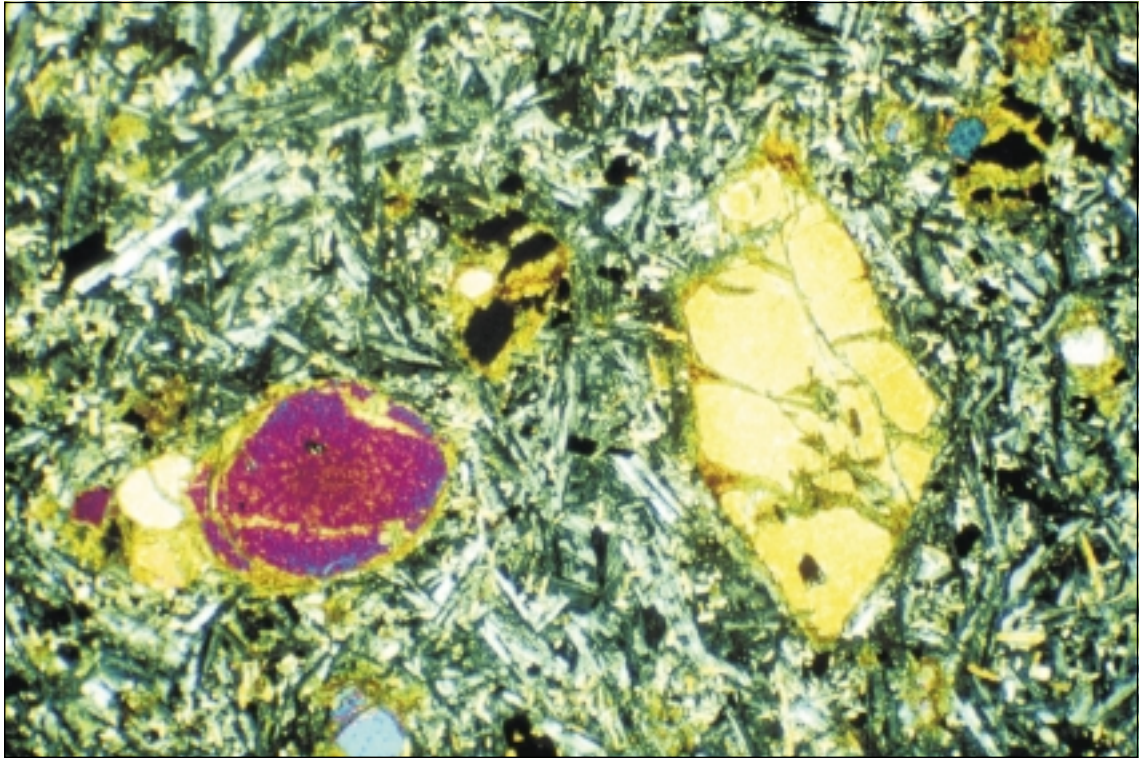


Plate 28

Sample RI1, Tertiary basalt (nepheline hawaiiite), Marys Island (Robbins Island). Olivine phenocrysts in a medium-grained intergranular groundmass. Crossed nicols, field of view 4.4×2.9 mm.

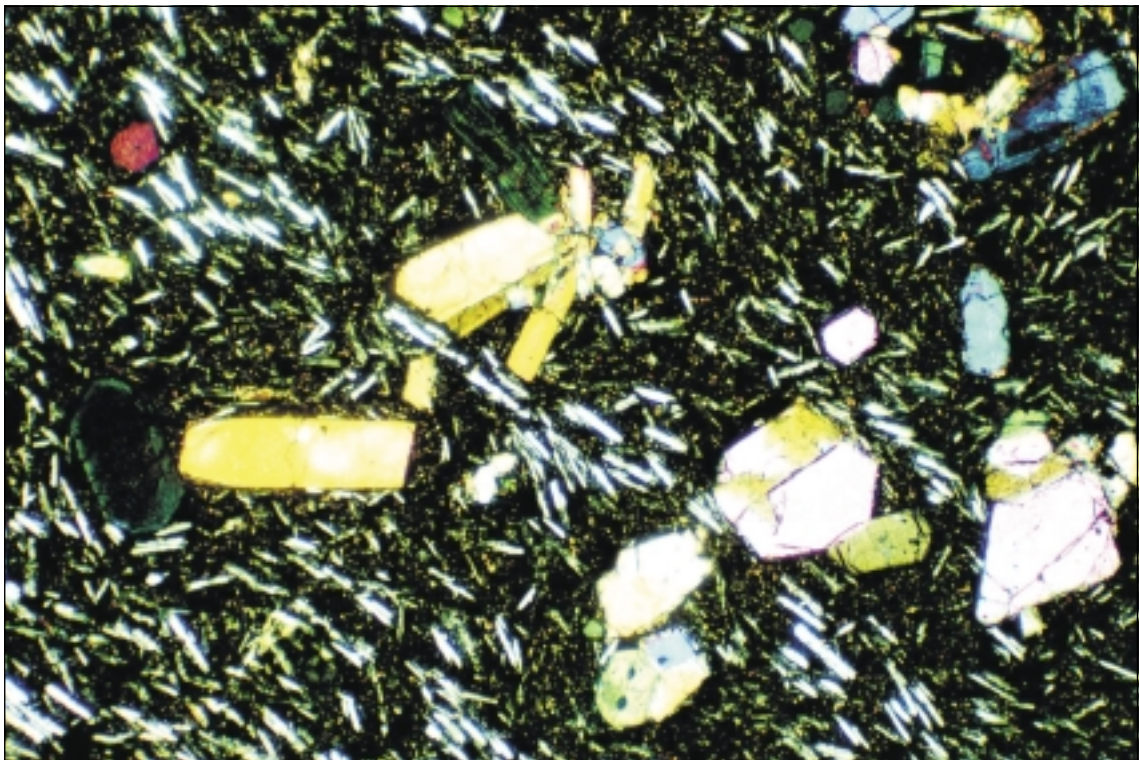


Plate 29

Sample RI3, Tertiary basalt (hawaiiite), Guyot Point (Robbins Island). Olivine and titanite phenocrysts in a fine-grained fluidal groundmass. Crossed nicols, field of view 4.4×2.9 mm.

euhedral to subhedral, slightly rounded olivine phenocrysts (500 μm to 2 mm across) and glomerocrysts, commonly altered to fine-grained green to brown iddingsite/bowlingite around their margins and along fractures. The relatively coarse-grained intergranular groundmass consists mainly of ragged elongate plagioclase subhedra (up to 500 μm , but commonly 100–200 μm) and pale pink, weakly titaniferous augite. There are some slightly coarser grained late segregations of strongly zoned plagioclase and zeolite. Opaque minerals and small quantities of finely acicular apatite are accessories. Zeolite also fills the scattered spherical amygdales. X-ray diffraction showed that the zeolite minerals are phillipsite and analcime; smectite, ilmenite and possible nepheline were also detected. Patches of greenish 'bowlingitic' alteration (probably the smectite phase) occur throughout the groundmass. The rock is petrographically an alkali basalt.

Two similar samples from the southern and northern sides of Guyot Point (RI3 and RI4) are difficult to distinguish from RI1 in hand specimen, but in thin section (plate 29) are much darker and texturally quite different. They also contain abundant but generally euhedral, angular and unrounded olivine phenocrysts (up to 1.5 mm), and also pale yellow-pink titanite phenocrysts (<1 mm), commonly clumped into rosette-like glomerocrysts. Both olivine and titanite grade down in grain size to a fine-grained fluidal groundmass of aligned small plagioclase laths (100–200 μm) and a dark mesostasis which under high magnification can be resolved into deep mauve-pink titanite and very abundant, mostly equant opaque minerals (10–20 μm across). Some patches of pale brownish-yellow alteration, probably a smectite group mineral, occur both in the groundmass and partly or completely replacing a few olivine phenocrysts. X-ray diffraction failed to detect any nepheline (or zeolite) in the mesostasis, but this phase may be occult as glass. The rocks are petrographically alkali basalts like RI1, and the textural differences are probably mainly due to more rapid cooling. They petrographically resemble Tertiary basanite from near Montagu, on the Tasmanian mainland ten kilometres to the southwest (Seymour and Baillie, 1992 J. L. Everard, unpublished data).

Geochemistry

The major element chemistry of all three samples (Tables 3, 4) is quite similar. The samples from Guyot Point (RI3 and RI4) are classified as hawaiites ($ne < 5$; $30 < An < 50$) in the nomenclature scheme of Johnson and Duggan (1989). The rock from Marys Island (RI1) differs mainly in having higher Na_2O and perhaps lower CaO . Because of the higher total alkali content, it is classified as a nepheline hawaiite ($ne > 5$; $30 < An < 50$). All are moderately potassic and moderately fractionated.

The trace element chemistry is also mostly typical of moderately fractionated, fairly alkalic basalts, with

depleted Ni and Cr, and high Nb/Y ratios. The Marys Island sample (RI1) has much lower Rb and Sr than the Guyot Point samples (or indeed than any similar basalt from northwest Tasmania; e.g. Everard, 1989; Brown, 1989), but other incompatible elements (P_2O_5 , Zr, Nb, Ce) are broadly similar. Although Rb and Sr are relatively mobile with weathering and alteration, and Sr may be depleted by plagioclase fractionation, there is little petrographic evidence for these processes in RI1. As such large variations in incompatible element ratios (e.g. Rb/Zr) are not attributable to low pressure crystal fractionation and are unlikely to be due to different degrees of partial melting, different mantle sources may be implied. In particular, the mantle source of RI1 may have lower Rb/Zr and Sr/Zr ratios, or contain a residual phase which buffered Rb and Sr at low levels. The similar REE and Y contents suggest that amphibole was not involved as a high pressure fractionating phase.

Petrel Islands and Walker Island

Whilst passing it was noted that the Petrel Islands and Cape Buache, at the northern tip of Walker Island, all consist of orthoquartzite. Dips of 35° to the west (Petrel Islands) and 30° to the southwest (Cape Buache) were estimated.

Dredging

The results of dredging are summarised in Table 8 and Table 9.

East of King Island (264 290 mE, 5 577 390 mN; 264 620 mE, 5 577 390 mN)

These localities lie in a NNE-trending zone of relatively subdued magnetics about six kilometres wide (fig. 3). This zone lies east of the main NNE-trending positive linear positive anomaly which extends onshore to southeast King Island and corresponds to a Neoproterozoic basalt sequence, and west of a similar trending but less well defined linear positive anomaly. A sedimentary or volcanosedimentary sequence of similar age was suspected.

Attempts to obtain samples from depths of 13 to 15 metres at these localities using the Vanveen dredge recovered only sand.

Hope Channel

A strong magnetic anomaly, thought to indicate the contact aureole of the Three Hummock Island Granite, occurs just offshore between Three Hummock Island and Hunter Island (fig. 14). A lobe of the anomaly extends onshore at Three Hummock Island, southeast of Chimney Corner, in an area mapped as 'stabilized recent dune terrain', without bedrock outcrops, by Jennings (1976).

Sixteen pipe dredge hauls over the inferred aureole, from water depths of from 10 m to 39 m, were attempted. Locations are plotted on Figure 14 and

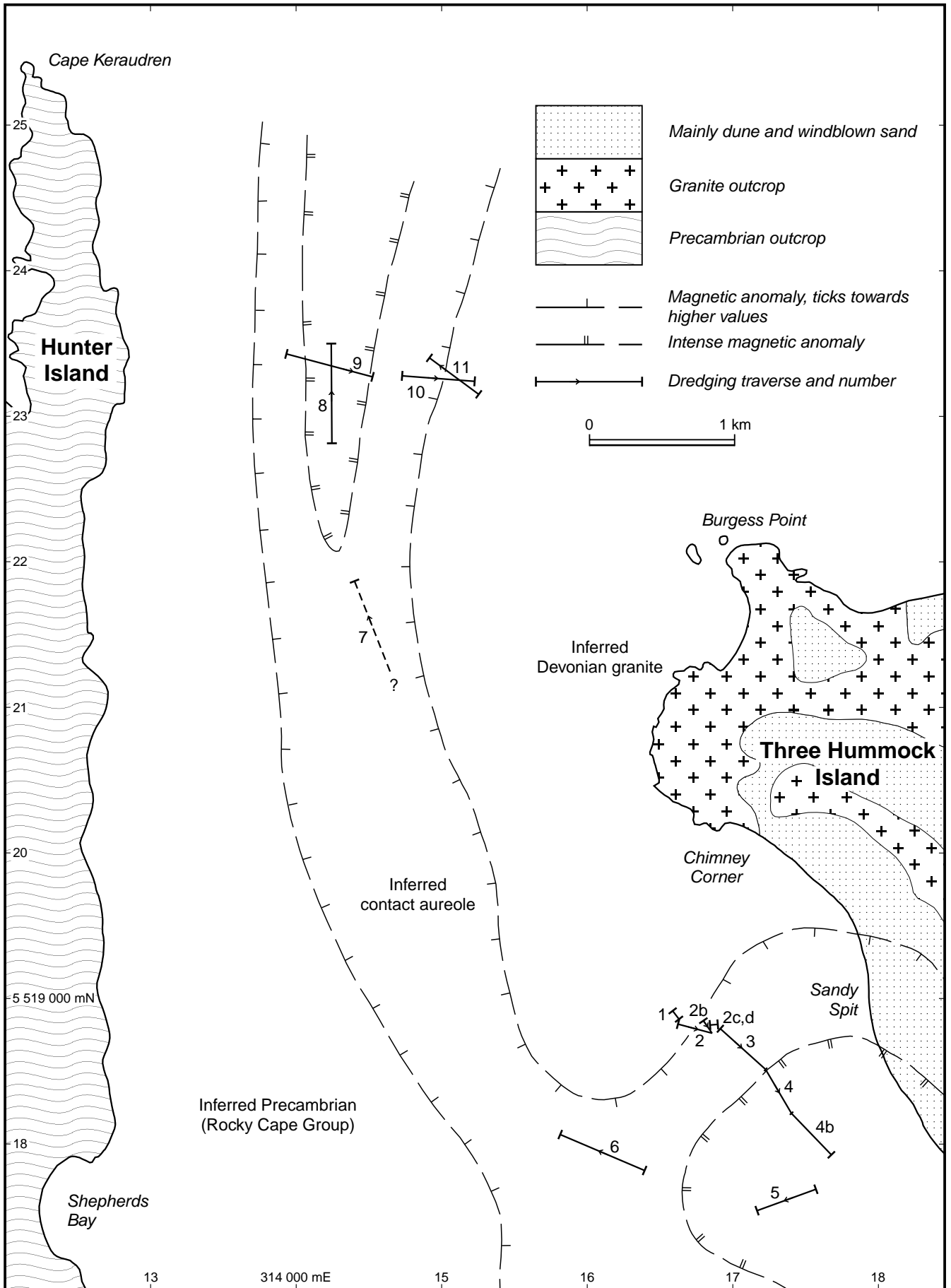


Figure 14

Location of dredging traverses, Hope Channel, showing onshore geology (after Jennings, 1976 and unpublished) and approximate position of magnetic anomaly, interpreted as contact metamorphic aureole of granite (after AGSO 1994 offshore survey, east-west flight lines 800 m apart).

Table 8
Summary of dredging results, Hope Channel

<i>Start of leg</i>	<i>Finish of leg</i>	<i>Distance (m)</i>	<i>Bearing (°)</i>	<i>Mean depth (m)</i>	<i>Sample</i>	<i>Reg. No.</i>	<i>Field description</i>	<i>Preparation</i>
16381904	16411901	40	135	19.7	HC1	004851	sandy limestone pebbles	
16411898	16621892	220	106	14.5	HC2	004852	sandy limestone pebbles	
16571901	16621892	100	151	18.5	-	-	no sample obtained	
16621898	16671899	50	79	17.7	-	-	no sample obtained	
16691896	17011869	420	130	15.0	HC3	004853	sandy limestone pebbles	
17011869	17201838	360	148	11.4	HC4	004854	sandy limestone pebbles	
17201838	17441811	360	138	10.5	-	-	sand, not collected	
17381786	16981770	590	248	23.6	HC5	004855	sandy limestone pebbles, sand, shells	
16201796	15721819	530	296	23.1	HC6	004856	sandy limestone pebbles, rare quartz, sand, shells	
c.14302120	13982185	c.720	334	22.5	HC7	004857	pebbles of basalt, quartzite and limestone; sand, shells	TS (basalt)
13792280	13752348	680	357	19.0	HC8	004848	sandy limestone pebbles	
13452341	14042327	610	103	39-14	HC9	004859	limestone solution tubes, sandy limestone	
14252328	14772326	520	92	19.0	HC10	004860	sandy limestone pebbles	
14892317	14442341	510	298	18.7	HC11	004861	two pebbles of sandy limestone	

Bearings true, relative to grid north
Location (AMG) determined by GPS (± 10 m)
Depths determined by echo sounder

details are given in Table 8. Unfortunately no definite bedrock samples were obtained.

The most varied sample was from near 313 960 mE, 5 521 820 mN at 22.5 m water depth. This included three small subrounded pebbles (<35 mm) of dark brown weathered Tertiary basalt, seven pebbles (8 to 20 mm) of pale yellow-brown quartzite similar to that of the Rocky Cape Group, and about 15 fragments of sandy textured Cainozoic limestone as flat subrounded pebbles (15 × 100 mm) to small irregular pebbles and granules (<10 mm).

At ten of the other dredge sites the only rock recovered was Cainozoic limestone, apart from rare quartz fragments at one site. The samples typically consisted of a few small (20–50 mm), irregularly rounded, subrounded, subangular to sometimes platy pebbles of grey to yellow brown or occasionally off-white, sometimes very porous sandy limestone. Large limestone solution tubes together with pebbles were also recovered at one site.

Only sand was recovered at one site, and no sample was obtained at four other sites.

Petrography – basalt

A thin section (HC7) of a basalt pebble shows that it is a vesicular, aphyric rock with an intersertal to slightly subophitic texture. It consists of plagioclase laths (<200 μ m), colourless augite granules (<100 μ m), angular and elongate to acicular opaque minerals and a brownish-green fine-grained altered interstitial

mesostasis. It is probably an evolved tholeiitic to transitional basalt, very likely of Tertiary age.

Discussion

The degree of rounding suggests that none of the material recovered was local basement. The source of the quartzite is very likely northwest Hunter Island, a few kilometres to the west. The origin of the Tertiary basalt pebbles is more problematical. No basalt is known on Hunter Island and a small area on Three Hummock Island is on the further eastern side. Petrographically similar basalt crops out at Cape Grim, Little Trefoil Island (Sutherland and Corbett, 1967) and probably Steep Island. These lie on the other side of Hunter Island, but it seems possible that the pebbles have been transported a considerable distance on the sea floor by the locally strong tidal currents. Alternatively there may be basalt flows, whether originally subaerial or subaqueous, concealed on the shallow sea floor in the more immediate area. Note that similar basalt beach pebbles occur on nearby Penguin Islet (see above).

Southeast of Albatross Island

(‘Anomaly Alpha’ – 302 110 mE, 5 525 770 mN)

This locality lies on the southern flank of a small positive magnetic anomaly centred about one kilometre ESE of Albatross Island (fig. 3).

A pipe dredge sample from a mean depth of 61 m contained, in addition to sand and shelly material, mostly well-rounded pebbles (20–120 mm) of basalt (about 40% by volume), and very irregularly shaped,

Table 9
Summary of dredging results, western Bass Strait

<i>Anomaly No.</i>	<i>Grid ref.</i>	<i>Locality</i>	<i>Mean water depth (m)</i>	<i>Dredge type</i>	<i>Material recovered</i>	<i>Sample</i>	<i>Preparation</i>
-	BR64297739	E of King Island	14	Vanveen	sand only		
-	BR64627812	E of King Island	14	Vanveen	sand only		
Anomaly alpha	BQ02112577	SE of Albatross Island	61	Pipe	Tertiary basalt	alpha-1 alpha-2 alpha-3	TS TS TS
					Cainozoic limestone Proterozoic(?) quartzite sand, shells		
Anomaly beta	BR95242355	SW of Albatross Is	59	Pipe	Tertiary basalt	beta-1	TS
					beta-2 beta-4 Proterozoic(?) orthoquartzite Recent(?) limestone sand, shells, organic material	TS TS beta-3	TS
Anomaly gamma-1	BR93163220	NW of Albatross Is	65	Pipe	Tertiary(?) basalt Cainozoic limestone sticky to clotted pale grey mud		
Anomaly gamma-2	BR92843349	NW of Albatross Is	44-58	Pipe	Tertiary basalt	gamma-2-1 gamma-2-2 gamma-2-3 gamma-2-4	TS TS TS, PA TS
					Cainozoic limestone Precambrian(?) orthoquartzite		
Anomaly delta	BR69321465	W of Black Pyramid	68	Pipe	Cainozoic limestone sand		

angular pebbles and cobbles (20–150 mm) of Tertiary (in part Recent?) limestone (about 50% by volume). A single well-rounded pebble (70 mm) of pale yellow-brown quartzite is cemented to smaller (20–30 mm) pebbles of limestone.

Petrography – basalt

A thin section (*alpha-1*) of a basalt pebble shows that it is a porphyritic to glomeroporphyritic basalt with a medium-grained intergranular to intersertal groundmass. Olivine euhedra up to 2 mm across are fairly abundant, equant, occasionally slightly resorbed and are fresh or partly to completely altered. Sparsely distributed phenocrysts (up to 3 mm × 300 μm) of plagioclase are at least as calcic as labradorite (An₆₀). Glomerocrysts up to 3 mm across consist of equant crystals of weakly coloured to colourless augite (<1 mm), subordinate plagioclase and less commonly olivine; they are probably cognate and cumulate in origin. The groundmass consists of plagioclase laths (typically 150–400 μm long) that are locally subparallel, defining domains with a pilotaxitic or ‘fluidal’ texture; augite and olivine granules (mostly <50 μm) and an interstitial poorly crystalline turbid mesostasis, enriched in opaque bladed iron-titanium oxides. The alteration product of olivine is fibrous to kelpyitic, pleochroic from khaki yellow-brown to almost

colourless, length slow and has high birefringence; it may be a ferroan talc.

A second thin section of basalt (*alpha-3*) shows some petrographic differences. The most common phenocryst phase is plagioclase, occurring as laths up to 4 mm long but grading downward in size into the mesostasis. Colourless augite (<2 mm) is less common as phenocrysts and small glomerocrysts. There are also a few composite glomerocrysts of augite and plagioclase. Olivine occurs sparsely as small (<500 μm) euhedral phenocrysts now completely altered to colourless fibrous talc (?) with dark brown rims of iddingsite. The intergranular groundmass is slightly finer grained but better crystallised than in sample *alpha-1*; it consists of plagioclase laths (mostly 100–500 μm long), small (mostly <25 μm) granules of a ferromagnesian phase (augite?) and fine-grained opaque minerals.

Another thin section (*alpha-2*) is of a much more glassy basalt. It consists of euhedral olivine phenocrysts (<4 mm), narrow to acicular disoriented plagioclase laths (up to 400 μm × 20 μm) and a turbid, partly altered and oxidised black to dark brown glass. Carbonate and ‘iddingsite’ are common secondary minerals.

Discussion

Although basalt, either Tertiary or older (Neoproterozoic?), remains the most likely explanation for the anomaly, the degree of rounding in the dredged basalt pebbles recovered makes it doubtful that they are locally derived.

They are Tertiary basalts. Their petrographic differences are attributable to different cooling rates, and they are probably chemically similar, most likely with transitional to mildly tholeiitic affinities. The least altered sample, *alpha-1*, petrographically resembles, for example, flow remnants at 'Kaywood' near Temma in far northwest Tasmania.

Southwest of Albatross Island (‘Anomaly Beta’ – 295 240 mE, 5 523 550 mN)

This site lies on the western flank of a similar but smaller positive magnetic anomaly centred about six kilometres southwest of Albatross Island (fig. 3).

A pipe dredge sample from a depth of 59 m retrieved well rounded pebbles (20–80 mm) of basalt (50% by volume), two well-rounded pebbles (30–50 mm) of pale yellow-brown weathered quartzarenite or orthoquartzite (15%), and several flattish to very irregularly shaped pieces of off-white Recent (?) limestone 20–50 mm across, in addition to sand, shells, sponges and other organic material.

Petrography – orthoquartzite

A thin section (*beta 3*) of a ‘quartzarenite’ pebble shows an orthoquartzite with a bimodal grain size distribution. The finer grains are about 200 μm and the coarser grains 500–700 μm in size, and well rounded with undulose extinction. There are rare chert and polycrystalline quartz grains. Convexo-concave contacts between many grains suggest considerable strain, either due to overburden or tectonic strain. The rock is most likely derived from a correlate of the Proterozoic Rocky Cape Group.

Petrography – basalt

Two thin sections (*beta-1* and *beta-2*) are essentially of similar basalt, consisting of plagioclase, augite, subordinate olivine and 30–50% black glass. Plagioclase ranges from oblong microphenocrysts (up to 2 mm \times 400 μm) to abundant smaller laths (commonly 200–500 μm \times 40–100 μm). Colourless augite is common as equant euhedral to subhedral microphenocrysts up to 1.5 mm across, and as smaller groundmass granules. Olivine is less abundant as smaller (<500 μm , to rarely 1 mm), often rounded or slightly embayed phenocrysts that may be rimmed with augite. Pigeonite was not observed. Glomerocrysts of crystals, mainly of augite with a few plagioclase and an occasional olivine grain, are common. The groundmass is a turbid, partly oxidised black to dark brown glass. Olivine, augite and glass are partly altered to a pale yellow-brown to deep orange-brown alteration.

These basalt samples are probably olivine tholeiites of Tertiary age.

A third thin section (*beta-4*) is quite different, and contains phenocrystal and glomerocrystal altered olivine, clinopyroxene and rare plagioclase in a fine-grained altered groundmass. The euhedral olivine phenocrysts (<1 mm) are now completely pseudomorphed by fine-grained chlorite, whilst equant euhedra of colourless clinopyroxene (mostly <500 μm) are quite fresh. A few poorly oblong plagioclase phenocrysts (<1 mm) are corroded and altered. A small anhedral quartz xenocryst (250 μm) is surrounded by a reaction rim 200 μm wide of fine-grained saccharoidal pyroxene. The groundmass consists of fine-grained ragged plagioclase laths, small grains of pale green chlorite, tiny granules <10 μm of clinopyroxene (?) and abundant highly prismatic to acicular opaque minerals (<150 μm \times 50–15 μm). In addition an orange-brown oxidised limonitic alteration product pervades the groundmass. More-or-less spherical chlorite-filled amygdalae up to 3 mm in diameter are abundant. This basalt is most likely also of Tertiary age, but it also has some textural similarities to the Neoproterozoic basalt of the Smithton Basin. However the groundmass opaque phases in the latter rocks are generally equant rather than acicular, and the complete phenocryst assemblage olivine-clinopyroxene-plagioclase has not been observed in them.

Discussion

Again, the pebbles are too well rounded for confidence that they are of local derivation. The orthoquartzite pebble could be either a transported fragment of Rocky Cape Group basement or a clast from a conglomerate similar to that of Albatross Island.

Northwest of Albatross Island (‘Anomaly Gamma’)

Anomaly gamma-1 (293 160 mE, 5 532 200 mN)

The site lies within an ellipsoidal (8 km \times 4 km) area of low, quiet magnetics on the colour image (fig. 3, 4). Outcropping granite, perhaps similar to that of Three Hummock Island, was thought possible on the sea floor, although the magnetic signature of the inferred aureole is much weaker.

A pipe dredge sample from a depth of 65 m obtained a sticky pale grey mud containing subrounded pebbles and cobbles (25–150 mm) of basalt (60% by volume). The basalt is dense, massive and black, apart from some of the smaller pebbles which may have soft weathered medium-brown surfaces. Small (<10 mm) irregular fragments of Cainozoic limestone (30% by volume) and clots of mud (<30 mm, 10%) were also present.

Anomaly gamma-2 (292 840 mE, 5 533 490 mN)

A second dredging from the same vicinity, at a depth varying between 58 m and 44 m, obtained several kilograms of material consisting of well-rounded

pebbles and small cobbles (10–100 mm) of basalt (60% by volume), irregular fragments (30–150 mm) of pale brown to off-white Cainozoic limestone (25%), and well-rounded pebbles of pale brown to yellow brown quartzite.

Petrography – orthoquartzite

Thin section *gamma 1* is a supermature orthoquartzite (0.1 to 0.5 mm grain size). The coarser grains show authigenic overgrowths and well-rounded detrital outlines. It appears to be a typical Rocky Cape Group quartzite.

Petrography – limestone

Thin section *gamma 2-3* is a poorly sorted bioclastic calcarenite, with fragmentary bryozoans, foraminifera, echinoderms, a gastropod and indeterminate fragments (comminuted shell hash) with porosity partly occluded by sparry calcite cement, in part as syntaxial overgrowths on echinoderm elements. The palaeontology of this sample is described in Appendix 1.

Petrography – basalt

A thin section (*gamma 2-1*) contains common euhedral phenocrysts of partly altered olivine (<2 mm) and nearly colourless augite (<1.5 mm, mostly <1 mm), the latter mostly clumped into glomerocrysts. The relatively medium to coarse-grained intergranular pilotaxitic groundmass consists of aligned plagioclase laths (mostly 200–600 μm long), interstitial augite granules (<5 μm) and bladed to acicular opaque grains. Some green chloritic alteration is present. The basalt is certainly Tertiary, and as some of the smaller granules of groundmass augite are distinctly pinkish (titaniferous), it may be mildly alkaline.

A small (1.5 mm) xenolith of well sorted quartzose siltstone, with a mean grain size of 50 μm , is probably an accidental high-level inclusion derived from Rocky Cape Group basement.

A second thin section (*gamma 2-2*) of another, vesicular and more altered, basalt pebble shows sparsely distributed, nearly completely altered phenocrysts of olivine (<1 mm) in a groundmass of aligned plagioclase laths (200–500 μm), small ferromagnesian granules (augite?) and abundant black to brown, altered and oxidised glass. This rock probably has tholeiitic affinities.

Discussion

The dredging obtained no evidence supporting the occurrence of granite, although the basalt and orthoquartzite pebbles are again well rounded and may not be locally derived.

Six kilometres west of Black Pyramid (‘Anomaly Delta’ - 269 320 mE, 5 514 650 mN)

This site lies over a strong positive magnetic anomaly (fig. 3, 4). It lacks the short wavelength structure, evident in the colour images, near known Tertiary

basalt at Reid Rocks and Black Pyramid, and more resembles anomalies associated with Neoproterozoic basalt.

The pipe dredge sample, obtained from a mean depth of 68 m, consisted only of sand and three irregular pieces of Cainozoic limestone, 40–50 mm across. Because of deteriorating sea conditions no further dredging attempts were possible. A similar but larger anomaly located 13 to 20 km south of Black Pyramid remains untested.

Note on Bass-3 drillhole

One of the petroleum exploration wells drilled in Bass Strait is marginal to the area discussed in this report. Bass-3, drilled by the Esso-BHP consortium in 1967, was sited 52 km NNE of Cape Rochon (Three Hummock Island) at the northern edge of the area covered by the new aeromagnetic data (253 390 mE, 5 671 090 mN). It was located near the western edge of a meridional positive magnetic anomaly of moderate intensity, and immediately east of a magnetically quiet area. The diffuse nature of the anomalies in the area indicate a considerable thickness of Tertiary Bass Basin sediments.

Details of the well are given by Anon (1967). After passing through marine sediments (to 1607 m below sea level) and the mainly continental ‘Delta Complex’ sequence (1607–2377 m) containing a mid-Eocene unconformity, pre-Tertiary basement was reached at a depth of 2377 m, and penetrated to a final depth of 2422 metres. The basement rocks were described in the log (Anon, 1967) as ‘interbedded quartzite and recrystallized siltstone and fine grained sandstone and black metamorphosed shale’. More detailed lithological descriptions mention very fine grained, sparsely pyritic, dense and very hard quartzite with apparent bands of silicified breccia. The shale was thought to be baked, with ‘recrystallized segregations of quartz-calcite-biotite’, irregular quartzite bodies, minor pyrite and rare chalcopyrite. A single sample, presumably containing biotite, from 2421 m yielded a K/Ar age of 418.0 Ma (‘Silurian, ... Ordovician and Devonian possible’).

Two thin sections of the basement rocks were re-examined for this study.

One (S4) contains fine-grained (<10 μm) dark brown carbonate, with a scattering of quartz-filled fenestral pores 20–200 μm in diameter. In abrupt conformable contact with the carbonate is a thinly laminated black (mostly opaque) shale, containing irregular sparry veinlets of carbonate. Partly conformable, and partly transgressing the laminae in the shale is a mass of fine-grained (mostly <5 to 20 μm) chert which has an ill-defined clastic or peloidal fabric suggestive of a carbonate (grainstone) precursor. Fine-grained (20–100 μm) aggregates of splintery phyllosilicate (probably talc rather than sericite, R. Bottrill, pers. comm.) appear to be locally replacing the chert, particularly near its margins.

The other thin section (S5) contains irregular bodies of chert and talc/sericite (as in S4), surrounded by thinly laminated carbonaceous (?) black shale. The lamination appears deformed by differential compaction or tectonic strain.

When compared lithologically to northwest Tasmanian sequences, the rocks more closely resemble certain lithologies within the Black River Dolomite of the Neoproterozoic Togari Group, rather than the mainly siliciclastic Mesoproterozoic Rocky Cape Group. The reported occurrence of biotite (not seen in these thin sections) is problematical. Possibly biotite and talc are contact metamorphic products, and they may indicate the proximity of a granitoid intrusion.

Conclusions

A recent magnetic interpretation of basement elements of the shelf between northwest Tasmania and King Island (Gunn *et al.*, 1996) shows:

- (i) a large (30 km) subcircular non-magnetic granite batholith embracing Three Hummock Island at its southwestern end;
- (ii) a broad (5–10 km) magnetic contact-metamorphic aureole partly surrounding this granite;
- (iii) meridional belts of magnetic Neoproterozoic basalt to the north and south of the granite; those to the south are continuous with basalt units within the Togari Group, confirmed by mapping on land (Seymour and Baillie, 1992);
- (iv) a major, complex, strongly magnetic meridional belt extending for at least 170 km from east of King Island to just off Sandy Cape, which is also provisionally interpreted as Neoproterozoic mafic units on the basis of outcropping units on the southeast coast of King Island (Waldron and Brown, 1993); and
- (v) several smaller, submerged areas between the Hunter Group and Black Pyramid, classed as 'weak magnetic anomalies sourced in or beneath Proterozoic units'.

The onshore geology of the small islands visited is of rather limited use in 'ground-truthing' this interpretation, particularly with regard to basement (here more-or-less meaning pre-Cretaceous) geology. The presumably Neoproterozoic picrites on Councillor Island confirm the offshore extension of similar units on southeast King Island. The presence of granite on Penguin Islet shows that the subsurface form of the Three Hummock granite is complex and of still greater extent, at least to the southwest, than is obvious in the magnetic image, but in accord with the (sparse) regional gravity data. The weak short wavelength negative anomalies between the Hunter Group and Black Pyramid are due to Tertiary basalt rather than sources in the presumably Neoproterozoic basement, as are similar but positive anomalies around Reid Rocks. Tertiary volcanism in the region is more varied

both temporally and geochemically than previous records indicate.

Possible areas for further onshore research in the region must include detailed systematic geological mapping of King Island. In particular, the relationship between the Proterozoic metasediments of the western part of the island and less metamorphosed sequences of the east is a key problem. The petrological affinities of the King Island and Councillor Island picrites and basalts need to be addressed in the context of similar sequences in northwest Tasmania, utilising isotopic and further geochemical data. Geological information on Robbins Island remains very sparse and systematic mapping is needed there. The work of Jennings (1976 and unpublished) provides a firm foundation for more detailed mapping on Three Hummock Island and Hunter Island, respectively. The former is an interesting area for further petrological studies of granite and, especially, their enclaves. There is scope for detailed volcanological studies of the Tertiary volcanic rocks of particularly Steep Island, on which we were unable to land, and Black Pyramid. Some of the Tertiary basalt samples collected on the voyage are being used in a wider geochemical and isotopic study of Tasmanian Tertiary volcanism, in collaboration with workers at Macquarie University.

It is clear that a much more concerted attempt must be made, if dredging is to yield more useful information about the basement geology of the region. The present results are not encouraging and the use of more sophisticated echo sounding to focus on sea floor topographic highs should perhaps be considered.

Economically the most interesting result of this work is the presence of weakly mineralised, highly fractionated granite on Penguin Islet. The strongly magnetic character of the contact aureole of the related Three Hummock Island granite is probably due to magnetite mineralisation. The aureole appears to extend onshore in the southwest of Three Hummock Island, but bedrock there is obscured by dune sand. The inferred Togari Group country rocks to the north and south of Three Hummock Island are likely to contain reactive carbonate units both stratigraphically above and below the inferred basalt units. Thus this area east of Hunter Island is considered to have high potential for skarn and carbonate replacement mineralisation, particularly of tin-tungsten. If most of the area were not 10–30 metres below sea level, it would be highly promising ground for mineral exploration.

Acknowledgements

We thank Charles Moore, founder and CEO of the Algalita Marine Research Foundation, for the opportunity to charter ORV *Algalita* as part of her 'shakedown cruise', and for his enthusiasm as skipper and head chef, in pursuing the objectives of the charter.

Technical assistance was provided by Geological Survey staff, notably Richie Woolley (x-ray diffraction), Shane Heawood and Mike Jacobson (lapidary), Peter

Sheridan and Les Hay (chemical analyses) and Anthony Hollick (drafting).

The Tasmanian Parks and Wildlife Service granted permits to collect geological samples from nature reserves.

Tony Yeates (AGSO) reviewed an earlier version of this report and made useful suggestions.

The boat charter and field expenses were funded under the National Geoscience Mapping Accord.

References

- ANONYMOUS, 1967. Ezzo Bass-3 Tasmania. *Well completion report*. Ezzo Exploration Australia Inc. [OR-332].
- BANKS, M. R. 1989. Notes on the geology and geomorphology of Albatross Island. *Records Queen Victoria Museum* 95.
- BLACK, L. P. 1994. The significance of current and proposed SHRIMP dating. *Report Mineral Resources Tasmania* 1994/16.
- BLEVIN, P. L.; CHAPPELL, B. W. 1992. The role of magma sources, oxidation states and fractionation in determining the granite metallogeny of eastern Australia. *Transactions Royal Society of Edinburgh (Earth Sciences)* 83:305–316.
- BLEVIN, P. L.; CHAPPELL, B. W. 1995. Chemistry, origin and evolution of mineralized granites in the Lachlan Fold Belt, Australia: the metallogeny of I- and S-type granites. *Economic Geology* 90:1604–1609.
- BOYNTON, W. V. 1984. Cosmochemistry of the rare earth elements: meteorite studies, in: HENDERSON, P. (ed.). *Rare earth element geochemistry*. 63–114. Elsevier.
- BROWN, A. V. 1986. Geology of the Dundas–Mt Lindsay–Mt Youngbuck region. *Bulletin Geological Survey Tasmania* 62.
- BROWN, A. V. (comp.). 1989. Geological Atlas 1:50 000 Series. Sheet 21 (7916S). Smithton. *Explanatory Report Geological Survey Tasmania*.
- CALVER, C. R.; CORBETT, K. D.; EVERARD, J. L.; GOSCOMBE, B. D.; PEMBERTON, J.; SEYMOUR, D. B. (Comp.). 1995. Geological Atlas 1:250 000 digital series. Geology of Northwest Tasmania. *Tasmanian Geological Survey*.
- CARTER, A. N. 1958. Tertiary foraminifera from the Aire district, Victoria. *Bulletin Geological Survey Victoria* 55.
- CAS, R. A. F. 1989. Physical volcanology: lava-forming eruptions and flow features, in: JOHNSON, R. W. (ed.). *Intraplate volcanism in Eastern Australia and New Zealand*. 57–68. Cambridge University Press : Cambridge.
- CHAPPELL, B. W.; ENGLISH, P. M.; KING, P. L.; WHITE, A. J. R.; WYBORN, D. 1991. Granites and related rocks of the Lachlan Fold Belt (1:1 250 000 scale map). *Bureau of Mineral Resources, Geology and Geophysics Australia*.
- CHAPPELL, B. W.; WHITE, A. J. R. 1974. Two contrasting granite types. *Pacific Geology* 8:173–174.
- CHAPPELL, B. W.; WHITE, A. J. R.; WYBORN, D. 1987. The importance of residual source material (restite) in granite petrogenesis. *Journal of Petrology* 28:1111–1138.
- CHAPPELL, B. W.; WHITE, A. J. R. 1992. I- and S-type granites in the Lachlan Fold Belt. *Transactions Royal Society of Edinburgh (Earth Sciences)* 83:1–26.
- CHEN, Y. D.; PRICE, R. C.; WHITE, A. J. R. 1989. Inclusions in three S-type granites from southeastern Australia. *Journal of Petrology* 30:1181–1218.
- COLLINS, W. J. 1996. Lachlan Fold Belt granitoids: products of three component mixing, in: BROWN, M.; CANDELA, P. A. *et al.* (ed.). The origin of granites and related rocks. *Transactions Royal Society of Edinburgh: Earth Sciences* 87:171–181.
- CRAWFORD, A. J.; BERRY, R. F. 1992. Tectonic implications of late Proterozoic–early Palaeozoic igneous rock associations in western Tasmania. *Tectonophysics* 214:37–56.
- CROMER, W. C. 1972. *The petrology and chemistry of the Circular Head teschenite*. B.Sc. (Hons) thesis, University of Tasmania.
- DIXON, G. 1996. *A reconnaissance inventory of sites of geoconservation significance on Tasmanian islands*. Parks and Wildlife Service Tasmania.
- DODGE, F. C. W.; KISTLER, R. W. 1990. Some additional observations on inclusions in the granitic rocks of the Sierra Nevada. *Journal of Geophysical Research* 95:17841–17848.
- EDWARDS, A. B. 1950. The petrology of the Cainozoic basaltic rocks of Tasmania. *Proceedings Royal Society of Victoria* 62:97–120.
- ELBURG, M. A.; NICHOLLS, I. A. 1995. Origin of microgranitoid enclaves in the S-type Wilson's Promontory Batholith, Victoria: evidence for magma mingling. *Australian Journal of Earth Sciences* 42:423–435.
- EVERARD, J. L. 1989. Petrology of the Tertiary basalt, in: SEYMOUR, D. B. (comp.). Geological Atlas 1:50 000 series. Sheet 36 (8015S). St Valentines. *Explanatory Report Geological Survey Tasmania* 79–142.
- FLINDERS, J.; CLEMENS, J. D. 1996. Non-linear dynamics, chaos, complexity and enclaves in granitoid magmas, in: BROWN, M.; CANDELA, P. A. *et al.* (ed.). The origin of granites and related rocks. *Transactions Royal Society of Edinburgh: Earth Sciences* 87:217–224.
- FLOOD, R. H.; SHAW, S. E. 1995. Granites and microgranitoid enclaves: the importance of cumulates, in: BROWN, M.; PICCOLI, P. M. (ed.). The origin of granites and related rocks. *Circular United States Geological Survey* 1129:53.
- FREY, F. A.; GREEN, D. H.; ROY, S. D. 1978. Integrated models of basalt petrogenesis: a study of quartz tholeiites to olivine melilitites from south eastern Australia utilizing geochemical and experimental petrological data. *Journal of Petrology* 19 463–513.
- GEE, R. D. 1971. Geological Atlas 1 mile series. Zone 7 Sheet 22 (8016S). Table Cape. *Explanatory Report Geological Survey Tasmania*.
- GEEVES, P. D. 1982. *The petrology, geochemistry and mineral chemistry of the basalts of the Wynyard area and the Table Cape teschenite*. B.Sc. (Hons) thesis, University of Tasmania.
- GUNN, P. J.; MACKAY, T. E.; RICHARDSON, R. G.; SEYMOUR, D. B.; MCCLENAGHAN, M. P.; CALVER, C. R.; ROACH, M. J.; YEATES, A. N. 1996. The basement elements of Tasmania. *Record Australian Geological Survey* 1996/29.

- HINE, R.; WILLIAMS, I. S.; CHAPPELL, B. W.; WHITE, A. J. R. 1978. Contrasts between I- and S-type granitoids of the Kosciusko Batholith. *Journal Geological Society of Australia* 25:219-234.
- ISHIHARA, S. 1977. The magnetite-series and ilmenite-series granitic rocks. *Mining Geology* 27:293-305.
- JENNINGS, D. J. 1976. The geology of Three Hummock Island. *Unpublished Report Tasmania Department of Mines* 1976/56.
- JENNINGS, D. J.; COX, S. F. 1978. Geological Atlas 1:250 000 Series. Sheet SK55-1 King Island and SK55-2 Flinders Island. *Tasmania Department of Mines*.
- JOHNSON, R. W.; DUGGAN, M. B. 1989. Rock classification and analytical databases, in: JOHNSON, R. W. (ed.). *Intraplate volcanism in Eastern Australia and New Zealand*. 12-13. Cambridge University Press : Cambridge.
- JONES, H. A.; DAVIES, P. J. 1983. Superficial sediments of the Tasmanian continental shelf and part of Bass Strait. *Bulletin Bureau of Mineral Resources, Geology and Geophysics Australia* 218.
- JONES, H. A.; HOLDGATE, G. R. 1980. Shallow structure and Late Cainozoic geological history of western Bass Strait and the west Tasmanian shelf. *BMR Journal of Australian Geology and Geophysics* 5:87-93.
- LEAMAN, D. E.; RICHARDSON, R. G. 1989. The granites of west and north-west Tasmania — a geophysical interpretation. *Bulletin Geological Survey Tasmania* 66.
- LE MAITRE, R. W. 1976. The chemical variability of some common igneous rocks. *Journal of Petrology* 17:589-637.
- MCCLENAGHAN, M. P.; CAMACHO, A.; HIGGINS, N. C.; REID, E. J. 1989. Mid-Palaeozoic granitoids, in: BURRETT, C. F.; MARTIN, E. L. (ed.). *Geology and mineral resources of Tasmania*. *Special Publication Geological Society of Australia* 15:253-270.
- MACDONALD, G. A.; KATSURA, T. 1964. Chemical composition of Hawaiian lavas. *Journal of Petrology* 5:82-133.
- MORRISON, K. C.; DAVIDSON, J. K. 1989. Bass Basin, in: BURRETT, C. F.; MARTIN, E. L. (ed.). *Geology and mineral resources of Tasmania*. *Special Publication Geological Society of Australia* 15:347-358.
- QUILTY, P. G. 1972. The biostratigraphy of the Tasmanian marine Tertiary. *Papers and Proceedings Royal Society of Tasmania* 106:25-44.
- REID, J. B.; EVANS, O. C.; FATES, D. G. 1983. Magma mixing in granitic rocks of the central Sierra Nevada, California. *Earth and Planetary Science Letters* 66:243-261.
- SAWKA, W. N.; HEIZLER, M. T.; KISTLER, R. W.; CHAPPELL, B. W. 1990. Geochemistry of highly fractionated I- and S-type granites from the tin-tungsten province of western Tasmania, in: STEIN, H. J.; HANNAH, J. L. (ed.). *Ore-bearing granite systems: petrogenesis and mineralizing processes*. *Special Paper Geological Society of America* 246:161-179.
- SCOTT, B. 1951. The petrology of the volcanic rocks of south east King Island. *Papers and Proceedings Royal Society of Tasmania* 85:113-136.
- SEYMOUR, D. B.; BAILLIE, P. W. 1992. Geological Atlas 1:50 000 Series. Sheet 20 (7816S). Woolnorth. *Department of Mines Tasmania*.
- SEYMOUR, D. B.; CALVER, C. R. 1995. Explanatory notes for the Time-Space Diagram and Stratotectonic Elements Map of Tasmania. *Record Tasmanian Geological Survey* 1995/01.
- SOLOMON, M. 1969. The nature and possible origin of the pillow lavas and hyaloclastite breccias of King Island, Australia. *Quarterly Journal Geological Society of London* 124:153-169.
- STRECKEISEN, A. L. 1973. Plutonic rocks: classification and nomenclature recommended by the IUGS subcommission on the systematics of igneous rocks. *Geotimes* 18(10):27-30.
- SUTHERLAND, F. L. 1980. Aquagene volcanism in the Tasmanian Tertiary, in relation to coastal seas and river systems. *Papers and Proceedings Royal Society of Tasmania* 114:177-199.
- SUTHERLAND, F. L.; BAILLIE, P. W.; COLWELL, J. B. 1989. Tasmania and Bass Strait, in: JOHNSON, R. W. (ed.). *Intraplate volcanism in Eastern Australia and New Zealand*. 143-149. Cambridge University Press : Cambridge.
- SUTHERLAND, F. L.; CORBETT, K. D. 1967. The Tertiary volcanic rocks of far north-western Tasmania. *Papers and Proceedings Royal Society of Tasmania* 101:71-90.
- SUTHERLAND, F. L.; EWART, A.; RAYNOR, L. R.; HOLLIS, J. D.; MCDONOUGH, W. D. 1989. Tertiary basaltic magmas and the Tasmanian lithosphere, in: BURRETT, C. F.; MARTIN, E. L. (ed.). *Geology and mineral resources of Tasmania*. *Special Publication Geological Society of Australia* 15:386-398.
- SUTHERLAND, F. L.; HENDRY, D. F.; BARRON, B. J.; MATTHEWS, W. L.; HOLLIS, J. D. 1996. An unusual Tasmanian Tertiary basalt sequence, near Boat Harbour, northwest Tasmania. *Records Australian Museum* 48:131-161.
- TURNER, N. J. 1989. Precambrian — correlates of the Rocky Cape Group, in: BURRETT, C. F.; MARTIN, E. L. (ed.). *Geology and mineral resources of Tasmania*. *Special Publication Geological Society of Australia* 15:15-17.
- VARNE, R. 1977. On the origin of spinel lherzolite inclusions in basaltic rocks from Tasmania and elsewhere. *Journal of Petrology* 18:1-23.
- VERNON, R. H. 1983. Restite, xenoliths and microgranitoid enclaves in granites. *Journal and Proceedings Royal Society of New South Wales* 116:77-103.
- VERNON, R. H. 1984. Microgranitoid enclaves in granites — globules of a hybrid magma quenched in a plutonic environment. *Nature* 309:438-439.
- WALDRON, H. M.; BROWN, A. V. 1993. Geological setting and petrochemistry of Eocambrian-Cambrian volcano-sedimentary rock sequences from southeast King Island. *Record Tasmanian Geological Survey* 1993/28.
- WHALEN, J. B.; CHAPPELL, B. W. 1988. Opaque mineralogy and mineral chemistry of I- and S-type granites of the Lachlan fold belt, southeast Australia. *American Mineralogist* 73:282-296.
- WHITE, A. J. R.; CHAPPELL, B. W. 1977. Ultrametamorphism and granitoid genesis. *Tectonophysics* 43:7-22.
- YAXLEY, G. M. 1981. *The geology and mineralisation of the Balfour district — a mineralogical and fluid inclusion study*. B.Sc. (Hons.) thesis, University of Tasmania.

[1 June 2000]

APPENDIX 1

Palaeontology and age of limestone from Black Pyramid and a dredged limestone pebble, Bass Strait

P. G. Quilty

Black Pyramid samples

Limestone occurs as a number of irregular bodies in Tertiary basalt, about 25 m above sea level.

Sample BPC 4a

The rock is an off white, massive, solid, biogenic limestone.

Slide description

The rock is a bryozoal/foraminiferid calcarenite. In contrast with the megascopic appearance, the rock appears to be quite well bedded and well sorted. Some beds are rich in well-sorted particles with abundant volcanic fragments. Others are dominated by the foraminiferid *Calcarina verriculata*.

Fauna

Apart from the foraminiferids recorded below, the sediment contains common calcareous algae, echinoid spines and echinoderm plates, bryozoans, and a few gastropods.

Foraminiferid fauna — this is of very low diversity and with high dominance.

Calcarina verriculata — abundant, with up to 12 chambers per whorl.

Cibicides sp.

Cassidulina sp. (rare)

Sherbornina sp. (probably *atkinsoni* identified tentatively in vertical section).

encrusting *Gypsina* (perhaps *Aceroulina*)

Carpenteria sp. (perhaps *balaniformis*)

agglutinated species (*Textularia*)

There are no planktonic species.

Age

The fauna is similar to that which occurs at Fossil Bluff, Cape Grim and other localities along the northwest and west coast of Tasmania (Quilty, 1972) where the age is early Miocene, correlating with Faunal Unit 6 of Carter (1958).

Environment of deposition

It is an inner neritic fauna, well within the range of light penetration. It appears to be a little warmer in aspect than the sediments recorded by Quilty from other early

Miocene sediments, perhaps reflecting the influence of an early version of the Leeuwin Current.

Sample BPC 4B

The specimen (a fawn massive indurated limestone) is essentially the same as BPC 4A but the volcanic fragments are coarser and more uniformly distributed.

The foraminiferid fauna is dominated again by *Calcarina verriculata* but it is less dominant than in BPC 4A. *Lenticulina* spp is common, there is a discoid form of *Gypsina*, fragments of planktonic species and generically identifiable *Textularia*.

The age is the same as BPC 4A.

Dredge sample γ 2 -3.

Location: 40°19.374'–40°19.413'S,
144°33.683–144°33.813'E

Depth: 44–58 m

Sample: A single highly rounded, dredged pebble, approximately 60 × 40 × 15 mm.

Megascopic description

The buff coloured cortex of the pebble surrounds a red centre. It is highly biogenic, calcareous and well sorted with abundant foraminiferids.

Thin section examination

In thin section the material is very poorly preserved and extensively recrystallised so that wall structure is seldom clear and much of the material is unidentifiable even at phylum level. Thus the comments made below are tentative. The sediment is massive without obvious bedding.

Fauna/flora

Apart from the foraminiferids recorded below, there are abundant bryozoa and molluscs with less abundant echinoderm fragments. Calcareous algae are rare and present as small broken fragments.

Foraminiferid fauna

Diversity is much higher than in the Black Pyramid samples and dominance much lower. Planktonic species make up about 20% of the fauna but that figure is very rough.

Agglutinated forms (*Textularia*, *Triraxia*, *Clavulina*, *Gaudryina*), miliolids (*Pyrgo*, *Quinqueloculina*, *Triloculina* [several species including an agglutinated

one]), abundant rotalids (*Anomalinoidea*, *Cibicides*, *Gavelinella*) and cassidulinids (*Cassidulina*, *Globocassidulina*) are common.

There seem to be only two planktonic species. One has a wall typical of the *Globigerina woodi* group and the other the thinner wall of the *G. bulloides* type. Globorotalids, sphaeroidinellids and *Globoquadrina* all appear to be absent.

Age

The material contains no age diagnostic forms and thus no definitive statement can be made. However, in northern Tasmania, faunas similar to this in benthic content and with low diversity planktonic fauna lacking anything other than globigerinids, are common

in the early Miocene sediments deposited during the widespread incursion that formed the Fossil Bluff/Cape Grim and related sediments.

Environment of deposition

The sediment appears to be a mid-shelf depth deposit, at the base of light penetration. Sediments formed in this environment commonly contain foraminiferid diversity similar to that recorded here, and with similar generic content in the benthic forms. The planktonic percentage is also consistent with this.

The sediment formed under fully marine conditions. There is not much evidence of terrigenous material. Water temperature was quite low, apparently lower than indicated in the Black Pyramid samples.

Appendix 2

Sample locations and treatment

<i>Island</i>	<i>Reg. No.</i>	<i>Field No.</i>	<i>AMG ref.</i>	<i>Locality</i>	<i>Description</i>	<i>Preparation</i>		
Councillor Island	004801	CN1	BR570872	15 m NW of gulch at north end	pillow basalt	TS	XRD	
	004802	CN2	BR569872	50 m NW of gulch	pillow basalt	TS	XRD	CA
	004803	CN3	BR569873	just SSE of north end	15 cm porphyry dyke	TS	XRD	CA ICPMS
	004804	CN4	BR569873	country rock to CN3	pillow basalt	TS	XRD	CA
	004805	CN5	BR568873	west shore, 100 m S of N end	pillow basalt	TS	XRD	CA
	004806	CN6	BR568871	Halfway down west shore	pillow basalt	TS	XRD	CA
	004807	CN7	BR566868	south end (Flying Squirrel Reef)	tabular basalt	TS	XRD	CA
	004808	CN8	BR570870	east side, SE of summit	tabular basalt, high X	TS	XRD	CA
	004809	CN9	BR570872	NW side of landing gulch	pillow basalt, high X	TS	XRD	CA ICPMS
	004810	CN10	BR571871	east shore	basalt dyke, high X	TS	XRD	
Reid Rocks	004811	RR1	BR581409	north side near east end	altered basalt	TS		
	004812	RR2	BR581409	north side near east end	altered basalt			
	004813	RR3	BR581409	north side near east end	altered basalt			
	004814	RR4	BR581409	north side near east end	altered basalt	TS		CA
	004815	RR5	BR581409	north side near east end	altered basalt			
	004816	RR6	BR581409	north side near east end	altered basalt			
	004817	RR7	BR581409	north side near east end	fracture material		XRD	
Black Pyramid	004818	BP1	BR753158	north side near east end, shore	basalt	TS		CA
	004819	BP2	BR753158	east end, base of cliff	pink limestone Neptunian dykes			
	004820	BP3	BR753158	east end, base of cliff	pink limestone	TS		
	004821	BP4	BR753158	east end, base of cliff	basalt, amygdaloidal			
	004822	BP5	BR750158	upper volcanoclastic unit	basalt, pillow fragments	TS		CA
	004823	BP6	BR751158	sedimentary horizon	bedded vitric tuff	TS	XRD	
	004824	BP7	BR753158	shore just west of BP1	basalt	TS		CA
Albatross Island	004825	AI1	CR009281	beach boulder, east shore	dolerite	TS	XRD	CA
	004826	AI1A	CR009281	beach boulder, east shore	dolerite			
	004827	AI2	CR009280	northern end	orthoquartzite clast	TS		
	004828	AI3	CR010279	northern end	from sandstone bed	TS		
Hunter Island (Cuvier Bay)	004829	CB1	CR071159	south of Cuvier Point	orthoquartzite	TS		
	904830	CB1A	CR071159	south of Cuvier Point	ankeritic vein		XRD	
	004831	CB4	CR072156	Cuvier Bay	black siltstone	TS		
	004832	CB5	CR072156	Cuvier Bay	altered dolerite dyke	TS		CA
	(Cave Bay)	004833	H1	CR114109	north end of Cave Bay	siltstone	TS	
Penguin Islet	004834	PI1	CR147060	eastern shore near north end	granite	TS		CA
	004835	PI2	CR146058	west shore, halfway along	granite	TS		CA
	004836	PI3	CR146057	beach cobble, west shore	basalt	TS		
Three Hummock Island	004837	TH1	CR167201	shore west of Chimney Corner	melanocratic enclave	TS		CA
	004838	TH2	CR165203	shore west of Chimney Corner	melanocratic enclave			
	004839	TH3	CR166203	shore west of Chimney Corner	melanocratic enclave, weathered			
	004840	TH4	CR166202	shore west of Chimney Corner	melanocratic enclave	TS	XRD	CA
	004841	TH5	CR168202	blasted outcrop at jetty	granite	TS		CA
	004842	TH6	CR198172	east end of beach east of spit	melanocratic enclave	TS		CA
	004843	TH7	CR198172	east end of beach east of spit	melanocratic enclave	TS		CA
	004844	TH8	CR198172	east end of beach east of spit	melanocratic enclave	TS	XRD	CA
	004845	TH9	CR198172	east end of beach east of spit	granite	TS		CA
	004846	TH10	CR198172	east end of beach east of spit	xenolith?	TS	XRD	
Robbins Island	004847	RI1	CQ348942	layered flow, Marys Island	platy basalt	TS	XRD	CA
	004848	RI2	CQ347946	south side of Guyot Point	mudstone/tuff			
	004849	RI3	CQ347946	as above, overlying mudstone	'knobby' basalt	TS	XRD	CA
	004850	RI4	CQ347948	north side of Guyot Point	columnar basalt	TS		CA

TS: thin section; XRD: x-ray diffraction; CA: chemical analysis; ICPMS: ICPMS analysis including rare earth elements

Appendix 3

Approximate mineralogy (approximate wt% by X-ray diffraction) of samples

Sample	>80%	60–80%	40–60%	25–40%	15–25%	10–15%	5–10%	<5%
CN1			amphibole, chlorite					
CN2			amphibole	chlorite				mica, ?zeolite
CN3				quartz	plagioclase, amphibole		chlorite, K-feldspar*	mica
CN4			chlorite, amphibole					
CN5			amphibole, chlorite					mica
CN6			chlorite	amphibole			clinopyroxene	
CN7			chlorite, amphibole					
CN8			amphibole		chlorite	clinopyroxene	epidote	
CN9			chlorite		amphibole, clinopyroxene			?quartz, ?epidote
CN10		chlorite		amphibole				clinopyroxene, mica
BP6	amorphous							anatase
AI1				amphibole, chlorite		quartz	epidote, plagioclase	mica
TH4		mica				quartz, plagioclase	chlorite	
TH8				mica, amphibole	plagioclase		chlorite, quartz	
TH10				quartz, clinopyroxene	plagioclase		amphibole	chlorite, mica
RI1				clinopyroxene, plagioclase		olivine	smectite, phillipsite	ilmenite, analcime ?nepheline
RI3			clinopyroxene	plagioclase	olivine			smectite, ?apatite

RR7 – minerals identified: white – apatite-group mineral (moderate crystallinity);
 beige – struvite (NH₄MgPO₄·6H₂O), monohydrocalcite (CaCO₃·H₂O)
 weathered – clinopyroxene, plagioclase, analcime, smectite

Peak overlap may interfere with identifications (e.g. K-feldspar* may mask clinopyroxene). Minerals present in trace amounts, or amorphous minerals, may not be detected.

Analyst: R. N. Woolley

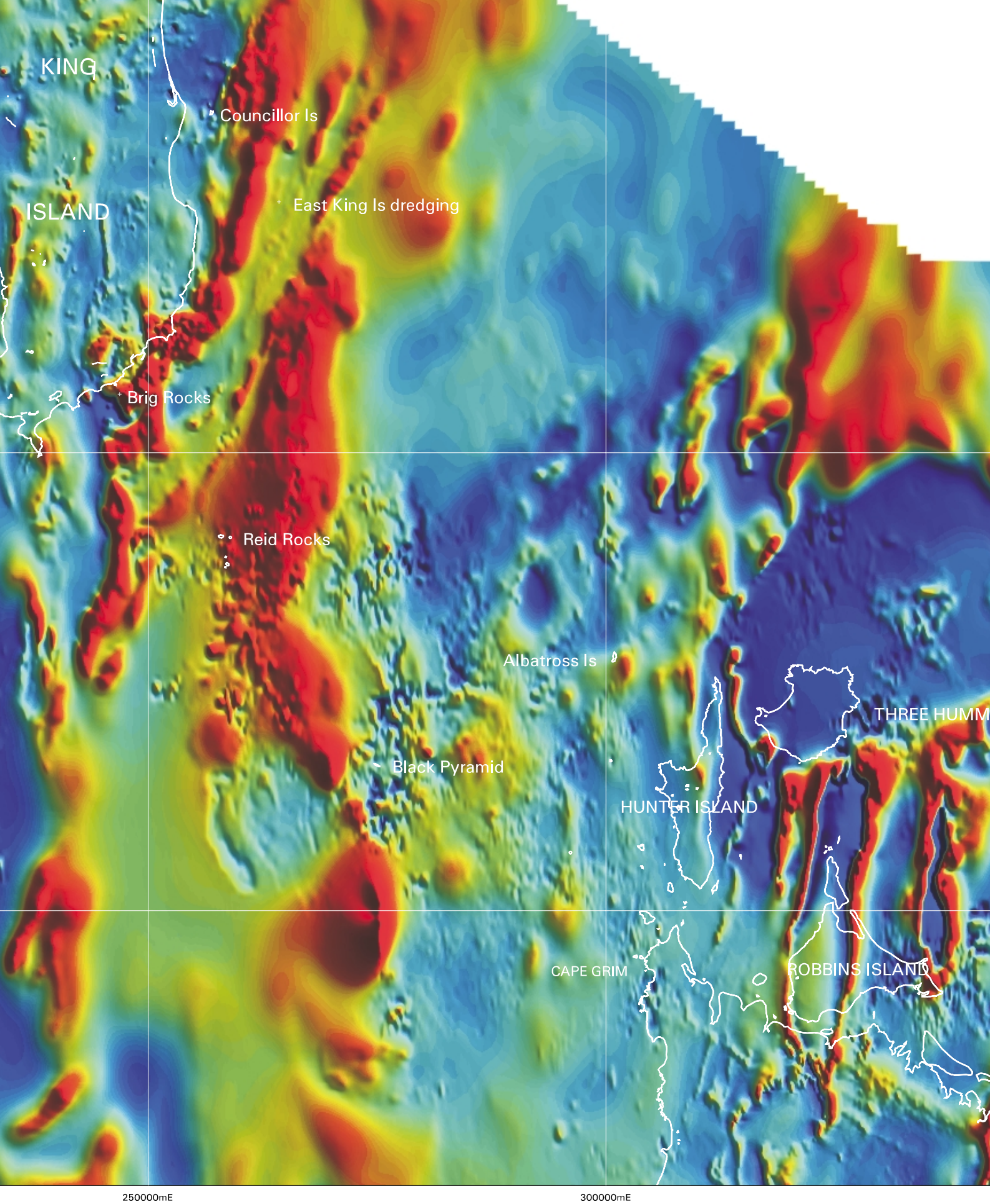


Figure 3

Image (total magnetic intensity) of southwestern Bass Strait (processed extract from 1994 AGSO aeromagnetic survey, east-west flight lines, 800 m interval)